Development and Analysis of New Integrated Energy Systems for Sustainable Buildings

By

FARRUKH KHALID

A Thesis Submitted in Partial Fulfilment

of the Requirements for the degree of

Master of Applied Science

in

Mechanical Engineering

Faculty of Engineering and Applied Science

University of Ontario Institute of Technology

Oshawa, Ontario, Canada

Abstract

Excessive consumption of fossil fuels in the residential sector and their associated negative environmental impacts bring a significant challenge to engineers within research and industrial communities throughout the world to develop more environmentally benign methods of meeting energy needs of residential sector in particular. This thesis addresses potential solutions for the issue of fossils fuel consumption in residential buildings. Three novel renewable energy based multigeneration systems are proposed for different types of residential buildings, and a comprehensive assessment of energetic and exergetic performances is given on the basis of total occupancy, energy load, and climate conditions.

System 1 is a multigeneration system based on two renewable energy sources. It uses biomass and solar resources. The outputs of System 1 are electricity, space heating, cooling, and hot water. The energy and exergy efficiencies of System 1 are 91.0% and 34.9%, respectively. The results of the optimisation analysis show that the net present cost of System 1 is $ 2,700,496 and that the levelised cost of electricity is $ 0.117/kWh.

System 2 is a multigeneration system, integrating three renewable energy based subsystems; wind turbine, concentrated solar collector, and Organic Rankine Cycle supplied by a ground source heat exchanger. The outputs of the System 2 are electricity, hot water, heating and cooling. The optimisation analysis shows that net present cost is $ 35,502 and levelised cost of electricity is $ 0.186/kWh. The energy and exergy efficiencies of System 2 are found to be 34.6% and 16.2%, respectively.

System 3 is a multigeneration system, comprising two renewable energy subsystems—geothermal and solar to supply power, cooling, heating, and hot water. The optimisation analysis shows that the net present cost of System 3 is $ 598,474, and levelised cost of electricity of $ 0.111/kWh. The energy and exergy efficiencies of System 3 are 20.2% and 19.2%, respectively, with outputs of electricity, hot water, cooling and space heating. A performance assessment for identical conditions indicates that System 3 offers the best performance, with the minimum net present cost of $ 26,001 and levelised cost of electricity of $ 0.136/kWh.

Acknowledgement

I would like to express my deepest gratitude to my supervisor Professor Dr. Ibrahim Dincer and my co-supervisor Professor Dr. Marc A Rosen for their exemplary guidance, care and patience and for providing me with a remarkable atmosphere for research.

I would like to thank my colleagues at UOIT for their assistance especially the people in my research room ACE3030B who helped me during the preparation of this thesis, especially Canan Acar, Fahad Suleman, Sayantan Ghosh, Karanvir Singh Thind and Shahid Zaman.

Last but not the least; I would like to express my gratitude to my parents for their limitless support, fortitude, inspiration and reassurance throughout my life. This thesis is dedicated to my mother, father, brothers, and uncles.

Furthermore, the financial support from the Natural Sciences and Engineering Research Council of Canada (NSERC) is greatly acknowledged.

Table of Contents

List of Tables

List of Figures

Nomenclature

A	area (m^2)
$\dot{C}$	cost rate ($/h)
COP	coefficient of performance
D	diameter (m)
ex	specific exergy (kJ/kg)
$\dot{E}x$	exergy rate (kW)
h	specific enthalpy (kJ/kg)
HHV	higher heating value (kJ/kg)
$\dot{m}$	mass flow rate (kg/s)
P	pressure (kPa)
q	solar radiation flux (W/m^2)
$\dot{Q}$	heat transfer rate (kW)
R	renewability ratio
s	specific entropy (kJ/kg K)
T	temperature (^0C or K)
U	overall heat transfer coefficient (W/m^2K)
$\dot{V}$	velocity (m/s)
$\dot{W}$	work rate or power (kW)

Greek Letters

η	efficiency
ρ	density (kg/m^3)
Φ	exergy to energy ratio of the fuel
λ	stoichiometric constant in biomass combustion reaction (moles)
$\alpha, \beta, \delta, \gamma$	number of atoms of carbon, hydrogen, nitrogen and oxygen in biomass (atoms/molecule)

Subscripts

a	absorber
ac	absorption chiller
c	condenser

cc	combustion chamber
ch	chemical
cv	control volume
d	destruction
e	evaporator
en	energy
ex	exergy
ev	expansion valve
f	fuel
g	generator
gen	generation
gshp	ground source heat pump
p	pump
ph	physical
s	source
she	solution heat exchanger
sol	solar
sp	solution pump
0	dead state
1, 2,...	state numbers
tv	throttle valve
wt	wind turbine

Acronyms

C	Compressor
CSP	Concentrated Solar Panel
EES	Engineering Equation Solver
GT	Gas Turbine
GTC	Gas Turbine Cycle
HEX	Heat Exchanger
HPST	High Pressure Steam Turbine
HPT	High Pressure Turbine

LPST Low Pressure Steam Turbine

LPT Low Pressure Turbine

MC Mixing Chamber

ORC Organic Rankine Cycle

ORCT Organic Rankine Cycle Turbine

RC Rankine Cycle

Chapter 1: Introduction

1.1 Energy Demand and Challenges

Global demand for energy has been increasing day by day. In the past 50 years this demand has increased tremendously as shown in Fig.1.1. This increase in demand of energy causes immense pressure on the resources which produces energy resulting in their rapid depletion. As shown in Fig.1.2, most of this demand is met by the use of fossil fuels which lead to their faster depletion. The other problem with the use of fossil fuel is of the emissions that they produce resulting in environmental problems. As given in Table 1.1, CO_2 emissions by the fossil fuels reached maximum in the year 2012. With the gradual depletion of conveniently available fossil fuel reserves and their environmental problems, people are seeking other energy sources which are sustainable as well as environmentally benign, for instance renewable energy sources.

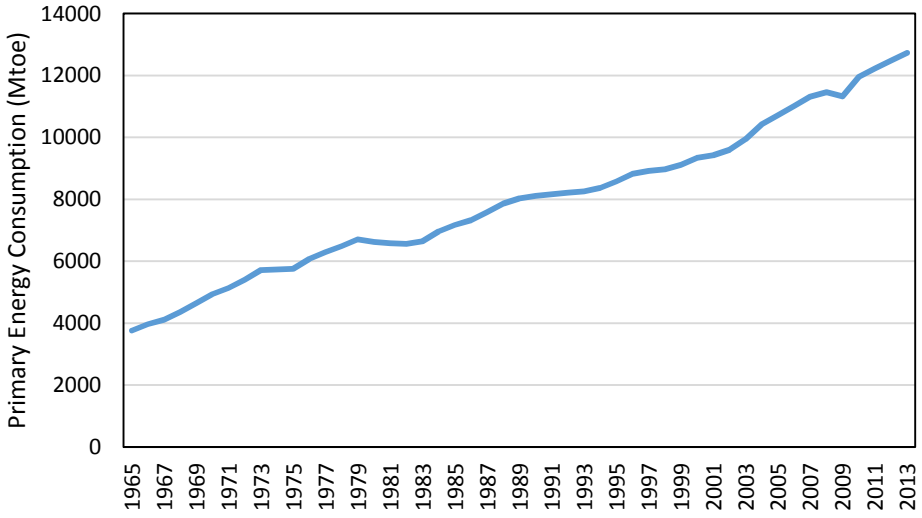

Fig. 1.1 Primary energy consumption of the world (Data from IEA, 2014).

Table 1.1 CO_2 emissions worldwide in 2012.

	Mtoe	%
Fossil Fuels	31575.33	99.50
Others	158.67	0.50
Total	31734	100.00

Source: (IEA, 2014).

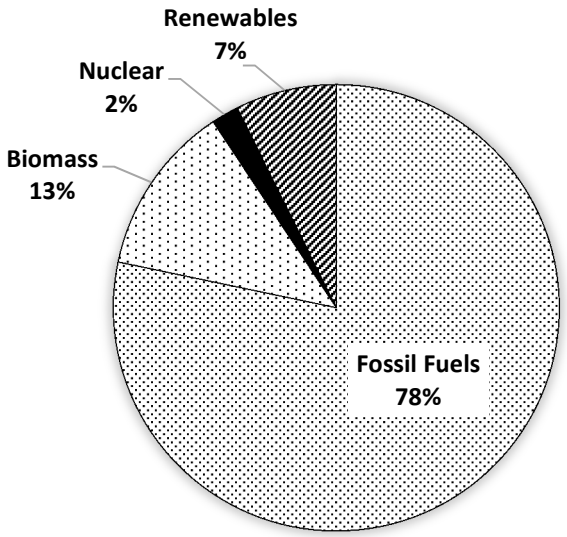

Fig. 1.2 Share of energy supply of the world by resources type in 2012 (Data from IEA, 2014).

1.2 Renewable as a Potential Source of Energy

As seen from Fig. 1.3a the energy produced by renewable energy is around 7% of the total energy in the year 2008 while there is a projection that this share could increase to around 22% in the year 2035 (Fig. 1.3b). These statistics clearly show that the use of renewable energy for the energy supply is a virtuous choice or the renewable energy sources have a great potential to meet the energy demand of the world in the upcoming years. Renewable energy are those sources of energy which are derived from natural processes and can be easily refilled. Currently, the leading and widely used renewable energy sources are solar, geothermal, wind, biomass and hydro (Cohce et al., 2011).

1.2.1 Solar

There are two ways of utilising solar energy into buildings. These are solar photovoltaic and solar thermal. A combination of these two is also available called as solar photovoltaic thermal. The photovoltaic directly converts solar energy to electricity. Its thermal part is utilised to heat water/organic fluid to change their phases to vapor which then expands in turbine to produces power which can be utilised for buildings.

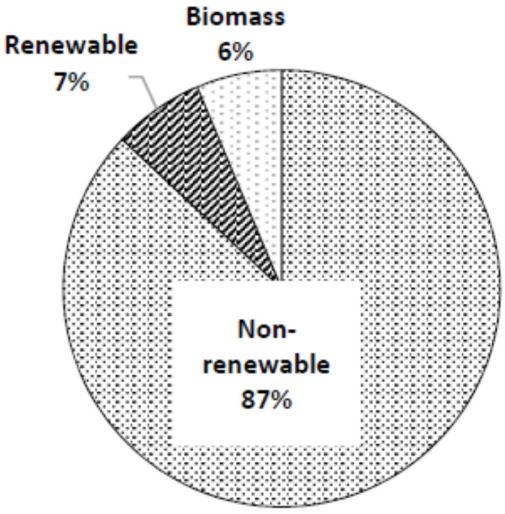

(a)

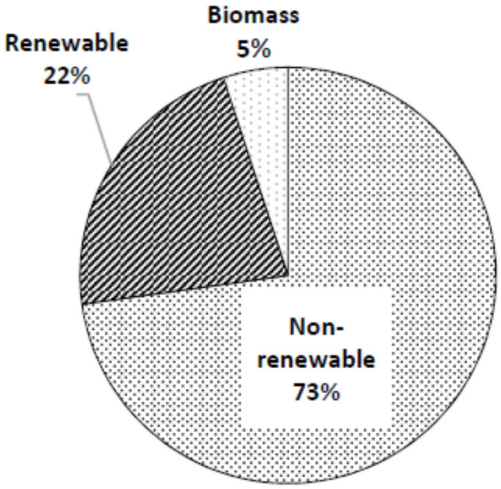

(b)

Fig 1.3 Primary energy share by resource type in (a) 2008 and (b) 2035 (Data from IEA, 2014).

1.2.2 Biomass

Biomass is mainly derived from living or dead matter present on earth (Cohce et al., 2011). There are various ways of utilising biomass in buildings. Some of them are listed as follows:

- Direct combustion: It is the most common technique used to produce electricity and power. In this technique, biomass is burned in a combustion chamber from where the hot combustion gases are expanded in the turbine to produce power. The exhaust gases can further be utilised for heating purposes.
- Gasification: In this technology, biomass is heated in absence of oxygen or in presence of partial oxygen. One of the useful products produced is syngas which can be utilised in heat engines to produce power and heat.
- Biogas: Biomass can be decayed and broken into elemental level with the help of microorganisms such as fungi, bacteria etc. resulting into biogas. This gas can be utilised for cooking and lighting in the house.

1.2.3 Geothermal

The word geothermal is derived from Greek words *geo* and *therme* which means earth and heat respectively. The total word signifies heat from earth. In this the earth energy is

utilised for power production or heat. There are generally three types of geothermal fields summarised as follows:

- Hot water fields: In these fields the water reservoirs are at around 60-80ºC best suited for space heating in the buildings. Their performance can be further enhanced by using the heat pump making it a ground source heat pump.
- Wet steam fields: In these types of fields, water reservoirs are around 100ºC and below atmospheric pressure. When this water is extracted to the earth surface, portion of it converts to steam. This steam can be utilised for producing power and space heating.
- Dry steam: These types of fields are quite similar to wet steam fields except the fact that the steam is at superheated state. These types of fields are generally uncommon in nature.

1.2.4 Wind

The extraction or obtaining power from the wind is a well-known technology nowadays. Power ranging from few watts to megawatts can be achieved or produced by using wind turbines. For example countries like India and China are increasing their power generation from wind progressively.

1.3 Renewable Energy Based Integrated Energy Systems

The drawbacks associated with these renewable energy sources are that the availability of a specific source depends upon the specific season and varies along the day. In order to overcome this problem, the integration of two or more renewable energy sources in the energy systems would be a good choice (Dagdougui et al., 2012). These integrated systems are found to be cost effective and reliable for the generation of energy. The advantage with these systems is that they reduce the energy storage necessities for providing stable operation (Deshmukh and Deshmukh, 2008). Table 1.2 shows the comparison between the renewable and conventional energy systems.

Table 1.2 Comparison of renewable and conventional energy systems.

	Renewable energy supplies	*Conventional energy supplies*
Examples	Solar, wind, biomass, tidal	Oil, natural gas, coal
Source	Local environment	Concentrated stock
Lifetime	Infinite	Finite
Cost at source	Free	Increasingly expensive
Location and use	Site and society specific	General and invariant use
Pollution	Very little	Intrinsic and common
Variation and control	Fluctuating	Steady

Source: (Twidell and Weir, 2006).

1.4 Renewable Energy Applications in Buildings

About 40% of the total energy produced in the world is consumed in the residential sectors of the developed countries (Dagdougui et al., 2012).

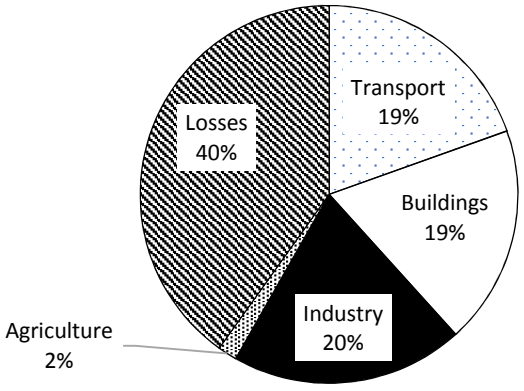

Fig. 1.4 The primary energy consumption share: sector wise in the year 2008 (Data from IEA, 2014).

Fig. 1.4 shows the primary energy consumption share by sector wise in the year 2008. It is clearly seen from the Fig. 1.4 that energy supply for the building is about 20% of the total energy consumption in the world which indicates the high energy requirements for buildings. This leads us to believe that the development of sustainable energy systems for buildings by using the renewable energy sources is crucial so that these buildings would have minimal impact on the environment. Fig. 1.5a shows the use of renewable energy i.e. about 9% in buildings in the year 2008 while it is predicted that this would increase to about 29% in the year 2035 (see Fig. 1.5b). The statistics clearly indicates that investment on the use of renewable energy sources in buildings is a worth.

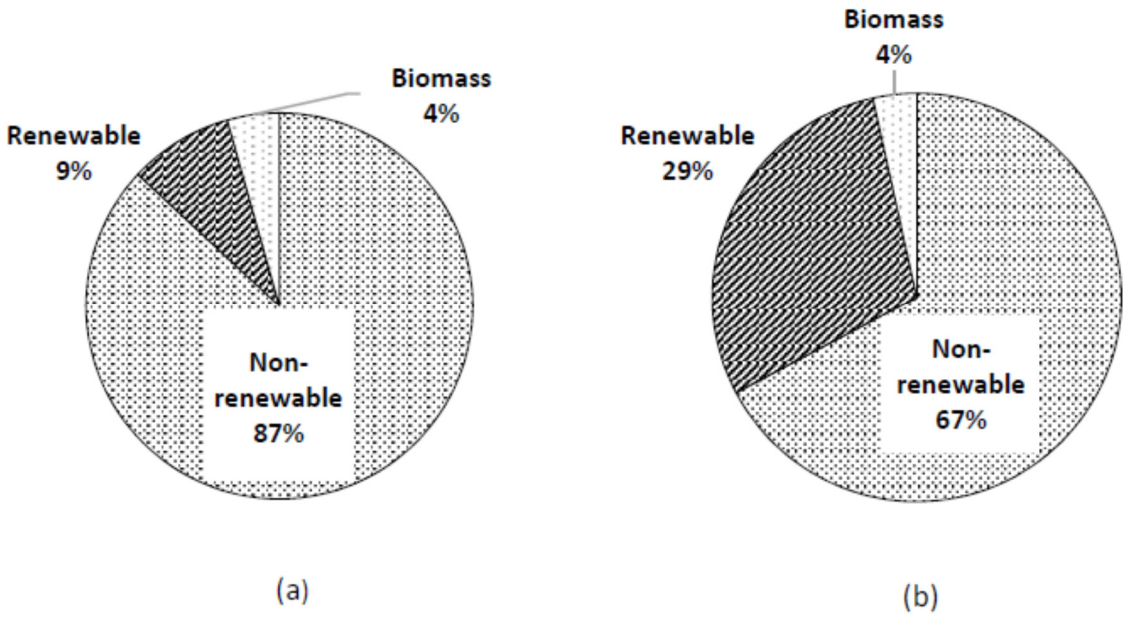

Fig.1. 5 Primary energy share in buildings: by resource type in (a) 2008 and (b) 2035 (Data from IEA, 2014).

1.5 Sustainable Energy Systems for Buildings

The other way to enhance the performance and to reduce the energy consumption in buildings is the use of multigeneration systems in place of single and cogeneration systems. Studies show that by using multigeneration the efficiency of the system can be enhanced further resulting in fewer emissions eventually leading to reduced impact on the environment.

Fig. 1.6 shows the sustainable energy systems for buildings based on the type of source, efficiency and the emissions. As the color changes from red to green it shows how the system becomes sustainable. The system with having red color is the least sustainable while the system having full green is the most sustainable. Dincer and Zamfirescu (2012) proposed that system would be greener or sustainable if it has better efficiency, better energy use and minimal environmental impact. Based on the above study an effort is made in this thesis to develop the sustainable energy systems for buildings that includes renewable energy resources as a source of energy and for better efficiency, multigeneration systems are proposed.

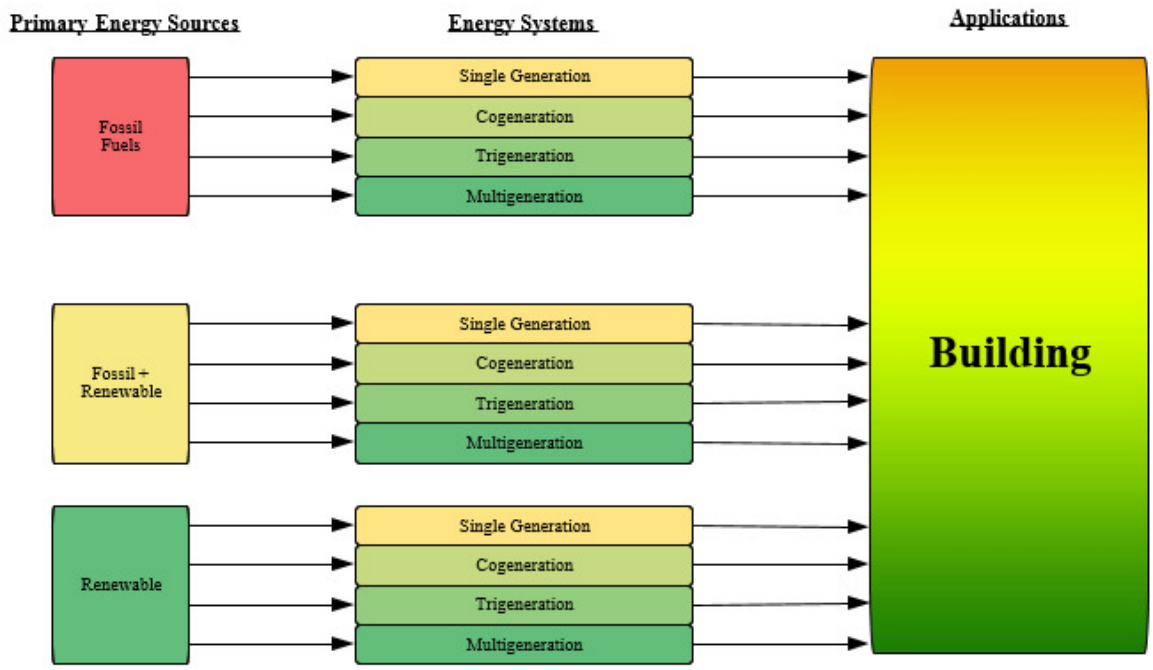

Fig. 1.6 Illustration of sustainable energy systems for buildings.

1.6 Motivation

The increase in the demand of energy for buildings, the environmental degradation and the increase in the living standard of individuals day by day drives me to find the solutions of these problems in a more sustainable manner. Therefore, the sustainable energy systems based on renewable energies become the main theme of this research. These energy systems need to be cost effective as well as efficient to meet all the requirement of the buildings. Thus, these buildings become grid independent and would generate the energy that would meet the requirements, if possible produce excessive energy which can be supplied to the grid.

1.7 Objectives

Most of the research in the literature focuses on the emissions from the energy systems for different applications in buildings, yet little focus is on the emissions from these applications. So, there is need to address this problem otherwise the proper objective of making the building sustainable would not be achieved to great extent. Thus in this study a detailed analysis of each component of the system is carried out by writing the balance equations and analysing them. To have a better insight, the exergy analysis is used with

the energy analysis. The analysis is carried out by putting all balance equations, energy and exergy efficiencies on the Engineering Equation Solver (EES) software. This software is a potential tool because of its large thermodynamic properties database of all the substances. To get the real data, a software called as HOMER is used. As HOMER's optimisation and sensitivity analysis allows evaluating the economic and technical feasibility of a large number of technology options and to account for variations in technology costs and energy resource types. In order to have a comprehensive view about the research, a parametric study is performed.

The specific objectives of this thesis study are listed as follows:

1. To develop the mathematical model for the new proposed systems, i.e., for multi-generation systems used for different applications, such as heating, cooling, electricity, hot water, etc. in buildings.
    - To write detailed thermodynamic balance equations for the proposed systems and their sub components, such as absorption chiller for cooling, heat exchangers, ground source heat pumps for heating.
    - To study energy and exergy efficiencies for the whole systems as well as for their components.
2. To perform a model validation study.
    - To develop the energy and exergy equations for each component and their codes and study in the EES.
    - To make more realistic analyses and simulations using actual data in the HOMER for various cases considered for the study.
3. To perform energy and exergy analyses of the newly developed systems.
    - To perform comprehensive energy and exergy analyses for each developed system.
    - To determine exergy losses and destructions for each developed system.
    - To study both energy and exergy efficiencies for a comparative assessment of each developed system.
    - To determine some dimensionless numbers, such as energetic renewable ratio and exergetic renewable ratio for the newly developed systems.

4. To perform enviroeconomic analyses for the newly developed systems.
    - To calculate the amount of CO_2 produced by each system.
5. To calculate the impose cost based on the amount of CO_2 produced by each system.
6. To perform a comprehensive parametric study and evaluation of the newly developed systems.
    - To do a comprehensive parametric study of each system separately to investigate the effects of design parameters on the system performance through energy and exergy efficiencies.
    - To investigate the effects of reference environment conditions on the performances of the overall systems and their subsystems.
7. To optimise the newly developed systems for better efficiency and cost.
    - To evaluate the optimized values for the proposed systems.

Chapter 2: Literature Review

Increase in energy consumption in buildings during the last decade has motivated the researchers to work in this area. In this section, the literature review for buildings is classified based on type of sources, systems, applications and products for buildings as follows:

2.1 Non-Renewable Energy Based Systems for Buildings

Li et al. (2012) developed a trigeneration system for electricity, heating and cooling using compressed air and thermal energy storage for a small office building in Chicago. In place of absorption chiller for cooling, direct expansion of compressed air is used. The system energy efficiency was approximately 50% in winter and it reduced to about 30% in summer due to more consumption of power in air compression process. Ebrahimi et al. (2012) presented a microsteam turbine system that produced combined cooling, heating, hot water and power for the residential building. Energy and exergy analyses were conduction and it was found that maximum exergy destruction takes place in the steam generator. Chen et al. (2014) presented the energy and exergy analyses of a trigeneration system working on vapor absorption cycle and Brayton cycles. Their analyses show that maximum destruction takes place in the combustor compared to all other components and the CO_2 emissions were reduced by a large percentage. Blieske et al. (2009) conducted the feasibility analysis of a system that produced heating, cooling and power for the residential purposes. The system used a gas turbine cycle and analyses show that the cost increased by 30%-40%., respectively. Toja-Silva and Rovira (2013) performed the energy and exergy analyses of a cogeneration system that produced heat and power for residential area. A gas turbine was used that ran on hydrogen and the exergy efficiency was found to be 45.7% and maximum exergy was destroyed in the combustion chamber.

2.2 Renewable Energy Based Systems for Buildings

Yang et al. (2014) studied the hybrid system for building that comprised of ground source heat pump and fuel cell. The main finding was that the hybrid system consumed less energy compared to the ground source system.

Beccali et al. (2008) studied the renewable energy based hydrogen system for residential buildings through energy and economic point of view. The analysis was conducted on a software called HOMER. The emissions of carbon dioxide and other pollutants were also found. Bingöl et al. (2011) performed the exergy based analysis of multi-generation systems for sustainable building. Two systems for multigeneration were considered and it was found that both the systems had better sustainability and green energy generation. Both systems exhibited more than 60% exergy efficiency and better energy savings. The primary energy savings (PES_R) for System 1 was calculated as 18.2% and 42.4% for System 2.

Calise et al. (2012) developed a novel polygeneration system for producing multiple outputs (electricity, space heating, cooling and domestic hot water). The system had Photovoltaic/Thermal (PVT) collector which provided electricity for building and heat to drive the absorption chiller. Energy and economic evaluation of the systems were done and it was found that a significant amount of energy could be saved and thus the system could be profitable from the economic point of view.

Ahmadi et al. (2013) performed the exergoeconomic and optimisation of a polygeneration system for the residential building. The main outputs were cooling, heating, power and hydrogen. An expression that related the exergy efficiency with the total cost of the system was also proposed. The main finding was that maximum destruction took place in heat recovery generator and on increasing the inlet pressure of turbine the exergy efficiency increased.

Hosseini et al. (2013) proposed a system for residential building that used solar PV and fuel cell to meet the heating and power demands. Analysis of the system was based on energy and exergy. The energy and exergy efficiency of the overall system was found to be 55.7% and 49.0% respectively. Ozgener (2010) proposed a geothermal heat pump that would assist with solar and wind turbine for a residential building. The results showed that the system was feasible from economic point of view if the location had good wind potential. Lubis et al. (2011) analysed a geothermal heat pump having a cooling tower as a heat rejecting device. The coefficient of performance evaluation and exergy analysis were conducted to assess the system. The main destruction of exergy in the system took

place in compressor and condenser. Caliskan et al. (2011) proposed a unique air cooling system for building. Comparison of the new system with the three other conventional system was done and it was found that the exergy efficiency of the new system was more compared to conventional systems. Their new system was also more sustainable compared to the conventional ones. Herrando et al. (2014) studied the system that comprised of photovoltaic and solar thermal collector for producing power and hot water in a building located in the United Kingdom. The results showed that the use of photovoltaic and solar thermal collector instead of photovoltaic reduced the emissions of carbon dioxide significantly resulting in better sustainability. Caliskan et al. (2013) studied the energy system for building including the energy storage option. The analysis of the system was done from thermoeconomic point of view, and it was found that as the cost of the system was more at higher ambient temperatures. It was also concluded that thermal energy system had the highest capital cost rate. Smith et al. (2013) studied system for different buildings including storage options. The study concluded that the system with energy storage options results in reduction in operation costs and carbon dioxide emissions. Ma et al. (2006) conducted the performance analysis of a hybrid system that comprised of a solar adsorption chiller and a compression heat pump. The system was designed for providing air conditioning to a building. The analysis showed that there was an increase of more than 40% in the performance if the proposed system was used in place of a conventional system.

Mammoli et al. (2010) evaluated the energetic, economic and environmental performance of a HVAC system which is assisted by solar energy. Roseik and Batlles (2013) considered different renewable energy options for cooling, heating and power in buildings, and found that solar absorption cooling, heating and power generation has the greatest energy saving potential. Zafar and Dincer (2014) presented the thermodynamic analysis of fuel cell and photovoltaic thermal collector for the generation of power, heat, fresh water and hydrogen for a residential building. The results show that when the heat from the fuel cell was consider to be as the useful output then the overall energy and exergy efficiencies of the system increased by 5.6% and 19.8% respectively.

2.3 Sustainable Assessment of Buildings

Mwasha et al. (2011) studied the performance of a residential building envelope and found that in order to have sustainable building, the sustainable assessment methods and energy performance indicator must be collaborated. Dincer and Rosen (2012) found that for the sustainable development the use of energy and the resource type must be assessed together.

Vučićević et al. (2014) assessed the sustainability of energy use in buildings and expressed the sustainability of building through sustainable index. Balta et al. (2010) assessed the performance and sustainability assessment of different energy options for buildings. Their main finding was that heating system based on solar had better sustainability compared to other three cases. Schmidt (2009) analysed the building on the basis of exergy used in the buildings. He found that the use of only energy analysis in the building calculation is insufficient. Hence, the concept of exergy analysis should be used. Sakulpipatsin et al. (2010) presented the application of exergy in analysing the residential buildings. They performed a detailed exergy analysis and calculated the emissions due to thermal sources and their effect on exergy efficiency.

Chapter 3: Description of Systems Studied

In this thesis, three sustainable energy systems for buildings are modeled and analysed based on energy and exergy analyses. The main goal of these systems is to produce multiple outputs such as electricity, cooling, heating and hot water without causing harm to the environment. The input source to all these systems is the combination of two or more renewable energy sources. The following chapter is divided into three subsections. Each subsection covers one system.

3.1 System 1

In System 1 two renewable sources (solar and biomass) are integrated to provide electricity, heating, cooling, and hot water for a building. Fig. 3.1 shows the schematic diagram of the multigeneration system consisting of concentrated solar collector and biomass powered gas turbine cycle. Overall, System 1 has a solar cycle, two organic Rankine cycles, one gas turbine cycle, and one vapor absorption cycle. Detailed descriptions of individual cycles have been summarised below.

- *Concentrated solar collector*

In this cycle, a concentrated solar collector is used to harvest the radiation from the sun. At state 33, Duratherm oil enters the collector and after being heated, leaves at state 12. The oil then enters the heat exchanger which also acts as a storage tank and utilised in heating the isopentane that enters the storage tank at state 12 to provide the energy requirement of organic Rankine cycle 1. The oil then goes to the heat exchanger which is used to heat stream 23 (isopentane) to stream 19 to preheat the stream to be used in organic Rankine cycle 2. Finally, the oil is sent back to the solar collector.

- *Organic Rankine Cycle*

In System 1, there are two organic Rankine cycles. The first ORC is supported only by solar energy while the second ORC is driven by both solar and biomass, depending on the availability. In total, there are two turbines, three heat exchangers, two pumps, and two condensers. More detailed description of each cycle can be summarised as:

Organic Rankine Cycle 1: Stream 16 (isopentane) enters the storage tank where it is heated at high pressure to be expanded in the ORCT 1 to generate electricity in this cycle. After leaving the turbine, stream 14 is sent to a condenser in which the rejected heat is used to provide heating for the community. After the condenser, stream 15 is pumped and sent back to heat exchanger/storage tank in order to be heated by the oil from the solar cycle.

Organic Rankine Cycle 2: ORC 1 and ORC work in similar fashion. In addition to the listed components in ORC 1, an additional heat exchanger is used in ORC 2 to harvest additional heat requirement for the ORCT 2. This heat is supplied by the biomass gas turbine cycle.

- *Gas Turbine Cycle*

In this cycle, atmospheric air enters to compressor and the resulting compressed air enters the combustion chamber where it mixes with biomass and burns to produce high temperature combustion gases. These highly pressurised gases pass through the gas turbine to produce power. The exhaust gases from gas turbine are used to provide the additional heat requirements of ORC 2. After leaving the heat exchanger, stream 30 is further utilised to provide heat for the generator in vapor absorption cycle.

- *Vapor absorption chiller*

Heat is transferred from the hot air at state 30 to the generator of the vapor absorption chiller and the air leaves the generator at state 31. After receiving the heat, a portion of the water in the generator is evaporated and enters the condenser. There, the water vapors are cooled and condensed using a cooling source, and throttled in an expansion valve. The water temperature drops as it enters the evaporator. After absorbing the cooling load in evaporator, the water is vaporized and enters the absorber, where it mixes with the lean mixture of LiBr–H_2O coming from the generator through a heat exchanger and expansion valve, and is converted to a rich mixture of LiBr–H_2O. Then, the mixture from the absorber is pumped to the generator through a solution heat exchanger. The evaporator in vapor absorption chiller also provides cooling for the community.

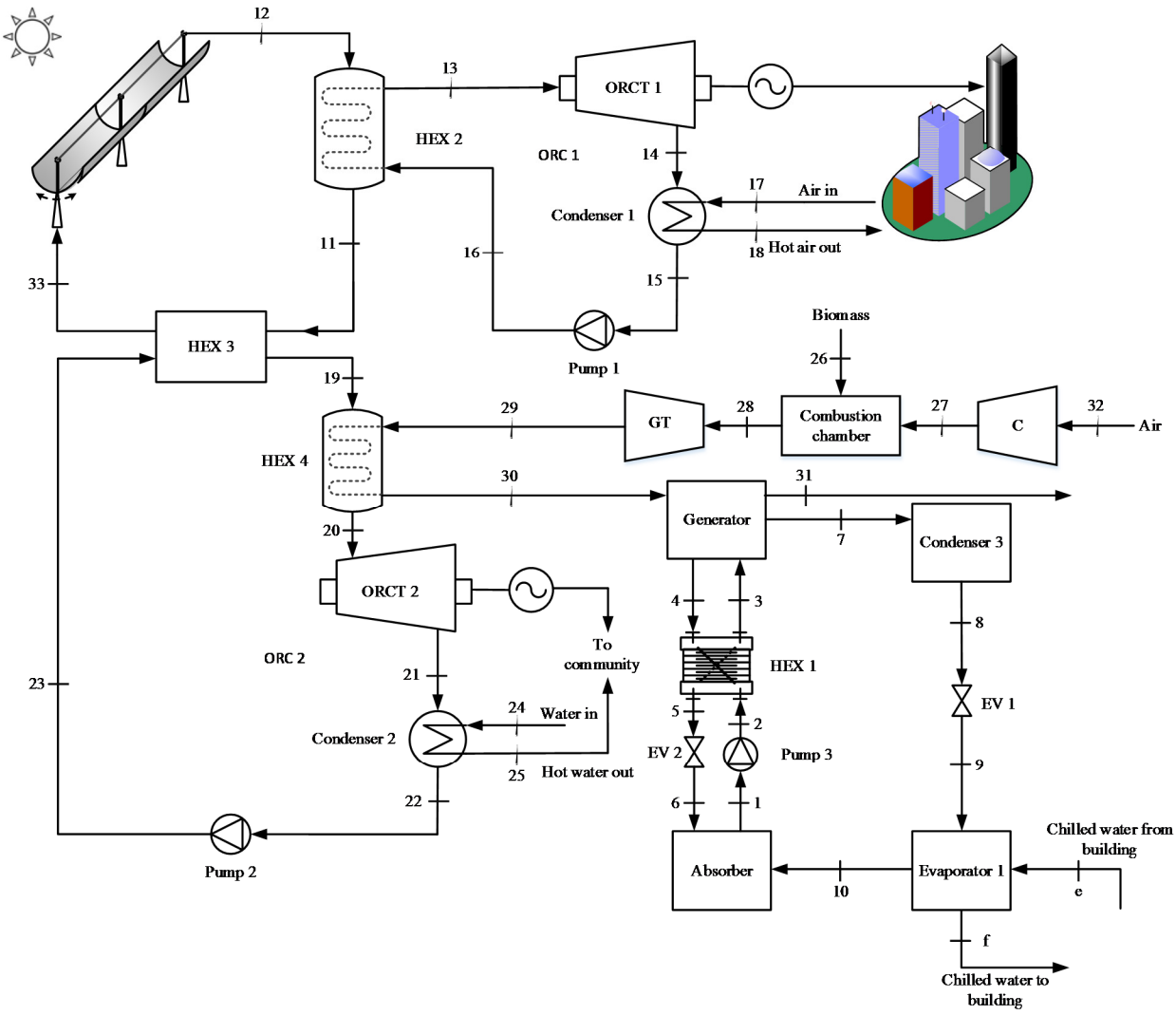

Fig. 3.1 Schematic illustration of System 1 (integrated solar-biomass multigeneration system).

3.2 System 2

A multigeneration system using solar, wind and ground source energy for producing electricity, hot water, heating and cooling is consider for a building. Fig. 3.2 shows the schematic diagram of a multigeneration system consisting of wind turbine, concentrated solar panel and ground source heat pump.

The system has following subsections:

- *Wind turbine system*

The electricity produce by wind turbine is used to meet the electricity requirement of the building. If there is any excess electricity produced by wind turbine then it is converted to heat and store in the form of hot water in the storage tank.

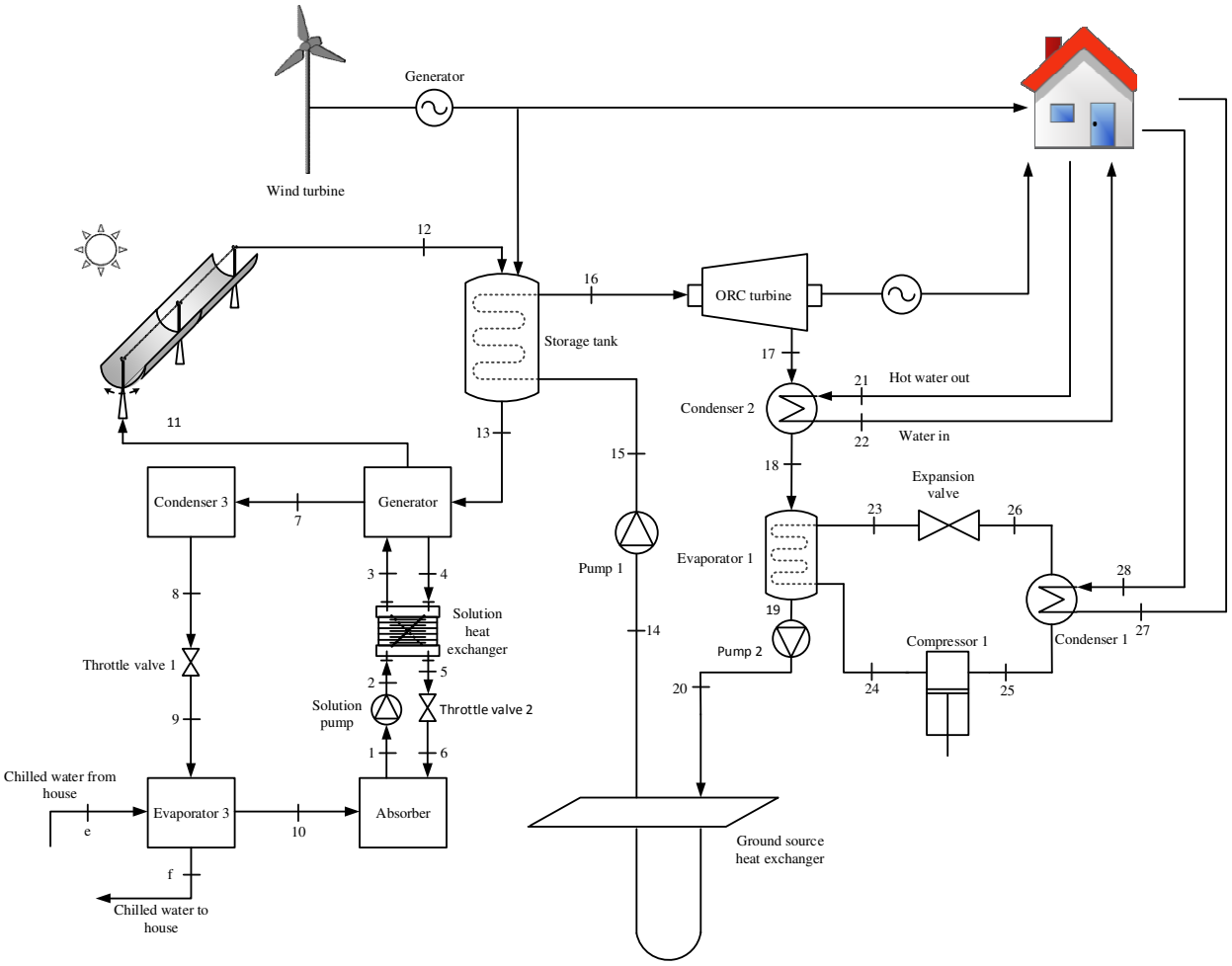

Fig. 3.2 Schematic illustration of System 2 (integrated solar-wind multigeneration system).

- *Concentrated solar collector*

The radiation from the sun falls on a concentrated solar collector and the Duratherm oil at state 11 enters the collector, after being heated, exits the collector at state 12. The oil then enters heat exchanger 2, which also acts as a storage tank and utilised in heating the isopentane that enters the storage tank at state 15. The oil then goes to the generator of vapor absorption chiller and then pumped back to the solar collector.

- *Vapor absorption chiller*

Heat is transferred from the hot oil at state 13 to the generator of the vapor absorption chiller and the oil leaves the generator at state 11 and is pumped back again to the solar collector. After receiving the heat, a portion of the water in the generator is evaporated and enters the condenser. There, the water vapor is cooled and condensed using a cooling source, and throttled in an expansion valve. The water temperature drops as it enters the evaporator. After absorbing the cooling load in evaporator, the water is vaporized and enters the absorber, where it mixes with the lean mixture of $LiBr - H_2O$ coming from the generator through a heat exchanger and expansion valve, and is converted to a rich mixture of $LiBr - H_2O$. The mixture from the absorber is then pumped to the generator through a solution heat exchanger.

- *Ground source heat pump*

As we know that ground has enormous amount of energy which can be utilised for producing useful output. In this case the ground energy is utilised by using isopentane (an organic fluid).The ground supplies the energy to the isopentane and which after getting heated enters the storage tank at state 14 where it get further heated. After leaving the storage tank the isopentane at state 16 goes to the ORC turbine where it gets expand and the power is produce. The exhaust of the ORC turbine at state 17 is get condensed in the condenser 2 .The condensed isopentane at state 18 goes to the evaporator 1 where it impart heat. After heating the evaporator 1 the isopentane at state 19 is pump back to the ground through pump 2. The refrigerant at state 24 enters into the compressor 1 as a vapor and is compressed to the condenser pressure. The compressed refrigerant enters the condenser at state 25 and is condensed by releasing heat (used for hot water). Then, the refrigerant enters the expansion valve at state 26, where its temperature drops due to the throttling effect. The low-temperature refrigerant enters the evaporator at state 23, where it is evaporated by absorbing the heat from the isopentane coming from the condenser at state 18. The cycle is then completed as refrigerant leaves the condenser and re-enters the compressor at state 24. The compressor of the heat pump is driven by part of the electricity generated by the wind turbine.

4.3 System 3

System 3 represents an integrated solar-geothermal multigeneration system to provide electricity, hot water, heating, and cooling for a community. Fig. 3.3 shows the schematic diagram of a multigeneration system consisting of a concentrated solar power, geothermal source, three Rankine cycles, and a vapor absorption chiller. The system has following subsections:

- *Concentrated solar collector*

The radiation from the sun falls on a concentrated solar collector and the Duratherm oil at state 13 enters the collector, after being heated, exits the collector at state 14. The oil then enters the heat exchanger 2, which also acts as a storage tank and utilised in heating the water that enters the storage tank at state 20 to provide the energy requirement of Rankine cycle 1. The oil is then goes to the heat exchanger 3 which is used to heat stream 35 (water) to stream 23 to support the high pressure stream turbine in Rankine cycle 2. Last, the oil is sent to the generator of vapor absorption chiller and then pumped back to the solar collector.

- *Vapor absorption chiller*

Heat is transferred from the hot oil at state 16 to the generator of the vapor absorption chiller and the oil leaves the generator at state 11 and is pumped back again to the solar collector. After receiving the heat, a portion of the water in the generator is evaporated and enters the condenser. There, the water vapor is cooled and condensed using a cooling source, and throttled in an expansion valve. The water temperature drops as it enters the evaporator. After absorbing the cooling load in evaporator, the water is vaporized and enters the absorber, where it mixes with the lean mixture of LiBr–H_2O coming from the generator through a heat exchanger and expansion valve, and is converted to a rich mixture of LiBr–H_2O. Then, the mixture from the absorber is pumped to the generator through a solution heat exchanger. The evaporator in vapor absorption chiller also provides cooling for the community.

- *Rankine Cycles*

In System 3, there are three Rankine cycle-based systems. Two of these cycles are supplied by solar and one of them is provided by geothermal energy. In total, there are four turbines (three high pressure turbines and one low pressure), two heat exchangers, two pumps, three condensers, two separators, two flash chambers, and a mixing chamber in these cycles. More detailed description of each cycle can be summarized as:

Rankine Cycle 1: Stream 17 (water) enters the high pressure turbine 1 to generate electricity in this cycle. After leaving the turbine, stream 18 is sent to a condenser in which the rejected heat is used to provide heating for the community. After the condenser, stream 19 is pumped and sent back to heat exchanger 2 in order to be heated by the oil from solar cycle.

Rankine Cycle 2: Heat exchanger 3 of solar cycle provides heating for stream 35 in this cycle. The stream leaving the heat exchanger 3 (23) is sent to high pressure turbine 2 to produce electricity. After the turbine, stream 24 is sent to a condenser, which provides hot water for the community. The stream leaving condenser is directed to the reinjection well.

Rankine Cycle 3: Unlike Rankine cycles 1 and 2 which are supported by solar cycle, this cycle uses geothermal as its energy source. The stream from geothermal production well (29) is sent to a flash chamber which is then separated in two streams (31 and 36). Stream 31 (vapor) enters the high pressure steam turbine 3 and then the mixing chamber. Stream 36 (liquid) is further separated and the liquid portion is directly sent to the reinjection well. The vapor from the second separator is sent to a low pressure turbine, where the exit stream is send to the mixing chamber along with stream 32. The outlet of the mixing chamber is condensed and pumped to heat exchanger 3 in order to be heated by solar cycle and used in high pressure turbine 2.

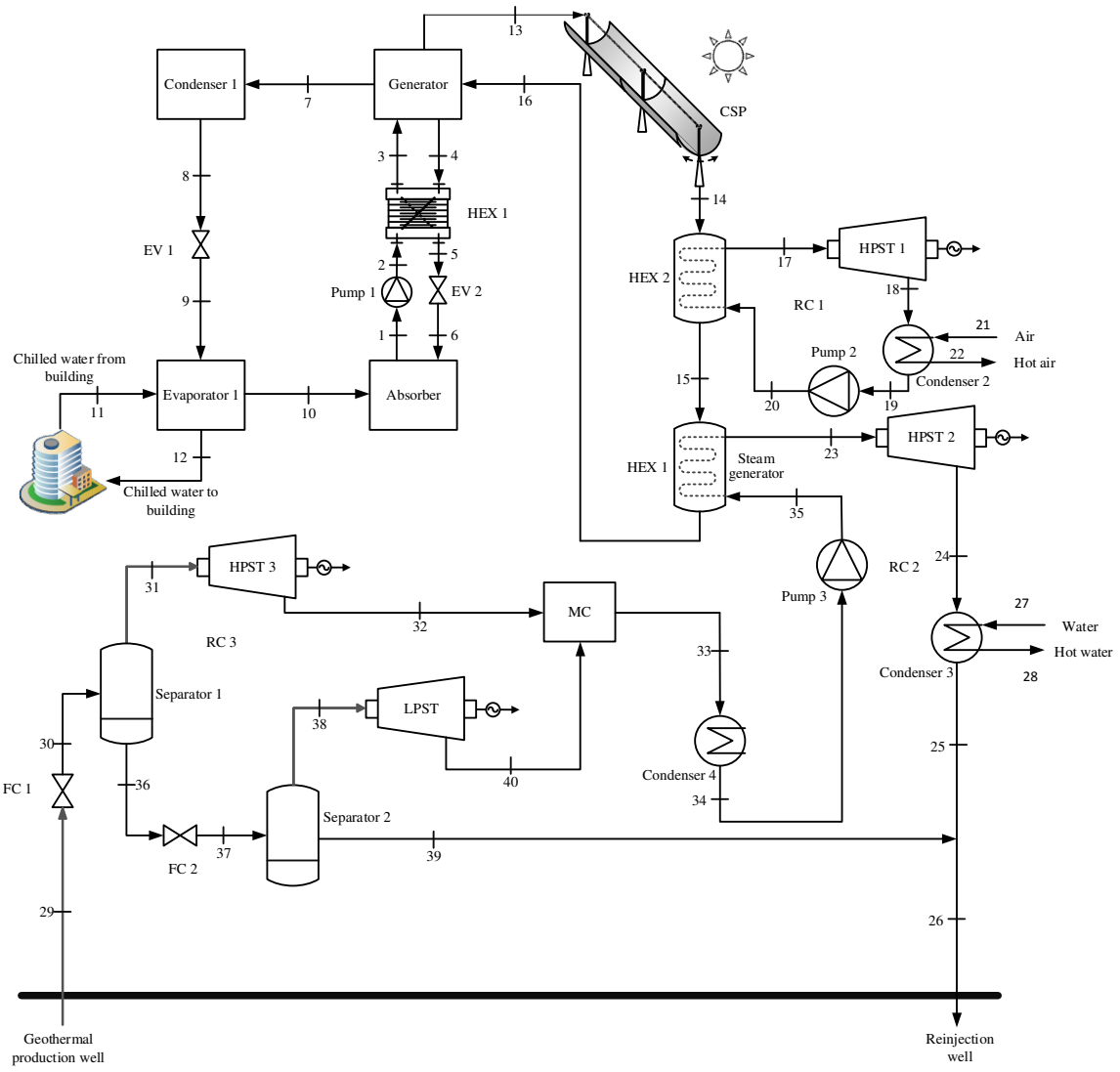

Fig. 3.3 Schematic illustration of System 3 (integrated solar-geothermal multigeneration system).

Chapter 4: Model Development and Analyses

In this chapter introduction about the thermodynamic principle to exergy and economics analyses are presented.

4.1 Thermodynamic Analysis

The detailed thermodynamic analyses are conducted to study mass, energy, entropy and exergy balance equations for each system and its components as presented in the following sections.

4.1.1 Mass Balance Equation

According to conservation of mass principle one can write the mass balance for the control volume as follows:

$$\sum_i \dot{m}_i - \sum_e \dot{m}_e = \frac{dm_{cv}}{dt} \tag{4.1}$$

where $\dot{m}$ and m represent the mass flow rate and mass, respectively and the subscripts i and e refers to the inlet and exit of the control volume, respectively while cv represent the control volume.

4.1.2 Energy Balance Equation

According to first law of thermodynamics the detailed energy balance equation for the control volume can be written as follows:

$$\dot{Q} - \dot{W} + \sum_i \dot{m}_i\left(h_i + \frac{V_i^2}{2} + gZ_i\right) - \sum_e \dot{m}_e\left(h_e + \frac{V_e^2}{2} + gZ_e\right) = \frac{dE_{cv}}{dt} \tag{4.2}$$

where $\dot{Q}, \dot{W}$, E and t are the heat transfer rate, work rate, energy and time, respectively while symbols h, V, g and Z stand for specific enthalpy, velocity, acceleration of gravity and elevation, respectively.

4.1.3 Entropy Balance Equation

The entropy that is generated within the process is called entropy generation denoted by S_{gen}. In Bejan (2002), the entropy generation rate over a control volume is given as

$$\dot{S}_{gen} = \frac{dS_{cv}}{dt} + \sum_i \dot{m}_e s_e - \sum_i \dot{m}_i s_i - \sum_k \frac{\dot{Q}_k}{T_k} \quad (4.3)$$

4.1.4 Exergy Balance Equation

Exergy analysis involves the concept of both first law and second laws of thermodynamics. The detailed provide by exergy analysis is valuable for understanding the details of the overall system. It would be useful in providing the guidelines and strategies for more efficient and effective use of energy and utilise it for various thermodynamic processes such as power generation, refrigeration etc. Basically the exergy consist of four substance, physical and chemical exergy are the most commonly and widely used as the other two kinetic and exergy terms are assumed to be neglected as there are very little change in velocity and elevation (Ameri et al., 2009, Dincer and Rosen, 2012, Ahmadi et al., 2013a). The physical exergy is defined as the maximum work that is obtained when the system interacts with environment which is in mechanical and thermal equilibrium. The chemical exergy is considered when the system is not in chemical equilibrium with the environment like in the case of combustion chamber and the processes where chemical change take place (Bejan et al., 1995). According to second law of thermodynamics the exergy balance for a control volume can be written as

$$\dot{E}x^Q + \sum_i \dot{m}_i ex_i = \sum_e \dot{m}_e ex_e + \dot{E}x_W + \dot{E}x_d \quad (4.4)$$

where i and e denotes the inlet and exit of the control volume, respectively while the exergy destruction is denoted by $\dot{E}x_d$ and the other terms are as follows:

$$\dot{E}x^Q = \dot{Q}_i \left(1 - \frac{T_0}{T_i}\right) \quad (4.5)$$

$$\dot{E}x_W = \dot{W} \quad (4.6)$$

$$ex = ex_{ph} + ex_{ch} \quad (4.7)$$

The physical exergy, ex_{ph} can be calculated as follows:

$$ex_{ph} = h - h_0 - T_0(s - s_0) \quad (4.8)$$

4.1.5 Dimensionless Parameters

There are some dimensional parameters to analyse the system based on renewable energy and exergy parameters namely energetic and exergetic renewability ratios.

- Energetic renewability ratio: According to Coskun et al. (2009) it is defined as the ratio of useful renewable energy to the total energy used by the system. The total energy used by the system includes both renewable and non-renewable energies.

$$R_{Ren_{en}} = \frac{\dot{En}_{useful}}{\dot{En}_{total}} \tag{4.9}$$

- Exergetic renewability ratio: According to Coskun et al. (2009) it is defined as the ratio of useful renewable exergy to the total exergy used by the system. The total exergy used by the system includes both renewable and non-renewable exergies.

$$R_{Ren_{ex}} = \frac{\dot{Ex}_{useful}}{\dot{Ex}_{total}} \tag{4.10}$$

4.2 Exergoeconomic Analysis

Economic analysis based on thermodynamics is called as thermoeconomics. It includes the cost of thermal systems considering capital and their running cost. The principle of exergy is generally utilised in determining the costs to the products as given by Dincer and Rosen (2012):

$$\dot{C}_{q,k} + \sum_i \dot{C}_{i,k} + \dot{Z}_k = \sum_e \dot{C}_{e,k} + \dot{C}_{w,k} \tag{4.11}$$

$$\dot{Z} = \frac{Z_k CRF \emptyset}{N*3600} \tag{4.12}$$

where Z_k is the purchase cost of the k^{th} component, and CRF is the capital recovery factor.

4.3 Exergoenvironmental Analysis

The main idea behind this thesis is to develop novel systems which produce no emissions or pollutants. The use of renewable energy in all the systems and having 100% renewable fraction results in no/reduced emissions. If there are any emissions by the systems, there

is a need to define a cost, based on the amount of CO_2 production, which results in an increase in the total cost of the system.

4.4 Optimisation

In this thesis the optimisation technique called as genetic algorithm is used to evaluate the best operating condition and to maximise the exergy efficiency. The genetic algorithms are the class of search techniques that primarily constructed on the biological procedure of growth. The genetic algorithm is based on the following four steps (Stender, 1993):

1. A string of population is created.
2. Each string is then evaluated based on the performance.
3. The best string is then survived based on the performance.
4. The manipulation is then carried out to create the new strings.

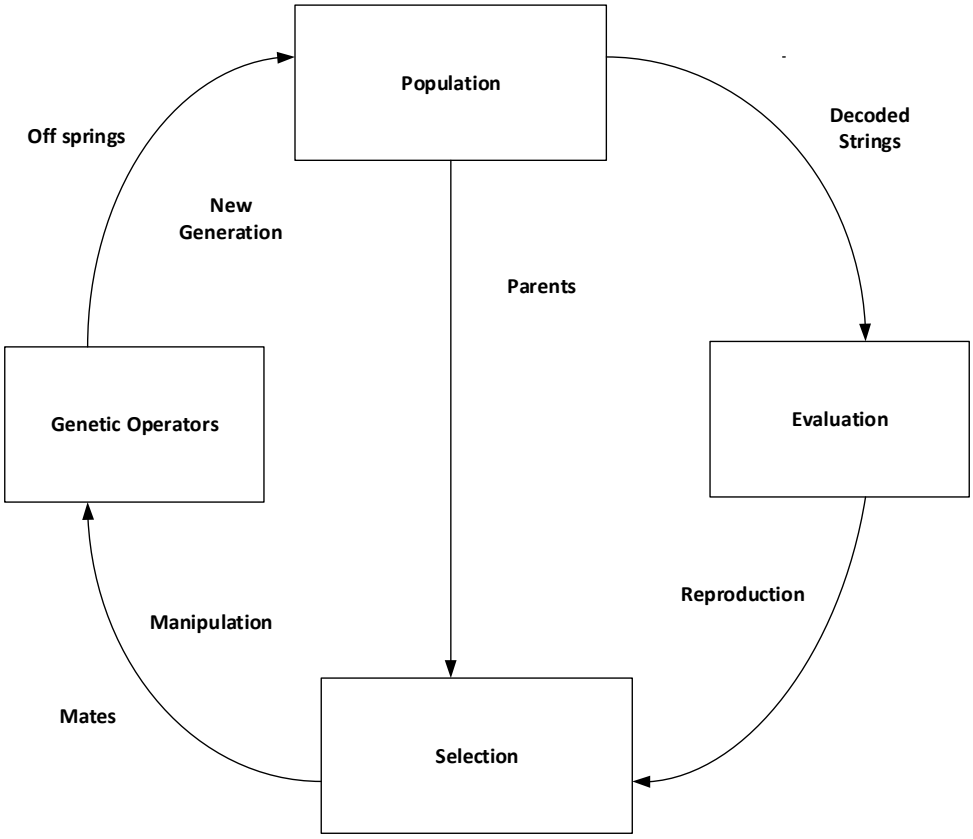

Fig. 4.1 Genetic algorithm cycle Adapted from (Stender, 1993).

4.5 Analyses of System 1

In this section, the thermodynamic analysis for System 1 is presented as follows:

4.5.1 Thermodynamic Analysis of System 1

Energy and exergy analyses are performed for the proposed system (see Fig. 3.1), in order to provide the information about its performances, efficiencies and emissions. The reference-environment state is specified as having a temperature $T_0 = 25\ ℃$ and a pressure $P_0 = 100\ \text{kPa}$.

The following assumptions are made for the analyses:

- The changes in kinetic and potential energy and exergy are negligible.
- The compressor and pumps are adiabatic.
- The isentropic efficiencies of the pumps and compressor are 85% (Srinivas et al., 2007).
- The pressure losses in all heat exchangers and pipelines are negligible.

4.5.1.1 Balance Equations

The balance equations for mass, energy, entropy and exergy are written for the components in System 1 as follows:

- *Concentrated Solar Panel (CSP)*

The mass balance for the concentrated solar panel can be written as follows:

$$\dot{m}_{33} = \dot{m}_{12} \tag{4.13}$$

The energy balance for the concentrated solar panel can be written as follows:

$$\dot{m}_{33}h_{33} + \dot{Q}_{sol} = \dot{m}_{12}h_{12} + \dot{Q}_{loss,csp} \tag{4.14}$$

The entropy balance for the concentrated solar panel can be written as follows:

$$\dot{m}_{33}s_{33} + \frac{\dot{Q}_{sol}}{T_0} + \dot{S}_{gen,csp} = \dot{m}_{12}s_{12} + \frac{\dot{Q}_{loss,csp}}{T_0} \tag{4.15}$$

The exergy balance for the concentrated solar panel can be written as follows:

$$\dot{m}_{33}ex_{33} + \dot{Q}_{sol}\left(1 - \frac{T_0}{T_s}\right) = \dot{m}_{12}ex_{12} + \dot{Q}_{loss,csp}\left(1 - \frac{T_0}{T_s}\right) + \dot{E}x_{d,csp} \quad (4.16)$$

Organic Rankine Cycle 1

- *Heat Exchanger 2*

The mass balance equation for HEX 2 can be written as follows:

For oil: $\dot{m}_{12} = \dot{m}_{11}$ (4.17)

For isopentane: $\dot{m}_{16} = \dot{m}_{13}$ (4.18)

The energy balance equation for HEX 2 can be written as follows:

$$\dot{m}_{12}h_{12} + \dot{m}_{16}h_{16} = \dot{m}_{11}h_{11} + \dot{m}_{13}h_{13} \quad (4.19)$$

The entropy balance equation for HEX 2 can be written as follows:

$$\dot{m}_{12}s_{12} + \dot{m}_{16}s_{16} + \dot{S}_{gen,HEX2} = \dot{m}_{11}s_{11} + \dot{m}_{13}s_{13} \quad (4.20)$$

The exergy balance equation for HEX 2 can be written as follows:

$$\dot{m}_{12}ex_{12} + \dot{m}_{16}ex_{16} = \dot{m}_{11}ex_{11} + \dot{m}_{13}ex_{13} + \dot{E}x_{d,HEX2} \quad (4.21)$$

- *Heat Exchanger 4*

The mass balance equation for HEX 4 can be written as follows:

For flue gases: $\dot{m}_{19} = \dot{m}_{20}$ (4.22)

For isopentane: $\dot{m}_{29} = \dot{m}_{30}$ (4.23)

The energy balance equation for HEX 4 can be written as follows:

$$\dot{m}_{19}h_{19} + \dot{m}_{29}h_{29} = \dot{m}_{20}h_{20} + \dot{m}_{30}h_{30} \quad (4.24)$$

The entropy balance equation for HEX 4 can be written as follows:

$$\dot{m}_{19}s_{19} + \dot{m}_{29}s_{29} + \dot{S}_{gen,HEX4} = \dot{m}_{20}s_{20} + \dot{m}_{30}s_{30} \quad (4.25)$$

The exergy balance equation for HEX 4 can be written as follows:

$$\dot{m}_{19}ex_{19} + \dot{m}_{29}ex_{29} = \dot{m}_{20}ex_{20} + \dot{m}_{30}ex_{30} + \dot{E}x_{d,HEX4} \quad (4.26)$$

- *For ORC Turbine 1*

The mass balance equation for ORC turbine 1 can be written as follows:

$$\dot{m}_{13} = \dot{m}_{14} \tag{4.27}$$

The energy balance equation for ORC turbine 1 can be written as follows:

$$\dot{m}_{13}h_{13} = \dot{m}_{14}h_{14} + \dot{W}_{ORCT1} \tag{4.28}$$

The entropy balance equation for ORC turbine 1 can be written as follows:

$$\dot{m}_{13}s_{13} + \dot{S}_{gen,ORCT1} = \dot{m}_{14}s_{14} \tag{4.29}$$

The exergy balance equation for ORC turbine 1 can be written as follows:

$$\dot{m}_{13}ex_{13} = \dot{m}_{14}ex_{14} + \dot{W}_{ORCT1} + \dot{E}x_{d,ORCT1} \tag{4.30}$$

- *Condenser 1*

The mass balance equation for condenser 1 can be written as follows:

For isopentane: $\dot{m}_{14} = \dot{m}_{15}$ (4.31)

For air: $\dot{m}_{17} = \dot{m}_{18}$ (4.32)

The energy balance equation for condenser 1 can be written as follows:

$$\dot{m}_{14}h_{14} + \dot{m}_{15}h_{15} = \dot{m}_{15}h_{15} + \dot{m}_{18}h_{18} \tag{4.33}$$

The entropy balance equation for condenser 1 can be written as follows:

$$\dot{m}_{14}s_{14} + \dot{m}_{15}s_{15} + \dot{S}_{gen,c1} = \dot{m}_{15}s_{15} + \dot{m}_{18}s_{18} \tag{4.34}$$

The exergy balance equation for condenser 1 can be written as follows:

$$\dot{m}_{14}ex_{14} + \dot{m}_{17}ex_{17} = \dot{m}_{15}ex_{15} + \dot{m}_{18}ex_{18} + \dot{E}x_{d,c1} \tag{4.35}$$

- *Pump 1*

The mass balance equation for pump 1 can be written as follows:

$$\dot{m}_{15} = \dot{m}_{16} \tag{4.36}$$

The energy balance equation for pump 1 can be written as follows:

$$\dot{m}_{15}h_{15} + \dot{W}_{P1} = \dot{m}_{16}h_{16} \tag{4.37}$$

The entropy balance equation for pump 1 can be written as follows:

$$\dot{m}_{15}s_{15} + \dot{S}_{gen,P1} = \dot{m}_{16}s_{16} \quad (4.38)$$

The exergy balance equation for pump 1 can be written as follows:

$$\dot{m}_{15}ex_{15} + \dot{W}_{P1} = \dot{m}_{16}ex_{16} + \dot{E}x_{d,P1} \quad (4.39)$$

- *Heat Exchanger 3*

The mass balance equation for HEX 3 can be written as follows:

For oil: $\dot{m}_{11} = \dot{m}_{33}$ (4.40)

For isopentane: $\dot{m}_{23} = \dot{m}_{19}$ (4.41)

The energy balance equation for HEX 3 can be written as follows:

$$\dot{m}_{11}h_{11} + \dot{m}_{23}h_{23} = \dot{m}_{33}h_{33} + \dot{m}_{19}h_{19} \quad (4.42)$$

The entropy balance equation for HEX 3 can be written as follows:

$$\dot{m}_{11}s_{11} + \dot{m}_{23}s_{23} + \dot{S}_{gen,HEX3} = \dot{m}_{33}s_{33} + \dot{m}_{19}s_{19} \quad (4.43)$$

The exergy balance equation for HEX 3 can be written as follows:

$$\dot{m}_{11}ex_{11} + \dot{m}_{23}ex_{23} = \dot{m}_{33}ex_{33} + \dot{m}_{19}ex_{19} + \dot{E}x_{d,HEX3} \quad (4.44)$$

Organic Rankine Cycle 2

- *For ORC turbine 2*

The mass balance equation for ORC turbine 2 can be written as follows:

$$\dot{m}_{20} = \dot{m}_{21} \quad (4.45)$$

The energy balance equation for ORC turbine 2 can be written as follows:

$$\dot{m}_{20}h_{20} = \dot{m}_{21}h_{21} + \dot{W}_{ORCT2} \quad (4.46)$$

The entropy balance equation for ORC turbine 2 can be written as follows:

$$\dot{m}_{20}s_{20} + \dot{S}_{gen,ORCT2} = \dot{m}_{21}s_{21} \quad (4.47)$$

The exergy balance equation for ORC turbine 2 can be written as follows:

$$\dot{m}_{20}ex_{20} = \dot{m}_{21}ex_{21} + \dot{W}_{ORCT2} + \dot{E}x_{d,ORCT2} \quad (4.48)$$

- *Condenser 1*

The mass balance equation for condenser 2 can be written as follows:

For isopentane: $\dot{m}_{21} = \dot{m}_{22}$ (4.49)

For water: $\dot{m}_{24} = \dot{m}_{25}$ (4.50)

The energy balance equation for condenser 2 can be written as follows:

$$\dot{m}_{21}h_{21} + \dot{m}_{24}h_{24} = \dot{m}_{22}h_{22} + \dot{m}_{25}h_{25} \quad (4.51)$$

The entropy balance equation for condenser 2 can be written as follows:

$$\dot{m}_{21}s_{21} + \dot{m}_{24}s_{24} + \dot{S}_{gen,c2} = \dot{m}_{22}s_{22} + \dot{m}_{25}s_{25} \quad (4.52)$$

The exergy balance equation for condenser 2 can be written as follows:

$$\dot{m}_{21}ex_{21} + \dot{m}_{24}ex_{24} = \dot{m}_{22}ex_{22} + \dot{m}_{25}ex_{25} + \dot{E}x_{d,c2} \quad (4.53)$$

- *Pump 2*

The mass balance equation for pump 2 can be written as follows:

$$\dot{m}_{22} = \dot{m}_{23} \quad (4.54)$$

The energy balance equation for pump 2 can be written as follows:

$$\dot{m}_{22}h_{22} + \dot{W}_{P2} = \dot{m}_{23}h_{23} \quad (4.55)$$

The entropy balance equation for pump 2 can be written as follows:

$$\dot{m}_{22}s_{22} + \dot{S}_{gen,P2} = \dot{m}_{23}s_{23} \quad (4.56)$$

The exergy balance equation for pump 2 can be written as follows:

$$\dot{m}_{22}ex_{22} + \dot{W}_{P2} = \dot{m}_{23}ex_{23} + \dot{E}x_{d,P2} \quad (4.57)$$

Gas Turbine Cycle

- *Compressor*

The mass balance equation for compressor can be written as follows:

$$\dot{m}_{32} = \dot{m}_{27} \quad (4.58)$$

The energy balance equation for compressor can be written as follows:

$$\dot{m}_{32}h_{32} + \dot{W}_C = \dot{m}_{27}h_{27} \quad (4.59)$$

The entropy balance equation for compressor can be written as follows:

$$\dot{m}_{32}s_{32} + \dot{S}_{gen,C} = \dot{m}_{27}s_{27} \quad (4.60)$$

The exergy balance equation for compressor can be written as follows:

$$\dot{m}_{32}ex_{32} + \dot{W}_C = \dot{m}_{27}ex_{27} + \dot{E}x_{d,C} \quad (4.61)$$

- *Combustion Chamber*

The mass balance equation for compressor can be written as follows:

$$\dot{m}_{27} + \dot{m}_{26} = \dot{m}_{28} \quad (4.62)$$

The energy balance equation for compressor can be written as follows:

$$\dot{m}_{27}h_{27} + \dot{m}_{26}h_{26} = \dot{m}_{28}h_{28} + \dot{Q}_{CC} \quad (4.63)$$

Where $h_{26} = \text{LHV of the fuel}$

The entropy balance equation for compressor can be written as follows:

$$\dot{m}_{27}s_{27} + \dot{m}_{26}s_{26} + \dot{S}_{gen,CC} = \dot{m}_{28}s_{28} + \frac{\dot{Q}_{CC}}{T_0} \quad (4.64)$$

The exergy balance equation for compressor can be written as follows:

$$\dot{m}_{27}ex_{27} + \dot{m}_{26}ex_{26} = \dot{m}_{28}ex_{28} + \dot{E}x_{d,CC} + \dot{Q}_{CC}\left(1 - \frac{T_0}{T_{CC}}\right) \quad (4.65)$$

where $T_{CC} = \text{combustion temperature}$

where $ex_{26} = \text{exergy of the fuel}$

- *Gas Turbine*

The mass balance equation for gas turbine can be written as follows:

$$\dot{m}_{28} = \dot{m}_{29} \quad (4.66)$$

The energy balance equation for gas turbine can be written as follows:

$$\dot{m}_{28}h_{28} = \dot{m}_{29}h_{29} + \dot{W}_{GT} \quad (4.67)$$

The entropy balance equation for gas turbine can be written as follows:

$$\dot{m}_{28}s_{28} + \dot{S}_{gen,GT} = \dot{m}_{29}s_{29} \quad (4.68)$$

The exergy balance equation for gas turbine can be written as follows:

$$\dot{m}_{28}ex_{28} = \dot{m}_{29}ex_{29} + \dot{W}_{GT} + \dot{E}x_{d,GT} \quad (4.69)$$

Absorption Chiller Cycle

- *Generator*

The mass balance equations for the generator of absorption cooling cycle can be written as follows:

For air: $\dot{m}_{30} = \dot{m}_{31}$ (4.70)

For LiBr: $\dot{m}_3 = \dot{m}_4 + \dot{m}_7$ (4.71)

The energy balance equation for the generator can be written as follows:

$$\dot{m}_3 h_3 + \dot{m}_{30} h_{30} = \dot{m}_4 h_4 + \dot{m}_7 h_7 + \dot{m}_{31} h_{31} \quad (4.72)$$

Here, the heat transfer rate to the generator, $\dot{Q}_d$ is written as

$$\dot{Q}_d = \dot{m}_{30}(h_{30} - h_{31}) \quad (4.73)$$

The entropy balance equation for the generator can be written as follows:

$$\dot{m}_3 s_3 + \dot{m}_{30} s_{30} + \dot{S}_{gen,g} = \dot{m}_4 s_4 + \dot{m}_7 s_7 + \dot{m}_{31} s_{31} \quad (4.74)$$

The exergy balance equation for the generator can be written as follows:

$$\dot{m}_3 ex_3 + \dot{m}_{30} ex_{30} = \dot{m}_4 ex_4 + \dot{m}_7 ex_7 + \dot{m}_{31} ex_{31} + \dot{E}x_{d,g} \quad (4.75)$$

- *Condenser 1*

The mass balance equation for the condenser 1 can be written as

$$\dot{m}_7 = \dot{m}_8 \quad (4.76)$$

The energy balance equation for the condenser 1 can be written as

$$\dot{m}_7 h_7 = \dot{m}_8 h_8 + \dot{Q}_{c1} \quad (4.77)$$

where $\dot{Q}_{c1}$ denotes the heat rejected from condenser 1.

The entropy balance equation for the condenser 1 can be written as

$$\dot{m}_7 s_7 + \dot{S}_{gen,c1} = \dot{m}_8 s_8 + \frac{\dot{Q}_{c1}}{T_0} \tag{4.78}$$

The exergy balance equation for the condenser can be written as

$$\dot{m}_7 ex_7 = \dot{m}_8 ex_8 + \dot{Q}_{c1}\left(1 - \frac{T_0}{T_S}\right) + \dot{E}x_{d,c1} \tag{4.79}$$

- *Expansion valve 1*

For expansion valve 1, we can write the following mass balance equation:

$$\dot{m}_8 = \dot{m}_9 \tag{4.80}$$

The energy balance equation for the expansion valve 1 can be written as

$$\dot{m}_8 h_8 = \dot{m}_9 h_9 \tag{4.81}$$

The entropy balance equation for the expansion valve 1 can be written as

$$\dot{m}_8 s_8 + \dot{S}_{gen,EV1} = \dot{m}_9 s_9 \tag{4.82}$$

The exergy balance equation for the expansion valve 1 can be written as

$$\dot{m}_8 ex_8 = \dot{m}_9 ex_9 + \dot{E}x_{d,EV1} \tag{4.83}$$

- *Evaporator 1*

The mass balance equation for the evaporator 1 can be written as follows

For LiBr: $\dot{m}_9 = \dot{m}_{10}$ (4.84)

For water: $\dot{m}_e = \dot{m}_f$ (4.85)

The energy balance equation for the evaporator 1 can be written as

$$\dot{m}_9 h_9 + \dot{Q}_{e1} = \dot{m}_{10} h_{10} \tag{4.86}$$

The entropy balance equation for the evaporator 1 can be written as follows:

$$\dot{m}_9 s_9 + \frac{\dot{Q}_{e1}}{T_0} + \dot{S}_{gen,e1} = \dot{m}_{10} s_{10} \tag{4.87}$$

The exergy balance equation for the evaporator 1 can be written as follows:

$$\dot{m}_9 ex_9 + \dot{Q}_{e1}\left(\frac{T_0}{T_{e1}} - 1\right) = \dot{m}_{10} ex_{10} + \dot{E}x_{d.e1} \tag{4.88}$$

- *Absorber*

The mass balance equation for the absorber can be written as follows:

$$\dot{m}_{10} + \dot{m}_6 = \dot{m}_1 \tag{4.89}$$

The energy balance equation for the absorber can be written as follows:

$$\dot{m}_{10} h_{10} + \dot{m}_6 h_6 = \dot{m}_1 h_1 + \dot{Q}_a \tag{4.90}$$

where $\dot{Q}_a$ denotes that heat loss rate from the absorber. The entropy balance equation for the absorber can be written as follows:

$$\dot{m}_{10} s_{10} + \dot{m}_6 s_6 + \dot{S}_{gen,a} = \dot{m}_1 s_1 + \frac{\dot{Q}_a}{T_0} \tag{4.91}$$

The exergy balance equation for the absorber can be written as follows:

$$\dot{m}_{10} ex_{10} + \dot{m}_6 ex_6 = \dot{m}_1 ex_1 + \dot{Q}_a\left(1 - \frac{T_0}{T_s}\right) + \dot{E}x_{d,a} \tag{4.92}$$

- *Pump 3*

The mass balance equation for the pump 3 can be written as follows:

$$\dot{m}_1 = \dot{m}_2 \tag{4.93}$$

The energy balance equation for the pump 3 can be written as follows:

$$\dot{m}_1 h_1 + \dot{W}_{p3} = \dot{m}_2 h_2 \tag{4.94}$$

The entropy balance equation for the pump 3 can be written as follows:

$$\dot{m}_1 s_1 + \dot{S}_{gen,p3} = \dot{m}_2 s_2 \quad (4.95)$$

The exergy balance equation for the pump 3 can be written as

$$\dot{m}_1 ex_1 + \dot{W}_{p3} = \dot{m}_2 ex_2 + \dot{E}x_{d,p3} \quad (4.96)$$

- *Heat Exchanger 1*

The mass balance equation for the heat exchanger 1 can be written as

$$\dot{m}_2 + \dot{m}_4 = \dot{m}_3 + \dot{m}_5 \quad (4.97)$$

The energy balance equation for the solution heat exchanger 1 can be written as

$$\dot{m}_2 h_2 + \dot{m}_4 h_4 = \dot{m}_3 h_3 + \dot{m}_5 h_5 \quad (4.98)$$

The entropy balance equation for the solution heat exchanger 1 can be written as

$$\dot{m}_2 s_2 + \dot{m}_4 s_4 + \dot{S}_{gen,HEX1} = \dot{m}_3 s_3 + \dot{m}_5 s_5 \quad (4.99)$$

The exergy balance equation for the solution heat exchanger 1 can be written as

$$\dot{m}_2 ex_2 + \dot{m}_4 ex_4 = \dot{m}_3 ex_3 + \dot{m}_5 ex_5 + \dot{E}x_{d,HEX1} \quad (4.100)$$

- *Expansion Valve 2*

The mass balance equation for the expansion valve 2 can be as:

$$\dot{m}_5 = \dot{m}_6 \quad (4.101)$$

The energy balance equation for the expansion valve 2 can be as

$$\dot{m}_5 h_5 = \dot{m}_6 h_6 \quad (4.102)$$

The entropy balance equation for the expansion valve 2 can be as

$$\dot{m}_5 s_5 + \dot{S}_{gen,EV2} = \dot{m}_6 s_6 \quad (4.103)$$

The exergy balance equation for the expansion valve 2 can be as

$$\dot{m}_5 ex_5 = \dot{m}_6 ex_6 + \dot{E}x_{d,EV2} \quad (4.104)$$

4.5.1.2 Energy Efficiencies

The energy efficiency can be defined for the systems considered here as the ratio of useful energy output to the total energy input. In this , the energy efficiencies for the gas turbine cycle, absorption chiller, organic Rankine cycle 1 and overall system are defined and evaluated.

- *Absorption Chiller*

For absorption chiller, a coefficient of performance can be used to express its energetic performance:

$$\mathrm{COP}_{\mathrm{en,ac}} = \frac{\dot{Q}_{e1}}{\dot{Q}_{d}} \tag{4.105}$$

- *Gas Turbine Cycle*

$$\eta_{\mathrm{en,GTC}} = \frac{\dot{W}_{GT} - \dot{W}_{c}}{\dot{m}_{26} h_{26}} \tag{4.106}$$

- *Organic Rankine Cycle 1*

$$\eta_{\mathrm{en,ORC1}} = \frac{(\dot{W}_{ORCT1} - \dot{W}_{P1})}{\dot{m}_{12} h_{12} - \dot{m}_{13} h_{13}} \tag{4.107}$$

- *Overall System*

The energy efficiency of the overall system (Fig. 3.1) can be written as follows:

$$\eta_{\mathrm{en,ov}} = \frac{(\dot{m}_{25} h_{25} - \dot{m}_{24} h_{24} + \dot{m}_{18} h_{18} - \dot{m}_{17} h_{17} + \dot{Q}_{e1} + \dot{W}_{ORCT1} + \dot{W}_{ORCT2} + \dot{W}_{GT} - \dot{W}_{C} - \dot{W}_{P1} - \dot{W}_{P2})}{\dot{m}_{26} h_{26} + \dot{Q}_{sol}} \tag{4.108}$$

4.5.1.3 Exergy Efficiencies

The exergy efficiency is defined here as the ratio of useful exergy output to the total exergy input. Exergy efficiencies for the gas turbine cycle, absorption chiller, organic Rankine cycle 1 and overall system are evaluated.

- *Absorption Chiller*

For an absorption chiller, the coefficient of performance can be used to express its exergetic performance as follows:

$$\mathrm{COP}_{\mathrm{ex,ac}} = \frac{\dot{Q}_{e1}\left(\frac{T_0}{T_{e1}}-1\right)}{\dot{Q}_d\left(1-\frac{T_0}{T_s}\right)} \tag{4.109}$$

- *Gas Turbine Cycle*

$$\eta_{\mathrm{ex,GTC}} = \frac{\dot{W}_{GT}-\dot{W}_c}{\dot{m}_{26}ex_{26}} \tag{4.110}$$

- *Organic Rankine Cycle 1*

$$\eta_{\mathrm{ex,ORC1}} = \frac{(\dot{W}_{ORCT1}-\dot{W}_{P1})}{\dot{m}_{12}ex_{12}-\dot{m}_{13}ex_{13}} \tag{4.111}$$

- *Overall System*

The exergy efficiency of the overall system (Fig. 3.1) can be written as follows:

$$\eta_{\mathrm{ex,ov}} = \frac{(\dot{m}_{25}ex_{25}-\dot{m}_{24}ex_{24}+\dot{m}_{18}ex_{18}-\dot{m}_{17}ex_{17}+\dot{Q}_{e1}\left(\frac{T_0}{T_{e1}}-1\right)+\dot{W}_{ORCT1}+\dot{W}_{ORCT2}+\dot{W}_{GT}-\dot{W}_C-\dot{W}_{P1}-\dot{W}_{P2})}{\dot{m}_{26}ex_{26}+Ex^{Q}_{sol}} \tag{4.112}$$

4.6 Analysis of System 2

4.6.1 Thermodynamic Analysis of System 2

Energy and exergy analyses are performed for the proposed system (see Fig. 3.2) in order to provide the information about its performances, efficiencies and emissions. The reference-environment state is specified as having a temperature $T_0 = 25\ ^\circ\mathrm{C}$ and a pressure $P_0 = 100$ kPa. The following assumptions are made for the analyses:

- The changes in kinetic and potential energy and exergy are negligible.
- The compressor and pumps are adiabatic.
- The isentropic efficiencies of the ORC pump and turbine are 75% and 85% respectively.

- The pressure losses in all heat exchangers and pipelines are negligible.

4.6.1.1 Balance Equations

The mass, energy, entropy and exergy balance are written for System 2 as shown in Fig. 3.2.

- *Concentrated solar panel*

The mass balance for the concentrated solar panel can be written as follows:

$$\dot{m}_{11} = \dot{m}_{12} \tag{4.113}$$

The energy balance for the concentrated solar panel can be written as follows:

$$\dot{m}_{11} h_{11} + \dot{Q}_{sol} = \dot{m}_{12} h_{12} + \dot{Q}_{loss,csp} \tag{4.114}$$

The entropy balance for the concentrated solar panel can be written as follows:

$$\dot{m}_{11} s_{11} + \frac{\dot{Q}_{sol}}{T_0} + \dot{S}_{gen,csp} = \dot{m}_{12} s_{12} + \frac{\dot{Q}_{loss,csp}}{T_0} \tag{4.115}$$

The exergy balance for the concentrated solar panel can be written as follows:

$$\dot{m}_{11} ex_{11} + \dot{Q}_{sol}\left(1 - \frac{T_0}{T_s}\right) = \dot{m}_{12} ex_{12} + \dot{Q}_{loss,csp}\left(1 - \frac{T_0}{T_s}\right) + \dot{E}x_{d,csp} \tag{4.116}$$

- *Storage tank*

The mass balance for the storage tank can be written as follows:

For oil: $\dot{m}_{12} = \dot{m}_{13}$ (4.117)

For isopentane: $\dot{m}_{15} = \dot{m}_{16}$ (4.118)

The energy balance for the storage tank can be written as

$$\dot{m}_{12} h_{12} + \dot{m}_{15} h_{15} + \dot{W}_{storage} = \dot{m}_{16} h_{16} + \dot{m}_{13} h_{13} \tag{4.119}$$

The entropy balance for the storage tank can be written as

$$\dot{m}_{12}s_{12} + \dot{m}_{15}s_{15} + \dot{S}_{gen,storage} = \dot{m}_{16}s_{16} + \dot{m}_{13}s_{13} \quad (4.120)$$

The exergy balance for the storage tank can be written as

$$\dot{m}_{12}ex_{12} + \dot{m}_{15}ex_{15} + \dot{W}_{storage} = \dot{m}_{16}ex_{16} + \dot{m}_{13}ex_{13} + \dot{E}x_{d,storage} \quad (4.121)$$

- *Pump 1*

The mass balance equation for the pump 1 can be written as follows:

$$\dot{m}_{14} = \dot{m}_{15} \quad (4.122)$$

The energy balance equation for the pump 1 can be written as follows:

$$\dot{m}_{14}h_{14} + \dot{W}_{p1} = \dot{m}_{15}h_{15} \quad (4.123)$$

The entropy balance equation for the pump 1 can be written as follows:

$$\dot{m}_{14}s_{14} + \dot{S}_{gen,p1} = \dot{m}_{15}s_{15} \quad (4.124)$$

The exergy balance equation for the pump 1 can be written as follows:

$$\dot{m}_{14}ex_{14} + \dot{W}_{p1} = \dot{m}_{15}ex_{15} + \dot{E}x_{d,p1} \quad (4.125)$$

- *ORC Turbine*

The mass balance equation for the ORC turbine can be written as follows:

$$\dot{m}_{16} = \dot{m}_{17} \quad (4.126)$$

The energy balance equation for the ORC turbine can be written as follows:

$$\dot{m}_{16}h_{16} = \dot{W}_{t} + \dot{m}_{17}h_{17} \quad (4.127)$$

The entropy balance equation for the ORC turbine can be written as follows:

$$\dot{m}_{16}s_{16} + \dot{S}_{gen,t} = \dot{m}_{17}s_{17} \quad (4.128)$$

The exergy balance equation for the ORC turbine can be written as follows:

$$\dot{m}_{16}ex_{16} = \dot{W}_{t} + \dot{m}_{17}ex_{17} + \dot{E}x_{d,t} \quad (4.129)$$

- *Condenser 2*

The mass balance for the condenser 2 can be written as:

For isopentane: $\dot{m}_{17} = \dot{m}_{18}$ (4.130)

For water: $\dot{m}_{21} = \dot{m}_{22}$ (4.131)

The energy balance equation for the condenser 2 can be written as:

$$\dot{m}_{17}h_{17} + \dot{m}_{21}h_{21} = \dot{m}_{22}h_{22} + \dot{m}_{18}h_{18} + \dot{Q}_{c2} \quad (4.132)$$

where $\dot{Q}_{c2}$ denotes the heat rejected from condenser 2.

The entropy balance equation for the condenser 2 can be written as:

$$\dot{m}_{17}s_{17} + \dot{m}_{21}s_{21} + \dot{S}_{gen,c2} = \dot{m}_{18}s_{18} + \dot{m}_{22}s_{22} + \frac{\dot{Q}_{c2}}{T_0} \quad (4.133)$$

The exergy balance equation for the condenser 2 can be written as

$$\dot{m}_{17}ex_{17} + \dot{m}_{21}ex_{21} = \dot{m}_{18}ex_{18} + \dot{m}_{22}ex_{22} + \dot{Q}_{c2}\left(1 - \frac{T_0}{T_S}\right) + \dot{E}x_{d,c} \quad (4.134)$$

- *Evaporator 1*

The mass balance equations for the evaporator 1 can be written as follows:

For isopentane: $\dot{m}_{18} = \dot{m}_{19}$ (4.135)

For R134a: $\dot{m}_{23} = \dot{m}_{24}$ (4.136)

The energy balance equation for the evaporator 1 can be written as follows:

$$\dot{m}_{18}h_{18} + \dot{m}_{23}h_{23} = \dot{m}_{24}h_{24} + \dot{m}_{19}h_{19} \quad (4.137)$$

The entropy balance equation for the evaporator 1 can be written as follows:

$$\dot{m}_{18}s_{18} + \dot{m}_{23}s_{23} + \dot{S}_{gen,e1} = \dot{m}_{24}s_{24} + \dot{m}_{19}s_{19} \quad (4.138)$$

The exergy balance equation for the evaporator 1 can be written as follows:

$$\dot{m}_{18}ex_{18} + \dot{m}_{23}ex_{23} = \dot{m}_{24}ex_{24} + \dot{m}_{19}ex_{19} + \dot{E}x_{d,e1} \quad (4.139)$$

- *Compressor 1*

The mass balance equation for the compressor 1 can be written as follows:

$$\dot{m}_{24} = \dot{m}_{25} \quad (4.140)$$

The energy balance equation for the compressor 1 can be written as follows:

$$\dot{m}_{24}h_{24} + \dot{W}_{comp} = \dot{m}_{25}h_{25} \quad (4.141)$$

The entropy balance equation for the compressor 1 can be written as follows:

$$\dot{m}_{24}s_{24} + \dot{S}_{gen,comp} = \dot{m}_{25}s_{25} \quad (4.142)$$

The exergy balance equation for the compressor 1 can be written as follows:

$$\dot{m}_{24}ex_{24} + \dot{W}_{comp} = \dot{m}_{25}ex_{25} + \dot{E}x_{d,comp} \quad (4.143)$$

- *Condenser 1*

The mass balance equations for the condenser 1 can be written as follows:

For R134a: $\dot{m}_{25} = \dot{m}_{26}$ (4.144)

For water: $\dot{m}_{27} = \dot{m}_{28}$ (4.145)

The energy balance equation for the condenser 1 can be written as follows:

$$\dot{m}_{25}h_{25} + \dot{m}_{27}h_{27} = \dot{m}_{26}h_{26} + \dot{m}_{28}h_{28} \quad (4.146)$$

The entropy balance equation for the condenser 1 can be written as follows:

$$\dot{m}_{25}s_{25} + \dot{m}_{27}s_{27} + \dot{S}_{gen,c1} = \dot{m}_{28}s_{28} + \dot{m}_{26}s_{26} \quad (4.147)$$

The exergy balance equation for the condenser 1 can be written as follows:

$$\dot{m}_{25}ex_{25} + \dot{m}_{27}ex_{27} = \dot{m}_{28}ex_{28} + \dot{m}_{26}ex_{26} + \dot{E}x_{d,c1} \quad (4.148)$$

- *Expansion Valve*

The mass balance equation for the expansion valve can be written as follows:

For R134a: $\dot{m}_{26} = \dot{m}_{23}$ (4.149)

The energy balance equation for the expansion valve can be written as follows:

$\dot{m}_{26}h_{26} = \dot{m}_{23}h_{23}$ (4.150)

The entropy balance equation for the expansion valve can be written as follows:

$\dot{m}_{26}s_{26} + \dot{S}_{gen,ev} = \dot{m}_{23}s_{23}$ (4.151)

The exergy balance equation for the expansion valve can be written as follows:

$\dot{m}_{26}ex_{26} = \dot{m}_{23}ex_{23} + \dot{E}x_{d,ev}$ (4.152)

- *Pump 2*

The mass balance equation for the pump 2 can be written as follows:

$\dot{m}_{19} = \dot{m}_{20}$ (4.153)

The energy balance equation for the pump 2 can be written as follows:

$\dot{m}_{19}h_{19} + \dot{W}_{p2} = \dot{m}_{20}h_{20}$ (4.154)

The entropy balance equation for the pump 2 can be written as follows:

$\dot{m}_{19}s_{19} + \dot{S}_{gen,p2} = \dot{m}_{20}s_{20}$ (4.155)

The exergy balance equation for the pump 2 can be written as follows:

$\dot{m}_{19}ex_{19} + \dot{W}_{p2} = \dot{m}_{20}ex_{20} + \dot{E}x_{d,p2}$ (4.156)

Absorption Chiller Cycle

- *Generator*

The mass balance equations for the generator of absorption cooling cycle can be written as follows:

For oil: $\dot{m}_{13} = \dot{m}_{11}$ (4.157)

For LiBr: $\dot{m}_3 = \dot{m}_7 + \dot{m}_4$ (4.158)

The energy balance equation for the generator can be written as follows:

$$\dot{m}_{13}h_{13} + \dot{m}_3h_3 = \dot{m}_7h_7 + \dot{m}_{11}h_{11} + \dot{m}_4h_4 \quad (4.159)$$

Here, the heat transfer rate to the generator, $\dot{Q}_d$ is present in this equation, since

$$\dot{Q}_d = \dot{m}_{13}(h_{13} - h_{11}) \quad (4.160)$$

The entropy balance equation for the generator can be written as follows:

$$\dot{m}_{13}s_{13} + \dot{m}_3s_3 + \dot{S}_{gen,g} = \dot{m}_7s_7 + \dot{m}_{11}s_{11} + \dot{m}_4s_4 \quad (4.161)$$

The exergy balance equation for the generator can be written as follows:

$$\dot{m}_3ex_3 + \dot{m}_{13}ex_{13} = \dot{m}_7ex_7 + \dot{m}_{11}ex_{11} + \dot{m}_4ex_4 + \dot{E}x_{d,g} \quad (4.162)$$

- *Condenser 3*

The mass balance equation for the condenser 3 can be written as

$$\dot{m}_7 = \dot{m}_8 \quad (4.163)$$

The energy balance equation for the condenser 3 can be written as

$$\dot{m}_7h_7 = \dot{m}_8h_8 + \dot{Q}_{c3} \quad (4.164)$$

where $\dot{Q}_{c3}$ denotes the heat rejected from condenser 3.

The entropy balance equation for the condenser 3 can be written as

$$\dot{m}_7s_7 + \dot{S}_{gen,c3} = \dot{m}_8s_8 + \frac{\dot{Q}_{c3}}{T_0} \quad (4.165)$$

The exergy balance equation for the condenser can be written as

$$\dot{m}_7ex_7 = \dot{m}_8ex_8 + \dot{Q}_{c3}\left(1 - \frac{T_0}{T_S}\right) + \dot{E}x_{d,c3} \quad (4.166)$$

- *Throttling Valve 1*

For throttling valve 1, we can write the following mass balance equation:

$$\dot{m}_8 = \dot{m}_9 \tag{4.167}$$

The energy balance equation for the throttle valve 1 can be written as

$$\dot{m}_8 h_8 = \dot{m}_9 h_9 \tag{4.168}$$

The entropy balance equation for the throttle valve 1 can be written as

$$\dot{m}_8 s_8 + \dot{S}_{gen,tv1} = \dot{m}_9 s_9 \tag{4.169}$$

The exergy balance equation for the throttle valve 1 can be written as

$$\dot{m}_8 ex_8 = \dot{m}_9 ex_9 + \dot{E}x_{d,tv1} \tag{4.170}$$

- *Evaporator 3*

The mass balance equation for the evaporator 3 can be written as follows

$$\dot{m}_9 = \dot{m}_{10} \tag{4.171}$$

The energy balance equation for the evaporator 3 can be written as

$$\dot{m}_9 h_9 + \dot{Q}_{e3} = \dot{m}_{10} h_{10} \tag{4.172}$$

where $\dot{Q}_{e3}$ denotes the heat absorption rate by the evaporator 3.

The entropy balance equation for the evaporator 3 can be written as follows:

$$\dot{m}_9 s_9 + \frac{\dot{Q}_{e3}}{T_0} + \dot{S}_{gen,e3} = \dot{m}_{10} s_{10} \tag{4.173}$$

The exergy balance equation for the evaporator 3 can be written as follows:

$$\dot{m}_9 ex_9 + \dot{Q}_{e3}\left(\frac{T_0}{T_{e3}} - 1\right) = \dot{m}_{10} ex_{10} + \dot{E}x_{d.e3} \tag{4.174}$$

- *Absorber*

The mass balance equation for the absorber can be written as follows:

$$\dot{m}_{10} + \dot{m}_6 = \dot{m}_1 \tag{4.175}$$

The energy balance equation for the absorber can be written as follows:

$$\dot{m}_{10}h_{10} + \dot{m}_6 h_6 = \dot{m}_1 h_1 + \dot{Q}_a \tag{4.176}$$

where $\dot{Q}_a$ denotes that heat loss rate from the absorber.

The entropy balance equation for the absorber can be written as follows:

$$\dot{m}_{10}s_{10} + \dot{m}_6 s_6 + \dot{S}_{gen,a} = \dot{m}_1 s_1 + \frac{\dot{Q}_a}{T_0} \tag{4.177}$$

The exergy balance equation for the absorber can be written as follows:

$$\dot{m}_{10}ex_{10} + \dot{m}_6 ex_6 = \dot{m}_1 ex_1 + \dot{Q}_a\left(1 - \frac{T_0}{T_s}\right) + \dot{E}x_{d,a} \tag{4.178}$$

- *Solution Pump*

The mass balance equation for the solution pump can be written as follows:

$$\dot{m}_1 = \dot{m}_2 \tag{4.179}$$

The energy balance equation for the solution pump can be written as follows:

$$\dot{m}_1 h_1 + \dot{W}_{sp} = \dot{m}_2 h_2 \tag{4.180}$$

The entropy balance equation for the solution pump can be written as follows:

$$\dot{m}_1 s_1 + \dot{S}_{gen,sp} = \dot{m}_2 s_2 \tag{4.181}$$

The exergy balance equation for the solution pump can be written as

$$\dot{m}_1 ex_1 + \dot{W}_{sp} = \dot{m}_2 ex_2 + \dot{E}x_{d,sp} \tag{4.182}$$

- *Solution Heat Exchanger*

The mass balance equation for the solution heat exchanger can be written as

$$\dot{m}_2 + \dot{m}_4 = \dot{m}_3 + \dot{m}_5 \quad (4.183)$$

The energy balance equation for the solution heat exchanger can be written as

$$\dot{m}_2 h_2 + \dot{m}_4 h_4 = \dot{m}_3 h_3 + \dot{m}_5 h_5 \quad (4.184)$$

The entropy balance equation for the solution heat exchanger can be written as

$$\dot{m}_2 s_2 + \dot{m}_4 s_4 + \dot{S}_{gen,she} = \dot{m}_3 s_3 + \dot{m}_5 s_5 \quad (4.185)$$

The exergy balance equation for the solution heat exchanger can be written as

$$\dot{m}_2 ex_2 + \dot{m}_4 ex_4 = \dot{m}_3 ex_3 + \dot{m}_5 ex_5 + \dot{E}x_{d,she} \quad (4.186)$$

- *Throttling valve 2*

The mass balance equation for the throttling valve 2 can be as:

$$\dot{m}_5 = \dot{m}_6 \quad (4.187)$$

The energy balance equation for the throttling valve 2 can be as

$$\dot{m}_5 h_5 = \dot{m}_6 h_6 \quad (4.188)$$

The entropy balance equation for the throttling valve 2 can be as

$$\dot{m}_5 s_5 + \dot{S}_{gen,tv2} = \dot{m}_6 s_6 \quad (4.189)$$

The exergy balance equation for the throttling valve 2 can be as

$$\dot{m}_5 ex_5 = \dot{m}_6 ex_6 + \dot{E}x_{d,tv2} \quad (4.190)$$

4.6.1.2 Energy Efficiencies

The energy efficiency can be defined for the systems considered here as the ratio of useful energy output to the total energy input. In this study, the energy efficiencies of the

Organic Rankine Cycle, ground source heat pump, wind power system, absorption chiller and the overall system are then evaluated.

- *Organic Rankine Cycle*

The energy efficiency of the Organic Rankine Cycle can be expressed as

$$\eta_{en,orc} = \frac{\dot{W}_{net,t}}{\dot{m}_{16}h_{16} - \dot{m}_{15}h_{15}} \tag{4.191}$$

where $\dot{W}_{net,t} = \dot{W}_t - \dot{W}_{p1}$ (4.192)

- *Ground source heat pump*

For the ground source heat pump, a coefficient of performance can be used to express energetic performance. The energetic COP of the ground source heat pump can be written as

$$COP_{en,gshp} = \frac{\dot{m}_{28}h_{28} - \dot{m}_{27}h_{27}}{\dot{W}_{comp}} \tag{4.193}$$

- *Absorption Chiller*

A coefficient of performance can also be used to express the energetic performance of the absorption chiller:

$$COP_{en,ac} = \frac{\dot{Q}_{e3}}{\dot{Q}_d} \tag{4.194}$$

- *Wind Turbine System*

The energy efficiency of the wind turbine can be expressed as

$$\eta_{en,wt} = \frac{\dot{W}_{wt,out}}{\dot{W}_{wt,in}} \tag{4.195}$$

where $\dot{W}_{wt,in} = \frac{1}{2} m_{air} \dot{V}^2$ (4.196)

and $m_{air} = \rho_{air} A_{wt} \dot{V}$ (4.197)

where $A_{wt} = \frac{\pi D^2}{4}$, D is the diameter of the rotor having value of 18.5 m.

- *Overall System*

The energy efficiency of the overall system (Fig. 3.2) can be written as follows:

$$\eta_{en,ov} = \frac{(\dot{Q}_{e3} + \dot{m}_{28}h_{28} - \dot{m}_{27}h_{27} + \dot{W}_{net,t} + \dot{W}_{wt,out} - \dot{W}_{comp} - \dot{W}_{storage})}{\dot{m}_{14}h_{14} - \dot{m}_{20}h_{20} + \dot{W}_{wt,in} + \dot{Q}_{sol}} \quad (4.198)$$

4.6.1.3 Exergy Efficiencies

The exergy efficiency is defined here as the ratio of useful exergy output to the total exergy input. Exergy efficiencies for the Organic Rankine Cycle, ground source heat pump, wind power system and the overall system are then evaluated.

- *Organic Rankine Cycle*

The exergy efficiency of the Organic Rankine Cycle can be expressed as

$$\eta_{ex,orc} = \frac{\dot{W}_{net,t}}{\dot{m}_{16}ex_{16} - \dot{m}_{15}ex_{15}} \quad (4.199)$$

where $\dot{W}_{net,t} = \dot{W}_t - \dot{W}_{p1}$ (4.200)

- *Ground Source Heat Pump*

For the ground source heat pump, a coefficient of performance can be used to express exergetic performance. The exergetic COP of the ground source heat pump can be written as

$$COP_{ex,gshp} = \frac{\dot{m}_{28}ex_{28} - \dot{m}_{27}ex_{27}}{\dot{W}_{comp}} \quad (4.201)$$

- *Wind Turbine System*

The exergy efficiency of the wind turbine can be expressed as

$$\eta_{ex,wt} = \frac{\dot{W}_{wt,out}}{\dot{W}_{wt,in}} \quad (4.202)$$

- *Overall System*

The exergy efficiency of the overall system (Fig. 3.2) can be written as follows:

$$\eta_{ex,ov} = \frac{(\dot{E}x^{Q}_{cooling} + \dot{m}_{28}ex_{28} - \dot{m}_{27}ex_{27} + \dot{W}_{net,t} + \dot{W}_{wt,out} - \dot{W}_{comp} - \dot{W}_{storage})}{\dot{m}_{14}ex_{14} - \dot{m}_{20}ex_{20} + \dot{W}_{wt,in} + \dot{E}x^{Q}_{sol}} \quad (4.203)$$

where $\dot{E}x^{Q}_{cooling} = \dot{Q}_{e3}\left(\frac{T_0}{Te3} - 1\right)$ (4.204)

4.7 Analysis of System 3

4.7.1 Thermodynamic Analysis of System 3

4.7.1.1 Balance Equations

The mass, energy, entropy, and exergy balance equations for System 3 (shown in Fig. 3.3) are described in detail below.

- *Concentrated Solar Panel (CSP)*

The mass balance for the concentrated solar panel can be written as follows:

$$\dot{m}_{13} = \dot{m}_{14} \quad (4.205)$$

The energy balance for the concentrated solar panel can be written as follows:

$$\dot{m}_{13}h_{13} + \dot{Q}_{sol} = \dot{m}_{14}h_{14} + \dot{Q}_{loss,csp} \quad (4.206)$$

The entropy balance for the concentrated solar panel can be written as follows:

$$\dot{m}_{13}s_{13} + \frac{\dot{Q}_{sol}}{T_0} + \dot{S}_{gen,csp} = \dot{m}_{14}s_{14} + \frac{\dot{Q}_{loss,csp}}{T_0} \quad (4.207)$$

The exergy balance for the concentrated solar panel can be written as follows:

$$\dot{m}_{13}ex_{13} + \dot{Q}_{sol}\left(1 - \frac{T_0}{T_s}\right) = \dot{m}_{14}ex_{14} + \dot{Q}_{loss,csp}\left(1 - \frac{T_0}{T_s}\right) + \dot{E}x_{d,csp} \quad (4.208)$$

- *Heat Exchanger 2*

The mass balance for the heat exchanger 2 can be written as follows:

For oil: $\dot{m}_{14} = \dot{m}_{15}$ (4.209)

For water: $\dot{m}_{20} = \dot{m}_{17}$ (4.210)

The energy balance for the heat exchanger 2 can be written as

$$\dot{m}_{14}h_{14} + \dot{m}_{20}h_{20} = \dot{m}_{15}h_{15} + \dot{m}_{17}h_{17} \quad (4.211)$$

The entropy balance for the heat exchanger 2 can be written as

$$\dot{m}_{14}s_{14} + \dot{m}_{20}s_{20} + \dot{S}_{gen,HEX2} = \dot{m}_{15}s_{15} + \dot{m}_{17}s_{17} \quad (4.212)$$

The exergy balance for the heat exchanger 2 can be written as

$$\dot{m}_{14}ex_{14} + \dot{m}_{20}ex_{20} = \dot{m}_{15}ex_{15} + \dot{m}_{17}ex_{17} + \dot{E}x_{d,HEX2} \quad (4.213)$$

- *Pump 2*

The mass balance equation for the pump 2 can be written as follows:

$$\dot{m}_{19} = \dot{m}_{20} \quad (4.214)$$

The energy balance equation for the pump 2 can be written as follows:

$$\dot{m}_{19}h_{19} + \dot{W}_{p2} = \dot{m}_{20}h_{20} \quad (4.215)$$

The entropy balance equation for the pump 2 can be written as follows:

$$\dot{m}_{19}s_{19} + \dot{S}_{gen,p2} = \dot{m}_{20}s_{20} \quad (4.216)$$

The exergy balance equation for the pump 2 can be written as follows:

$$\dot{m}_{19}ex_{19} + \dot{W}_{p2} = \dot{m}_{20}ex_{20} + \dot{E}x_{d,p2} \quad (4.217)$$

- *Condenser 2*

The mass balance for the condenser 2 can be written as

For water: $\dot{m}_{18} = \dot{m}_{19}$ (4.218)

For air: $\dot{m}_{21} = \dot{m}_{22}$ (4.219)

The energy balance equation for the condenser 2 can be written as

$$\dot{m}_{18}h_{18} + \dot{m}_{21}h_{21} = \dot{m}_{19}h_{19} + \dot{m}_{22}h_{22} + \dot{Q}_{c2} \quad (4.220)$$

where $\dot{Q}_{c2}$ denotes the heat rejected from condenser 2. The entropy balance equation for the condenser 2 can be written as

$$\dot{m}_{18}s_{18} + \dot{m}_{21}s_{21} + \dot{S}_{gen,c2} = \dot{m}_{19}s_{19} + \dot{m}_{22}s_{22} + \frac{\dot{Q}_{c2}}{T_0} \quad (4.221)$$

The exergy balance equation for the condenser 2 can be written as

$$\dot{m}_{18}ex_{18} + \dot{m}_{21}ex_{21} = \dot{m}_{19}ex_{19} + \dot{m}_{22}ex_{22} + \dot{Q}_{c2}\left(1 - \frac{T_0}{T_S}\right) + \dot{E}x_{d,c2} \quad (4.222)$$

- *High Pressure Steam Turbine 1*

The mass balance equation for the high pressure steam turbine 1 can be written as follows:

$$\dot{m}_{17} = \dot{m}_{18} \quad (4.223)$$

The energy balance equation for the high pressure steam turbine 1 can be written as follows:

$$\dot{m}_{17}h_{17} = \dot{W}_{HPST1} + \dot{m}_{18}h_{18} \quad (4.224)$$

The entropy balance equation for the high pressure steam turbine 1 can be written as follows:

$$\dot{m}_{17}s_{17} + \dot{S}_{gen,HPST1} = \dot{m}_{18}s_{18} \quad (4.225)$$

The exergy balance equation for the high pressure steam turbine 1can be written as follows:

$$\dot{m}_{17}ex_{17} = \dot{W}_{HPST1} + \dot{m}_{18}ex_{18} + \dot{E}x_{d,HPST1} \quad (4.226)$$

- *Heat Exchanger 3*

The mass balance equations for the heat exchanger 3 can be written as follows:

For oil: $\dot{m}_{15} = \dot{m}_{16}$ (4.227)

For water: $\dot{m}_{35} = \dot{m}_{23}$ (4.228)

The energy balance equation for the heat exchanger 3 can be written as follows:

$$\dot{m}_{15}h_{15} + \dot{m}_{35}h_{35} = \dot{m}_{16}h_{16} + \dot{m}_{23}h_{23} \quad (4.229)$$

The entropy balance equation for the heat exchanger 3 can be written as follows:

$$\dot{m}_{15}s_{15} + \dot{m}_{35}s_{35} + \dot{S}_{gen,HEX3} = \dot{m}_{16}s_{16} + \dot{m}_{23}s_{23} \quad (4.230)$$

The exergy balance equation for the heat exchanger 3 can be written as follows:

$$\dot{m}_{15}ex_{15} + \dot{m}_{35}ex_{35} = \dot{m}_{16}ex_{16} + \dot{m}_{23}ex_{23} + \dot{E}x_{d,HEX3} \quad (4.231)$$

- *Pump 3*

The mass balance equation for the pump 3 can be written as follows:

$$\dot{m}_{34} = \dot{m}_{35} \quad (4.232)$$

The energy balance equation for the pump 3 can be written as follows:

$$\dot{m}_{34}h_{34} + \dot{W}_{p3} = \dot{m}_{35}h_{35} \quad (4.233)$$

The entropy balance equation for the pump 3 can be written as follows:

$$\dot{m}_{34}s_{34} + \dot{S}_{gen,p3} = \dot{m}_{35}s_{35} \quad (4.234)$$

The exergy balance equation for the pump 3 can be written as follows:

$$\dot{m}_{34}ex_{34} + \dot{W}_{p3} = \dot{m}_{35}ex_{35} + \dot{E}x_{d,p3} \quad (4.235)$$

- *Condenser 3*

The mass balance for the condenser 3 can be written as

For water: $\dot{m}_{24} = \dot{m}_{25}$ (4.236)

For hot water: $\dot{m}_{27} = \dot{m}_{28}$ (4.237)

The energy balance equation for the condenser 3 can be written as

$$\dot{m}_{24}h_{24} + \dot{m}_{27}h_{27} = \dot{m}_{25}h_{25} + \dot{m}_{28}h_{28} + \dot{Q}_{c3} \quad (4.238)$$

where $\dot{Q}_{c3}$ denotes the heat rejected from condenser 3. The entropy balance equation for the condenser 3 can be written as:

$$\dot{m}_{24}s_{24} + \dot{m}_{27}s_{27} + \dot{S}_{gen,c3} = \dot{m}_{25}s_{25} + \dot{m}_{28}s_{28} + \frac{\dot{Q}_{c3}}{T_0} \quad (4.239)$$

The exergy balance equation for the condenser 2 can be written as

$$\dot{m}_{24}ex_{24} + \dot{m}_{27}ex_{27} = \dot{m}_{25}ex_{25} + \dot{m}_{28}ex_{28} + \dot{Q}_{c3}\left(1 - \frac{T_0}{T_S}\right) + \dot{E}x_{d,c3} \quad (4.240)$$

- *High Pressure Steam Turbine 2*

The mass balance equation for the high pressure steam turbine 2 can be written as follows:

$$\dot{m}_{23} = \dot{m}_{24} \quad (4.241)$$

The energy balance equation for the high pressure steam turbine 2 can be written as follows:

$$\dot{m}_{23}h_{23} = \dot{W}_{HPST2} + \dot{m}_{24}h_{24} \quad (4.242)$$

The entropy balance equation for the high pressure steam turbine 2 can be written as follows:

$$\dot{m}_{23}s_{23} + \dot{S}_{gen,HPST2} = \dot{m}_{24}s_{24} \quad (4.243)$$

The exergy balance equation for the high pressure steam turbine 2 can be written as follows:

$$\dot{m}_{23}ex_{23} = \dot{W}_{HPST2} + \dot{m}_{24}ex_{24} + \dot{E}x_{d,HPST2} \quad (4.244)$$

- *Condenser 4*

The mass balance for the condenser 4 can be written as

$$\dot{m}_{33} = \dot{m}_{34} \tag{4.245}$$

The energy balance equation for the condenser 4 can be written as

$$\dot{m}_{33}h_{33} = \dot{m}_{34}h_{34} + \dot{Q}_{c4} \tag{4.246}$$

where $\dot{Q}_{c4}$ denotes the heat rejected from condenser 4. The entropy balance equation for the condenser 4 can be written as:

$$\dot{m}_{33}s_{33} + \dot{S}_{gen,c4} = \dot{m}_{34}s_{34} + \frac{\dot{Q}_{c4}}{T_0} \tag{4.247}$$

The exergy balance equation for the condenser 4 can be written as

$$\dot{m}_{33}ex_{33} = \dot{m}_{34}ex_{34} + \dot{Q}_{c4}\left(1 - \frac{T_0}{T_S}\right) + \dot{E}x_{d,c4} \tag{4.248}$$

- *Mixing Chamber*

The mass balance equation for the mixing chamber can be written as follows:

$$\dot{m}_{32} + \dot{m}_{40} = \dot{m}_{33} \tag{4.249}$$

The energy balance equation for the mixing chamber can be written as follows:

$$\dot{m}_{32}h_{32} + \dot{m}_{40}h_{40} = \dot{m}_{33}h_{33} \tag{4.250}$$

The entropy balance equation for the mixing chamber can be written as follows:

$$\dot{m}_{32}s_{32} + \dot{m}_{40}s_{40} + \dot{S}_{gen,MC} = \dot{m}_{33}s_{33} \tag{4.251}$$

The exergy balance equation for the mixing chamber can be written as follows:

$$\dot{m}_{32}ex_{32} + \dot{m}_{40}ex_{40} = \dot{m}_{33}ex_{33} + \dot{E}x_{d,MC} \tag{4.252}$$

- *High Pressure Steam Turbine 3*

The mass balance equation for the high pressure steam turbine 3 can be written as follows:

$$\dot{m}_{31} = \dot{m}_{32} \tag{4.253}$$

The energy balance equation for the high pressure steam turbine 3 can be written as follows:

$$\dot{m}_{31}h_{31} = \dot{W}_{HPST3} + \dot{m}_{32}h_{32} \quad (4.254)$$

The entropy balance equation for the high pressure steam turbine 3 can be written as follows:

$$\dot{m}_{31}s_{31} + \dot{S}_{gen,HPST3} = \dot{m}_{32}s_{32} \quad (4.255)$$

The exergy balance equation for the high pressure steam turbine 3 can be written as follows:

$$\dot{m}_{31}ex_{31} = \dot{W}_{HPST3} + \dot{m}_{32}ex_{32} + \dot{E}x_{d,HPST3} \quad (4.256)$$

- *Low Pressure Steam Turbine*

The mass balance equation for the low pressure steam turbine can be written as follows:

$$\dot{m}_{38} = \dot{m}_{40} \quad (4.257)$$

The energy balance equation for the low pressure steam turbine can be written as follows:

$$\dot{m}_{38}h_{38} = \dot{W}_{LPST} + \dot{m}_{40}h_{40} \quad (4.258)$$

The entropy balance equation for the low pressure steam turbine can be written as follows:

$$\dot{m}_{38}s_{38} + \dot{S}_{gen,LPST} = \dot{m}_{40}s_{40} \quad (4.259)$$

The exergy balance equation for the low pressure steam turbine can be written as follows:

$$\dot{m}_{38}ex_{38} = \dot{W}_{LPST} + \dot{m}_{40}ex_{40} + \dot{E}x_{d,LPST} \quad (4.260)$$

- *Separator 1*

The mass balance equation for the separator 1 can be written as follows:

$$\dot{m}_{30} = \dot{m}_{31} + \dot{m}_{36} \quad (4.261)$$

The energy balance equation for the separator 1 can be written as follows:

$$\dot{m}_{30}h_{30} = \dot{m}_{31}h_{31} + \dot{m}_{36}h_{36} \quad (4.262)$$

The entropy balance equation for the separator 1 can be written as follows:

$$\dot{m}_{30}s_{30} + \dot{S}_{gen,S1} = \dot{m}_{31}s_{31} + \dot{m}_{36}s_{36} \quad (4.263)$$

The exergy balance equation for the separator 1 can be written as follows:

$$\dot{m}_{30}ex_{30} = \dot{m}_{31}ex_{31} + \dot{m}_{36}ex_{36} + \dot{E}x_{d,S1} \quad (4.264)$$

- *Separator 2*

The mass balance equation for the separator 2 can be written as follows:

$$\dot{m}_{37} = \dot{m}_{38} + \dot{m}_{39} \quad (4.265)$$

The energy balance equation for the separator 2 can be written as follows:

$$\dot{m}_{37}h_{37} = \dot{m}_{38}h_{38} + \dot{m}_{39}h_{39} \quad (4.266)$$

The entropy balance equation for the separator 2 can be written as follows:

$$\dot{m}_{37}s_{37} + \dot{S}_{gen,S2} = \dot{m}_{38}s_{38} + \dot{m}_{39}s_{39} \quad (4.267)$$

The exergy balance equation for the separator 2 can be written as follows:

$$\dot{m}_{37}ex_{37} = \dot{m}_{38}ex_{38} + \dot{m}_{39}ex_{39} + \dot{E}x_{d,S2} \quad (4.268)$$

- *Flash Chamber 1*

The mass balance equation for the flash chamber 1 can be written as follows:

$$\dot{m}_{29} = \dot{m}_{30} \quad (4.269)$$

The energy balance equation for the flash chamber 1 can be written as follows:

$$\dot{m}_{29}h_{29} = \dot{m}_{30}h_{30} \quad (4.270)$$

The entropy balance equation for the flash chamber 1 can be written as follows:

$$\dot{m}_{29}s_{29} + \dot{S}_{gen,FC1} = \dot{m}_{30}s_{30} \quad (4.271)$$

The exergy balance equation for the flash chamber 1 can be written as follows:

$$\dot{m}_{29}ex_{29} = \dot{m}_{30}ex_{30} + \dot{E}x_{d,FC1} \quad (4.272)$$

- *Flash Chamber 2*

The mass balance equation for the flash chamber 2 can be written as follows:

$$\dot{m}_{36} = \dot{m}_{37} \quad (4.273)$$

The energy balance equation for the flash chamber 2 can be written as follows:

$$\dot{m}_{36}h_{36} = \dot{m}_{37}h_{37} \quad (4.274)$$

The entropy balance equation for the flash chamber 2 can be written as follows:

$$\dot{m}_{36}s_{36} + \dot{S}_{gen,FC2} = \dot{m}_{37}s_{37} \quad (4.275)$$

The exergy balance equation for the flash chamber 2 can be written as follows:

$$\dot{m}_{36}ex_{36} = \dot{m}_{37}ex_{37} + \dot{E}x_{d,FC2} \quad (4.276)$$

Absorption Chiller

- *Generator*

The mass balance equations for the generator of vapor absorption cycle can be written as follows:

For oil: $\dot{m}_{13} = \dot{m}_{16}$ (4.277)

For LiBr: $\dot{m}_{3} = \dot{m}_{4} + \dot{m}_{7}$ (4.278)

The energy balance equation for the generator can be written as follows:

$$\dot{m}_{3}h_{3} + \dot{m}_{13}h_{13} = \dot{m}_{4}h_{4} + \dot{m}_{7}h_{7} + \dot{m}_{16}h_{16} \quad (4.279)$$

Here, the heat transfer rate to the generator, $\dot{Q}_d$ is present in this equation, since

$$\dot{Q}_d = \dot{m}_{13}(h_{16} - h_{13}) \quad (4.280)$$

The entropy balance equation for the generator can be written as follows:

$$\dot{m}_3 s_3 + \dot{m}_{13} s_{13} + \dot{S}_{gen,g} = \dot{m}_4 s_4 + \dot{m}_7 s_7 + \dot{m}_{16} s_{16} \quad (4.281)$$

The exergy balance equation for the generator can be written as follows:

$$\dot{m}_3 ex_3 + \dot{m}_{13} ex_{13} = \dot{m}_4 ex_4 + \dot{m}_7 ex_7 + \dot{m}_{16} ex_{16} + \dot{E}x_{d,g} \quad (4.282)$$

- *Condenser 1*

The mass balance equation for the condenser 1 can be written as

$$\dot{m}_7 = \dot{m}_8 \quad (4.283)$$

The energy balance equation for the condenser 1 can be written as

$$\dot{m}_7 h_7 = \dot{m}_8 h_8 + \dot{Q}_{c1} \quad (4.284)$$

where $\dot{Q}_{c1}$ denotes the heat rejected from condenser 1.

The entropy balance equation for the condenser 1 can be written as

$$\dot{m}_7 s_7 + \dot{S}_{gen,c1} = \dot{m}_8 s_8 + \frac{\dot{Q}_{c1}}{T_0} \quad (4.285)$$

The exergy balance equation for the condenser can be written as

$$\dot{m}_7 ex_7 = \dot{m}_8 ex_8 + \dot{Q}_{c1}\left(1 - \frac{T_0}{T_S}\right) + \dot{E}x_{d,c1} \quad (4.286)$$

- *Expansion Valve 1*

For expansion valve 1, we can write the following mass balance equation:

$$\dot{m}_8 = \dot{m}_9 \quad (4.287)$$

The energy balance equation for the expansion valve 1 can be written as

$$\dot{m}_8 h_8 = \dot{m}_9 h_9 \quad (4.288)$$

The entropy balance equation for the expansion valve 1 can be written as

$$\dot{m}_8 s_8 + \dot{S}_{gen,EV1} = \dot{m}_9 s_9 \quad (4.289)$$

The exergy balance equation for the expansion valve 1 can be written as

$$\dot{m}_8 ex_8 = \dot{m}_9 ex_9 + \dot{E}x_{d,EV1} \quad (4.290)$$

- *Evaporator 1*

The mass balance equation for the evaporator 1 can be written as follows

For LiBr: $\dot{m}_9 = \dot{m}_{10}$ (4.291)

For water: $\dot{m}_{11} = \dot{m}_{12}$ (4.292)

The energy balance equation for the evaporator 1 can be written as

$$\dot{m}_9 h_9 + \dot{Q}_{e1} = \dot{m}_{10} h_{10} \quad (4.293)$$

$$\dot{m}_9 s_9 + \frac{\dot{Q}_{e1}}{T_0} + \dot{S}_{gen,e1} = \dot{m}_{10} s_{10} \quad (4.294)$$

The exergy balance equation for the evaporator 1 can be written as follows:

$$\dot{m}_9 ex_9 + \dot{Q}_{e1}\left(\frac{T_0}{T_{e1}} - 1\right) = \dot{m}_{10} ex_{10} + \dot{E}x_{d.e1} \quad (4.295)$$

- *Absorber*

The mass balance equation for the absorber can be written as follows:

$$\dot{m}_{10} + \dot{m}_6 = \dot{m}_1 \quad (4.296)$$

The energy balance equation for the absorber can be written as follows:

$$\dot{m}_{10} h_{10} + \dot{m}_6 h_6 = \dot{m}_1 h_1 + \dot{Q}_a \quad (4.297)$$

where $\dot{Q}_a$ denotes that heat loss rate from the absorber. The entropy balance equation for the absorber can be written as follows:

$$\dot{m}_{10}s_{10} + \dot{m}_6 s_6 + \dot{S}_{gen,a} = \dot{m}_1 s_1 + \frac{\dot{Q}_a}{T_0} \quad (4.298)$$

The exergy balance equation for the absorber can be written as follows:

$$\dot{m}_{10}ex_{10} + \dot{m}_6 ex_6 = \dot{m}_1 ex_1 + \dot{Q}_a\left(1 - \frac{T_0}{T_s}\right) + \dot{E}x_{d,a} \quad (4.299)$$

- *Pump 1*

The mass balance equation for the pump 1 can be written as follows:

$$\dot{m}_1 = \dot{m}_2 \quad (4.300)$$

The energy balance equation for the pump 2 can be written as follows:

$$\dot{m}_1 h_1 + \dot{W}_{p1} = \dot{m}_2 h_2 \quad (4.301)$$

The entropy balance equation for the solution pump can be written as follows:

$$\dot{m}_1 s_1 + \dot{S}_{gen,p1} = \dot{m}_2 s_2 \quad (4.302)$$

The exergy balance equation for the solution pump can be written as

$$\dot{m}_1 ex_1 + \dot{W}_{p1} = \dot{m}_2 ex_2 + \dot{E}x_{d,p1} \quad (4.303)$$

- *Heat Exchanger 1*

The mass balance equation for the heat exchanger 1 can be written as

$$\dot{m}_2 + \dot{m}_4 = \dot{m}_3 + \dot{m}_5 \quad (4.304)$$

The energy balance equation for the solution heat exchanger can be written as

$$\dot{m}_2 h_2 + \dot{m}_4 h_4 = \dot{m}_3 h_3 + \dot{m}_5 h_5 \quad (4.305)$$

The entropy balance equation for the solution heat exchanger can be written as

$$\dot{m}_2 s_2 + \dot{m}_4 s_4 + \dot{S}_{gen,HEX1} = \dot{m}_3 s_3 + \dot{m}_5 s_5 \quad (4.306)$$

The exergy balance equation for the solution heat exchanger can be written as

$$\dot{m}_2 ex_2 + \dot{m}_4 ex_4 = \dot{m}_3 ex_3 + \dot{m}_5 ex_5 + \dot{E}x_{d,HEX1} \quad (4.307)$$

- *Expansion Valve 2*

The mass balance equation for the expansion valve 2 can be as:

$$\dot{m}_5 = \dot{m}_6 \quad (4.308)$$

The energy balance equation for the expansion valve 2 can be as

$$\dot{m}_5 h_5 = \dot{m}_6 h_6 \quad (4.309)$$

The entropy balance equation for the expansion valve 2 can be as

$$\dot{m}_5 s_5 + \dot{S}_{gen,EV2} = \dot{m}_6 s_6 \quad (4.310)$$

The exergy balance equation for the expansion valve 2 can be as

$$\dot{m}_5 ex_5 = \dot{m}_6 ex_6 + \dot{E}x_{d,EV2} \quad (4.311)$$

4.7.1.2 Energy Efficiencies

The energy efficiency can be defined for the systems considered here as the ratio of useful energy output to the total energy input. In this study the energy efficiencies of the Rankine Cycle 1, absorption chiller and the overall system are presented and evaluated.

- *Rankine Cycle 1*

The energy efficiency of the Rankine Cycle 1 can be expressed as

$$\eta_{en,rc1} = \frac{\dot{W}_{HPST1} - \dot{W}_{P1}}{\dot{m}_{14} h_{14} - \dot{m}_{15} h_{15}} \quad (4.312)$$

- *Absorption Chiller*

A coefficient of performance can also be used to express the energetic performance of the absorption chiller:

$$COP_{en,ac} = \frac{\dot{Q}_{e1}}{\dot{Q}_d} \quad (4.313)$$

- *Overall System*

The energy efficiency of the overall system (Fig. 3.3) can be written as follows:

$$\eta_{en,ov} = \frac{(\dot{Q}_{e1}+\dot{m}_{28}h_{28}-\dot{m}_{27}h_{27}+\dot{m}_{22}h_{22}-\dot{m}_{21}h_{21}+\dot{W}_{HPST1}+\dot{W}_{HPST2}+\dot{W}_{LPST}-\dot{W}_{P2}-\dot{W}_{P3})}{\dot{m}_{29}h_{29}-\dot{m}_{26}h_{26}+\dot{Q}_{sol}} \quad (4.314)$$

4.7.1.3 Exergy Efficiencies

The exergy efficiency is defined here as the ratio of useful exergy output to the overall exergy input. Exergy efficiencies for the Rankine Cycle 1, absorption chiller and the overall system are presented and evaluated.

- *Rankine Cycle 1*

The exergy efficiency of the Rankine Cycle 1 can be expressed as

$$\eta_{ex,rc1} = \frac{\dot{W}_{HPST1}-\dot{W}_{P1}}{\dot{m}_{14}ex_{14}-\dot{m}_{15}ex_{15}} \quad (4.315)$$

- *Vapor Absorption Chiller*

A coefficient of performance can also be used to express the exergetic performance of the vapor absorption chiller:

$$COP_{ex,ac} = \frac{\dot{Q}_{e1}\left(\frac{T_0}{T_{e1}}-1\right)}{\dot{Q}_d\left(1-\frac{T_0}{T_s}\right)} \quad (4.316)$$

- *Overall System*

The exergy efficiency of the overall system (Fig. 3.3) can be written as follows:

$$\eta_{ex,ov} = \frac{(\dot{E}x^{Q}_{cooling}+\dot{m}_{28}ex_{28}-\dot{m}_{27}ex_{27}+\dot{m}_{22}ex_{22}-\dot{m}_{21}ex_{21}+\dot{W}_{HPST1}+\dot{W}_{HPST2}+\dot{W}_{LPST}-\dot{W}_{P2}-\dot{W}_{P3}}{\dot{m}_{29}ex_{29}-\dot{m}_{26}ex_{26}+\dot{E}x^{Q}_{sol}} \quad (4.317)$$

$$\text{where } \dot{E}x^{Q}_{cooling} = \dot{Q}_{e1}\left(\frac{T_0}{Te1}-1\right) \quad (4.318)$$

Chapter 5: Results and Discussion

The design of sustainable energy systems for buildings can be achieved by using the procedure presented in section 4. The systems that meet the different energy requirement of the buildings are shown in Figures. 3.1 to 3.3.

The electricity load of each building is determined and the optimum power system is chosen based on the minimum NPC cost, emissions and greater renewability. The renewability is measured in terms of renewable fraction. The energy and exergy analyses are also conducted to analyse the overall performance of systems for each case, and the effects of various parameters on the energy and exergy efficiencies are examined. Some dimensionless parameters to analyse the systems have also been evaluated.

5.1 Results of System 1

5.1.1 Energy and Exergy Analyses of System 1

The exergy destruction rate for the major components of System 1 are determined and shown in Fig. 5.1. The maximum destruction rate occurs in the combustion chamber and the next highest takes place in the CSP and the third highest destruction rate occurs in the HEX 2. To improve the performance of the overall system, efforts need to be made to reduce the exergy destruction in the combustion chamber, CSP, HEX 2 etc. These efforts need to be more cost effective.

The energetic and exergetic renewability ratio for the System 1 are found to be 0.91 and 0.34 respectively. Table 5.1 provide the energy and exergy efficiencies of various components in System 1.

A parametric study is carried on system component by varying different parameters. EES is used to calculated and develop the parametric study. In parametric study various parameters like ambient temperature, evaporator temperature, solar intensity etc. are varied and their effect on overall energy and exergy efficiencies of System 1 and its sub systems are studied. The ambient temperature affects the performance of most thermodynamic systems. For example, variations in the surrounding temperature can increase or decrease the systems' performance.

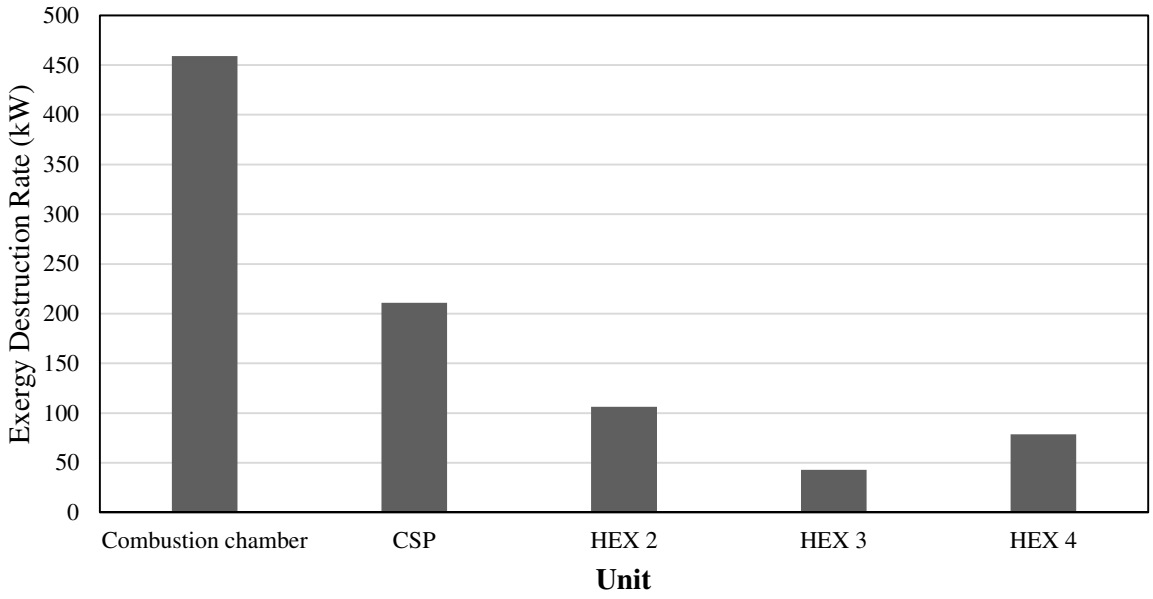

Fig. 5.1 Exergy destruction rates of selected units of System 1.

Table 5.1 Parameter values from modeling and energy and exergy analyses of System 1.

Parameter	Value
Energy efficiency of GTC (%)	43.6
Exergy efficiency of GTC (%)	32.8
Overall energy efficiency of the system (%)	91.0
Overall exergy efficiency of the system (%)	34.9
Energetic COP of the absorption chiller	0.77
Exergetic COP of the absorption chiller	0.25
Energy efficiency of ORC 1 (%)	16.4
Exergy efficiency of ORC 1 (%)	18.0

The effects of variation in the ambient temperature on the energetic and exergetic COPs of the absorption chiller are shown in Fig. 5.2. As the ambient temperature changes from 5℃ to 35℃, the energetic COP does not change while the exergetic COP varies from 0.028 to 0.397. This is due to the fact that as the ambient temperature increases the exergetic output of the evaporator increases resulting in the increase in exergetic COP. There is no change in the energetic COP of the absorption chiller because it is not a function of ambient temperature i.e. it is not associated with ambient temperature. The result shows that exergy analysis provides a better insight than energy analysis.

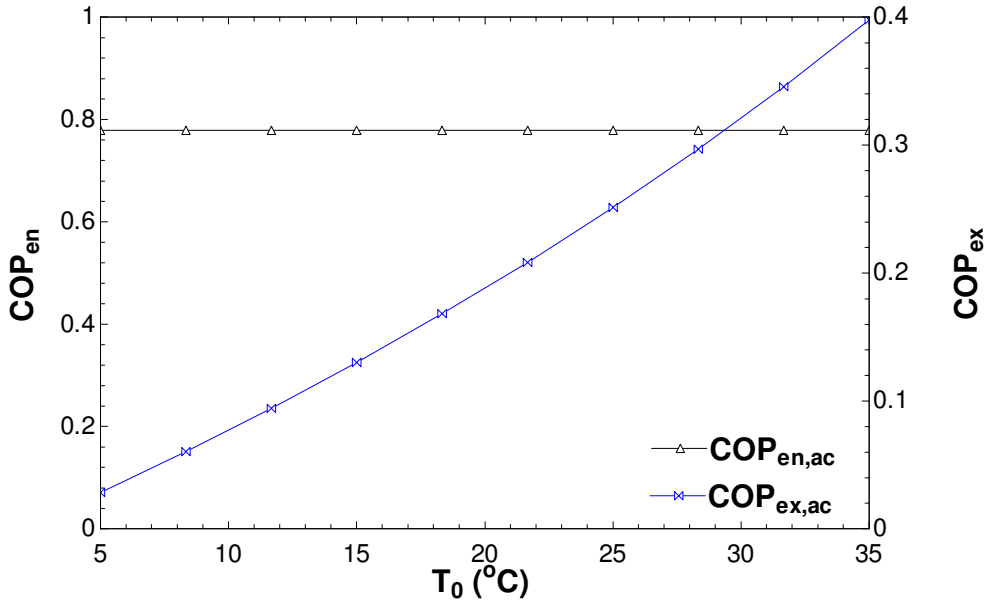

Fig. 5.2 Effect of ambient temperature on energetic and exergetic COPs of the vapor absorption chiller.

The effects of ambient temperature on the overall energy and exergy efficiencies of System 1 are shown in Fig. 5.3. As the ambient temperature increases from 5℃ to 35℃ the overall energy efficiency of System 1 does not change while the overall exergy efficiency decreases from 37.2% to 33.7%. The increase in ambient temperature decreases the exergetic output of the hot water as well as of hot air resulting in the decrease in overall exergy efficiency of System 1.

Fig. 5.4 shows the effects of combustion temperature on the energy and exergy efficiencies of Gas Turbine Cycle. As the combustion temperature changes from 700℃ to 900℃ the energy efficiency of the Gas Turbine Cycle increases from 35.0% to 52.4% while the exergy efficiency of the Gas Turbine Cycle increases from 26.3% to 39.3%.

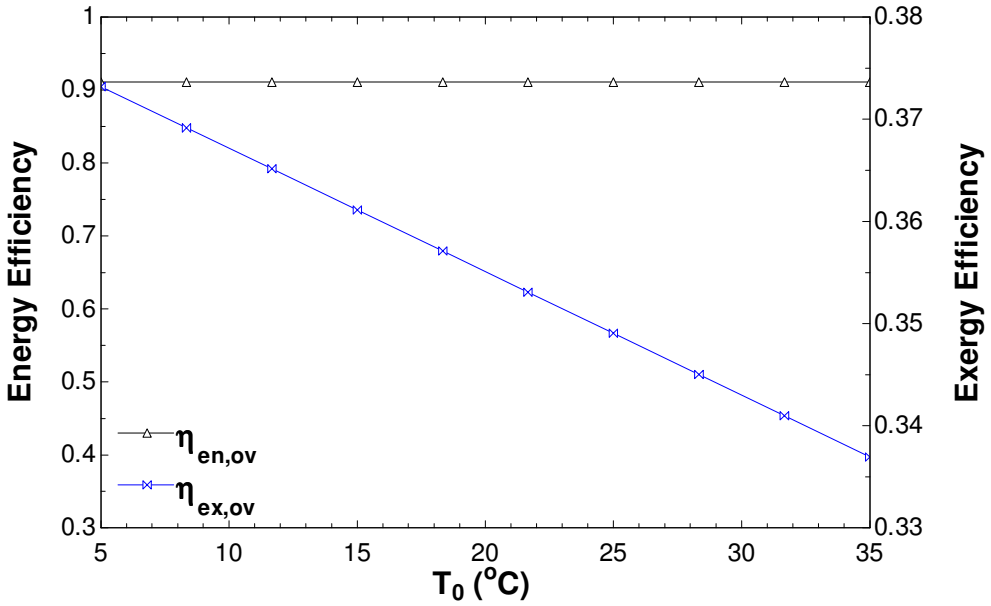

Fig. 5.3 Effect of ambient temperature on the overall energy and exergy efficiencies of System 1.

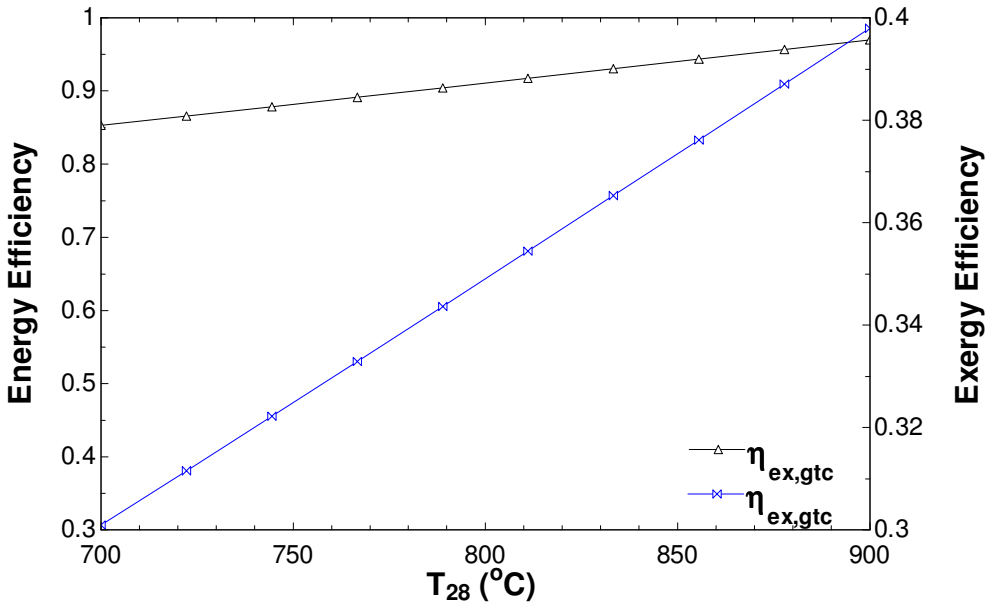

Fig. 5.4 Effect of combustion temperature on the energy and exergy efficiencies of the Gas Turbine Cycle.

Fig. 5.5 shows the effects of combustion temperature on the overall energy and exergy efficiencies of System 1. It is clearly seen that as the combustion temperature increases from700℃ to 900℃ the overall energy efficiency of System 1 increases from 85.2% to 97.0% while the overall exergy efficiency of System 1 changes from 30.0% to 39.8%.

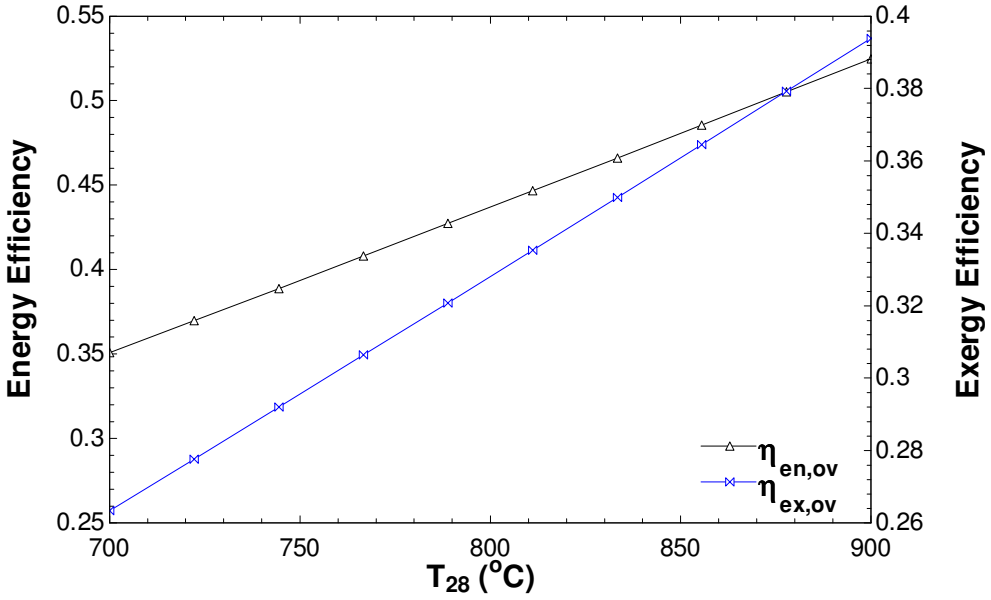

Fig. 5.5 Effect of combustion temperature (T_{28}) on the overall energy and exergy efficiencies of System 1.

Fig. 5.6 shows the effects of pressure ratio of the Gas Turbine on the energy and exergy efficiencies of the Gas Turbine Cycle. With increase in pressure ratio, both energy and exergy efficiencies first increases then decreases after reaching the optimum pressure ratio. After the optimum pressure ratio is achieved the work done by the compressor is more than the work done by the Gas Turbine resulting in decrease in energy and exergy efficiencies of the Gas Turbine Cycle.

Fig. 5.7 shows the effects of pressure ratio of the Gas Turbine on the overall energy and exergy efficiencies of System 1. As the pressure ratio increases, both the overall energy and exergy efficiencies first increases then decreases after reaching the optimum pressure ratio.

Fig. 5.8 shows the variations of energy and exergy efficiencies of the ORC 1 versus the turbine inlet pressure. As the turbine inlet pressure changes from 1000 kPa to 1400 kPa, the exergy efficiency of the ORC 1 increases from 18.0% to 22.4% while the energy efficiency of the ORC 1 increases from 16.4% to 20.5%. The increase in the turbine inlet pressure results in the increase in work output of the ORC 1 turbine.

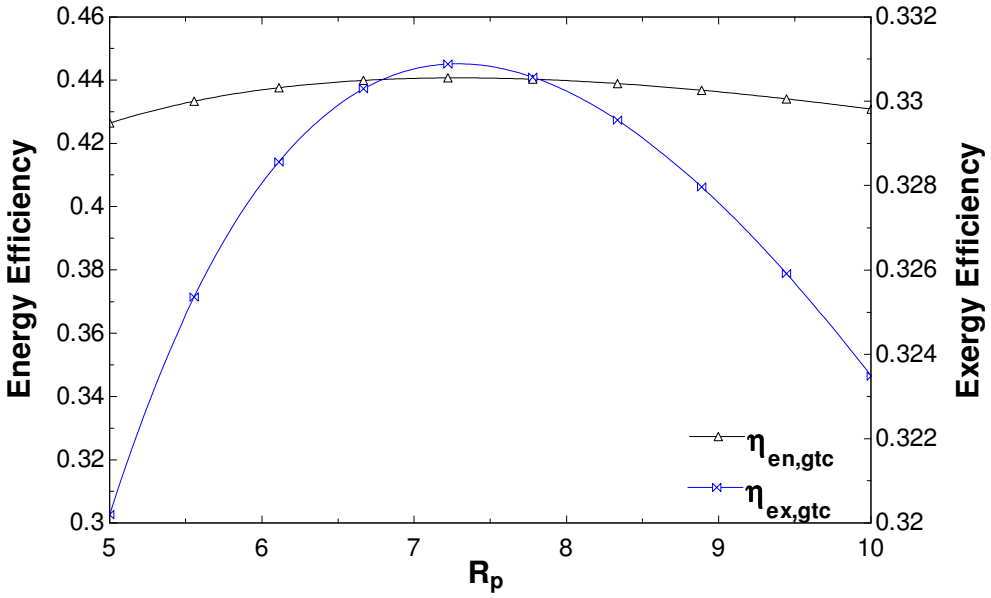

Fig. 5.6 Effect of pressure ratio of the Gas Turbine on the energy and exergy efficiencies of the Gas Turbine Cycle.

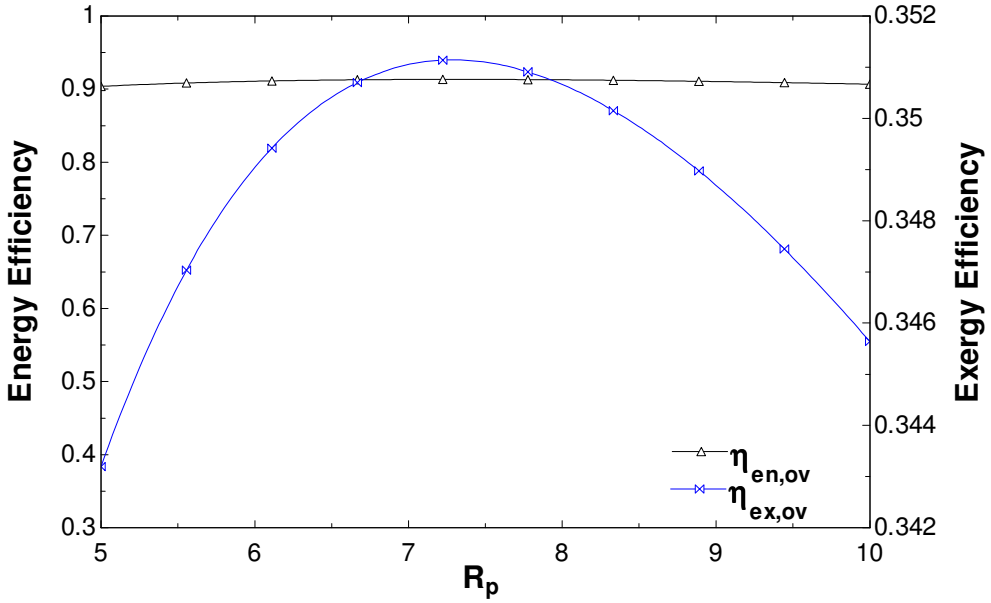

Fig. 5.7 Effect of pressure ratio on the overall energy and exergy efficiencies of System 1.

Fig. 5.9 shows the effects of ORC 1 turbine inlet pressure (P_{13}) on the overall energy and exergy efficiency of System 1. As the inlet pressure of the turbine increases from 1000 kPa to 1400 kPa, the exergy efficiency of the overall system increases from 34.9% to 35.4% while the energy efficiency of the overall system increases from 91.0% to 91.7%.

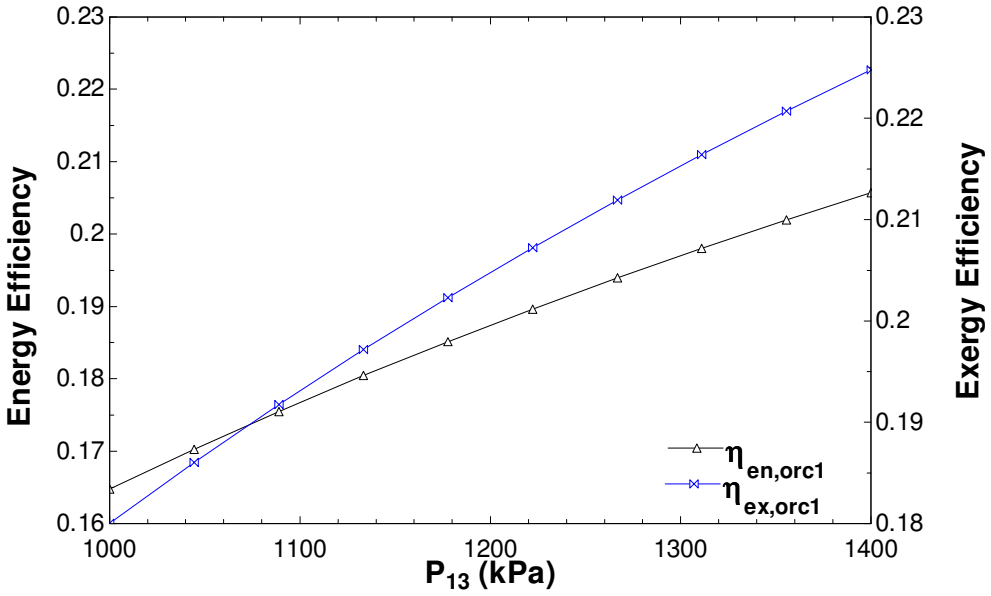

Fig. 5.8 Effect of ORC 1 turbine inlet pressure (P_{13}) on the energy and exergy efficiencies of ORC 1.

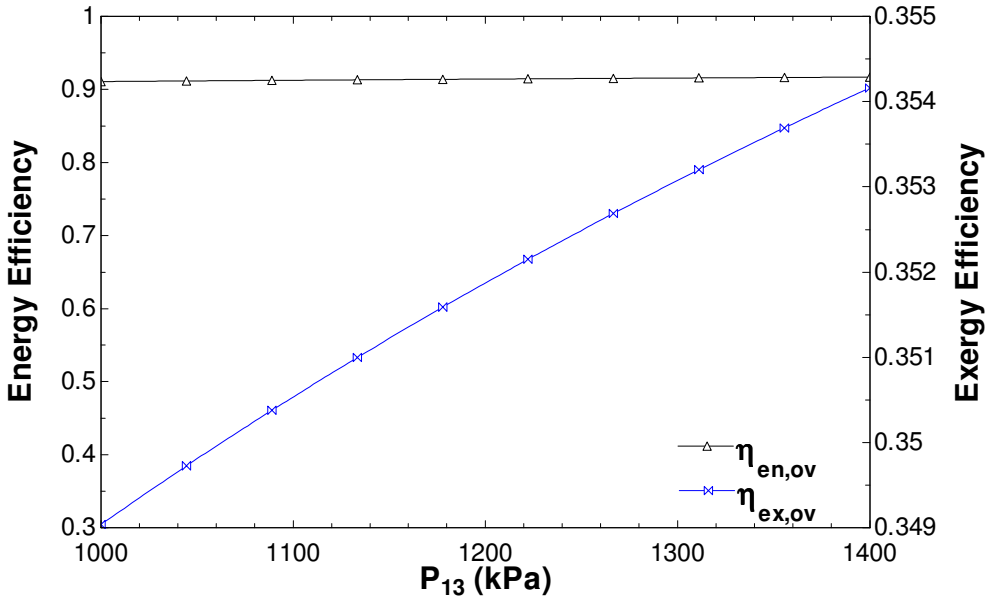

Fig. 5.9 Effect of ORC turbine inlet pressure (P_{13}) on the overall energy and exergy efficiencies of System 1.

Fig. 5.10 shows the effects of compressor inlet temperature (T_{32}) on the energy and exergy efficiencies of the Gas Turbine Cycle. As the compressor inlet temperature increases both the energy and exergy efficiencies of the Gas Turbine Cycle decreases. This is because of the fact that the increase in inlet temperature of the compressor results

in a higher compressor work which finally leads to a decrease in energy and exergy efficiencies of the Gas Turbine Cycle.

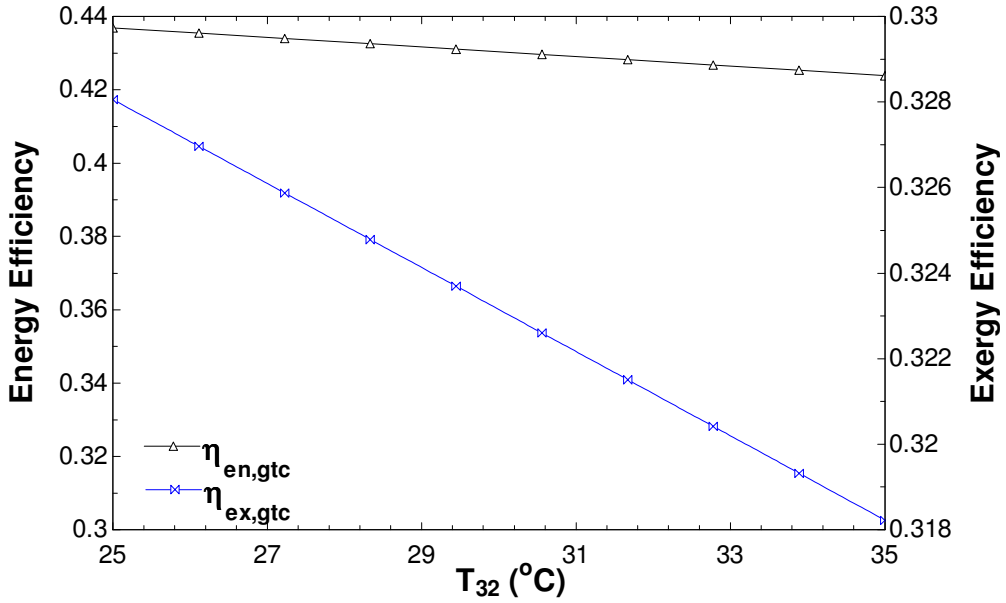

Fig. 5.10 Effect of inlet temperature (T_{32}) of compressor on the energy and exergy efficiencies of the Gas Turbine Cycle.

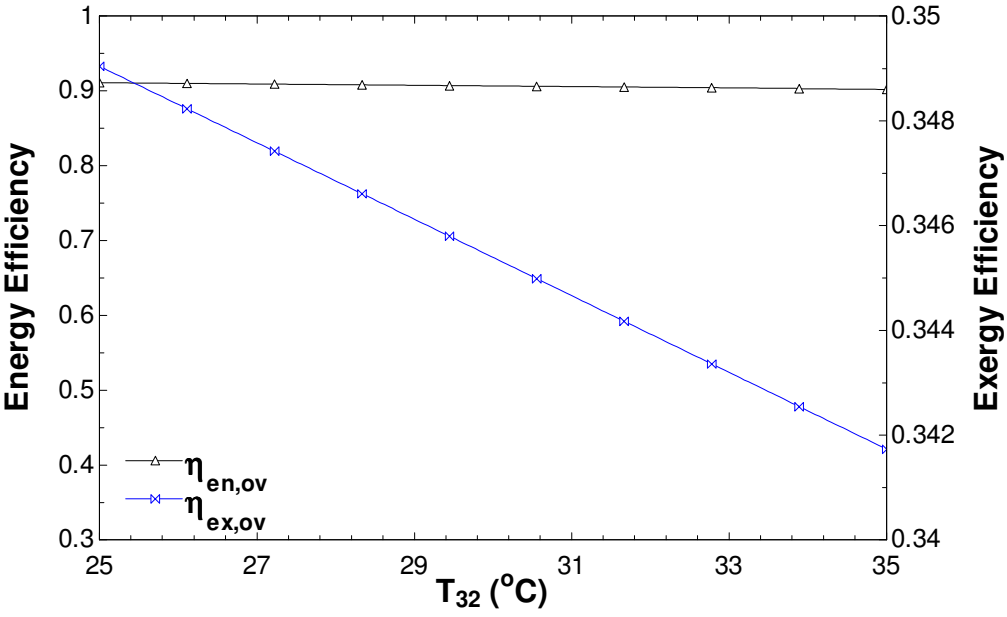

Fig. 5.11 Effect of inlet temperature (T_{32}) of compressor on the overall energy and exergy efficiencies of System 1.

Fig. 5.11 shows the effects of inlet temperature (T_{32}) of compressor on the overall energy and exergy efficiencies of system 1. The increase in inlet temperature of the compressor results in the decrease in the overall energy and exergy efficiencies of System 1.

5.1.2 Optimised power System 1

Optimisation of renewable energy power systems in this thesis study is based on the minimisation of total net present cost and the carbon dioxide emissions. Fig. 5.12 shows the optimised power system considered in the study for System 1. A large number of simulations are conducted on the HOMER, and the best suited results are presented in Table 5.2. It shows that it requires 150 kW biomass generator, 220 kW ORC turbine, 100 batteries of 6 Volt capacity each, 90 kW rectifier and 90 kW inverter. Table 5.3 shows the cost summary of the optimised system having the cost of electricity as $0.117/kWh and the total cost of the System 1 as $2,700,496.

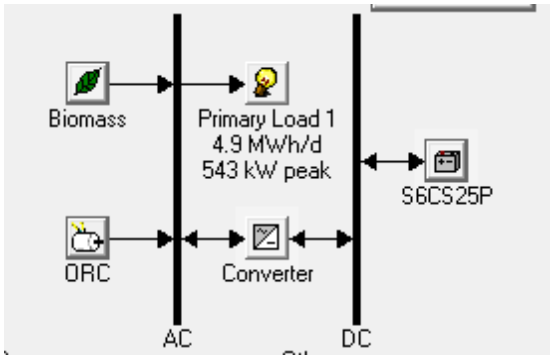

Fig. 5.12 Optimised power System 1.

Table 5.2 Architecture of the optimised power System 1.

Biomass generator	150 kW
ORC	100 kW
Battery	100 Surrette 6CS25P
Inverter	90 kW
Rectifier	90 kW

Table 5.3 Cost summary of the optimised power System 1.

Total net present cost	$ 2,700,496
Levelised cost of energy	$ 0.117/kWh
Operating cost	$ 174,875/yr

Table 5.4 shows the total net present cost of the optimised renewable energy system based on all components which is further divided as capital, replacement, salvage and other costs. Fig. 5.13 shows the cash flow summary of the optimised renewable energy system. The capital cost of the ORC is around 48% of the total capital cost of the system while on the other hand the biomass generator is cheaper in terms of initial capital cost as well as in terms of operation cost.

Table 5.4 Optimised power System 1 net present costs.

Component	Capital Cost ($)	Replacement Cost ($)	Operation and Maintenance Cost ($)	Fuel Cost ($)	Salvage Cost ($)	Total Cost ($)
Biomass generator	150,000	156,951	37,411	216,646	-20,923	540,083
ORC	220,000	1,406,241	242,283	0	-29,603	1,838,921
Surrette 6CS25P	50,000	37,526	63,917	0	-2,227	149,216
Converter	45,000	1,502	115,050	0	-2,796	172,276
System	465,000	1,615,739	458,8661	216,646	-55,549	2,700,497

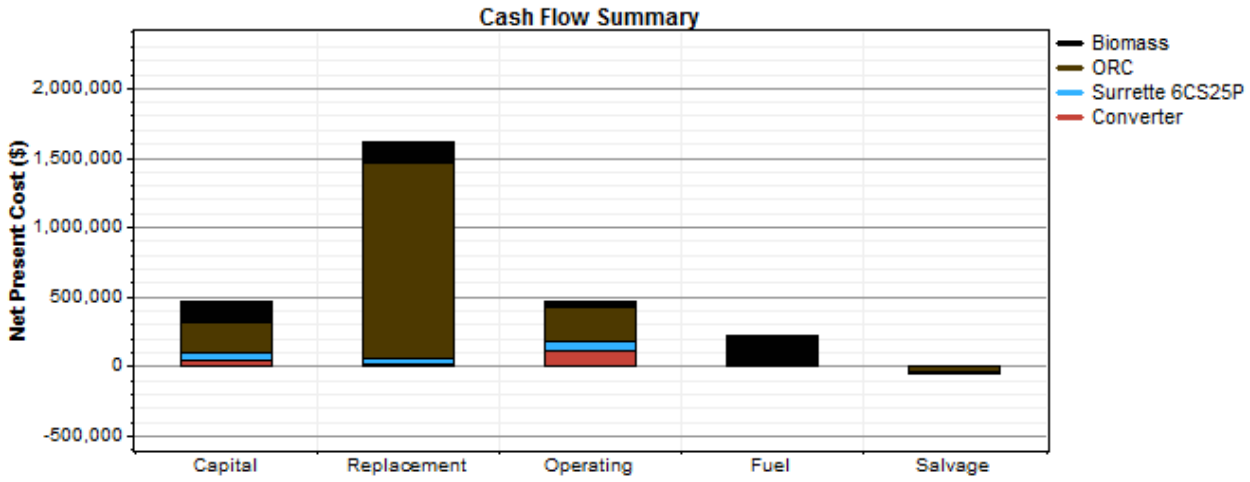

Fig. 5.13 Cash flow summary of the optimised power System 1 based on the selected component.

Table 5.5 shows the annualised cost of the optimised system with detailed cost type. The annual cost for the ORC is found to be more compared to biomass generator. The annualised cost helps in determining the levelised cost of electricity. Fig. 5.14 shows the annualised cash flow summary of the optimised system. The salvage value is taken as negative (-ve) since it is added value or it the money we actually save at the end of the

project. The salvage cost of any component depends on its replacement cost instead of the initial capital cost.

Table 5.5 Optimised power System 1 annualised costs.

Component	Capital Cost ($)	Replacement Cost ($)	Operation and Maintenance Cost ($)	Fuel Cost ($)	Salvage Cost ($)	Total Cost ($)
Biomass generator	11,734	12,278	2,927	16,947	-1,637	42,249
ORC	17,210	110,006	18,953	0	-2,316	143,853
Surrette 6CS25P	3,911	2,936	5,000	0	-174	11,673
Converter	3,520	1,175	9,000	0	-219	13,477
System	36,375	126,394	35,800	16,947	-4,345	211,251

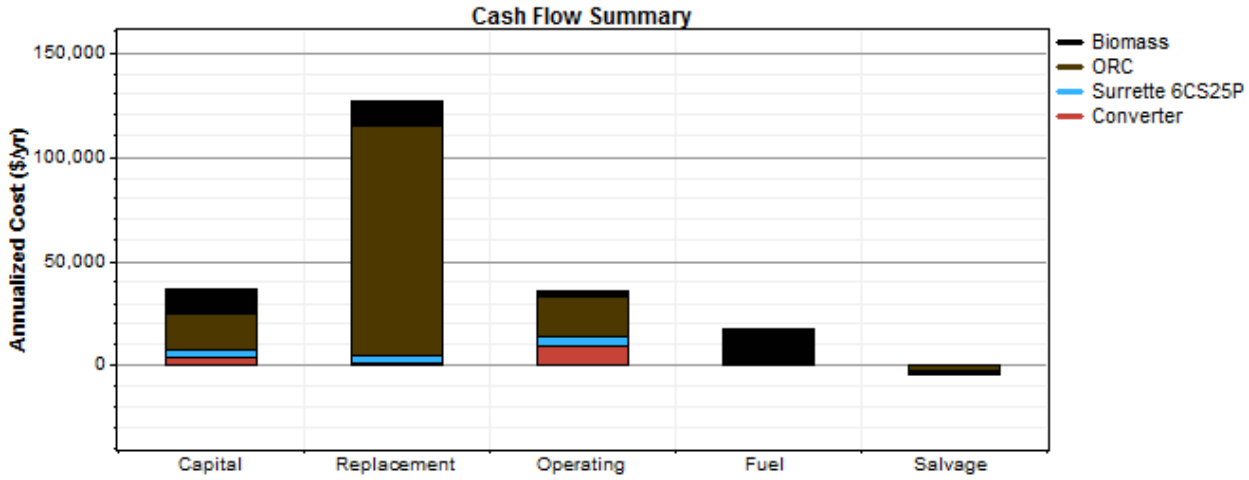

Fig. 5.14 Annual cash flow summary of the optimised power System 1 based on the selected component.

The nominal cash summary of the optimised renewable energy system is presented in Fig. 5.15. The nominal cash is the amount that one gets after subtracting the annual income from the actual cost. Fig. 5.16 shows the discounted cash flow summary of the optimised renewable energy system with the detailed component.

As seen from Table 5.7 the electricity produced by ORC is 92% of the total electricity produced i.e. 1,708,035 kWh annually while the electricity produced by biomass generator annually is 145,215 kWh that makes 8% of the total electricity production.

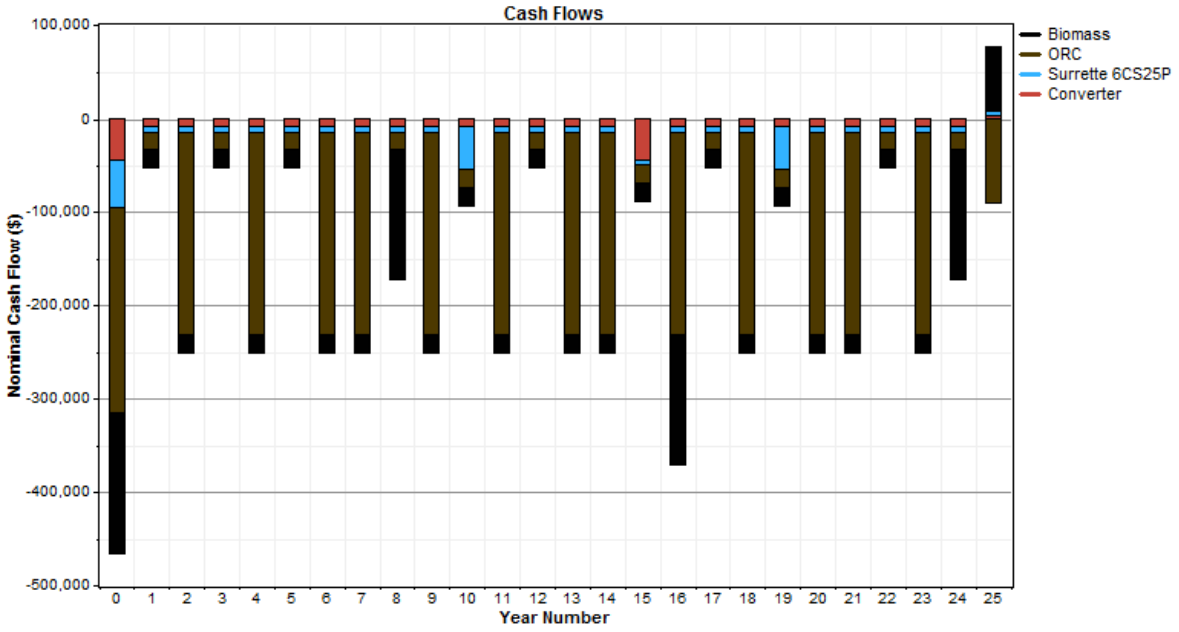

Fig. 5.15 Nominal cash flow summary of the optimised power System 1.

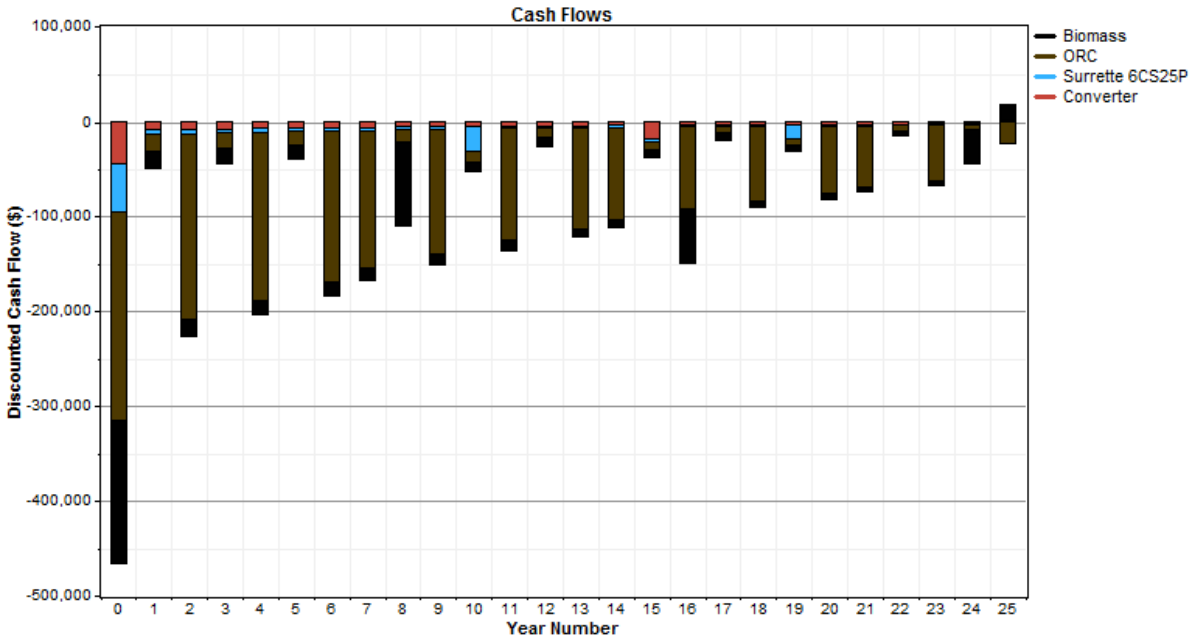

Fig. 5.16 Discounted cash flow summary of the optimised power System 1.

The excess electricity produced by the system is found to be negligible. Fig. 5.17 shows the monthly production of electricity production by ORC turbine and biomass generator. It is clear from the Fig. 5.17 that the electricity produced by ORC becomes more compared to biomass generator.

Table 5.6 Optimised power System 1 electrical configuration.

Component	Production (kWh/yr)	Fraction (%)
Biomass generator	145,215	8
ORC	1,708,035	92
Excess electricity	0.0181	0.00

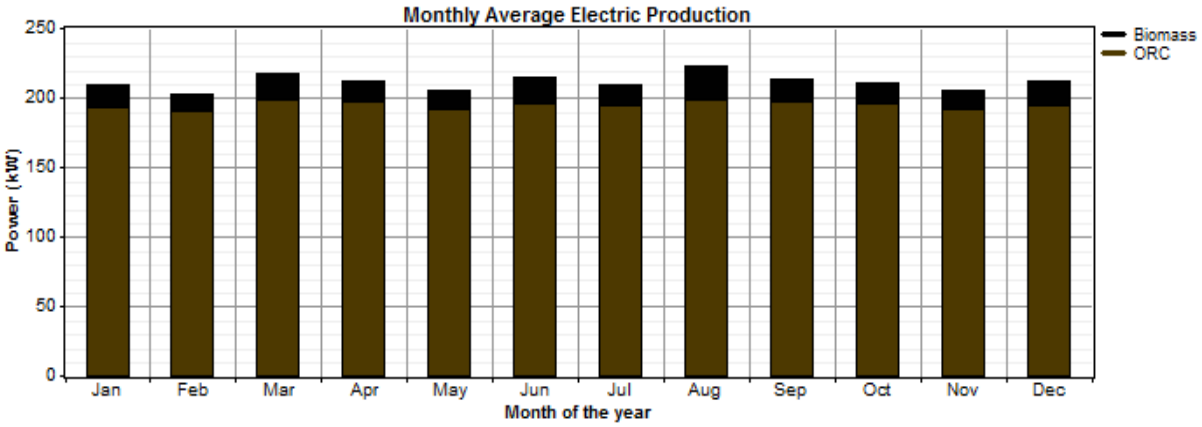

Fig. 5.17 Monthly production of electricity for the optimised power System 1.

Table 5.7 shows the detailed configuration of the biomass generator for System 1. The rated capacity of the biomass generator is 150 kW, and the mean output is 74.4 kW. The nominal efficiency of the biomass generator is 11.1% while its operation hours are 1,951 per year. Fig. 5.18 shows the monthly electrical output of the biomass generator utilized in the system.

Table 5.7 Biomass generator electrical configuration for optimised power System 1.

Quantity	Value	Units
Rated capacity	150.0	kW
Mean output	74.4	kW
Minimum output	45.0	kW
Capacity factor	11.1	%
Total production	15,432	kWh/yr
Maximum output	150	kW
Hours of operation	1,951	h/yr
Biomass feedstock consumption	314	t/yr
Specific fuel consumption	2.16	kg/kWh

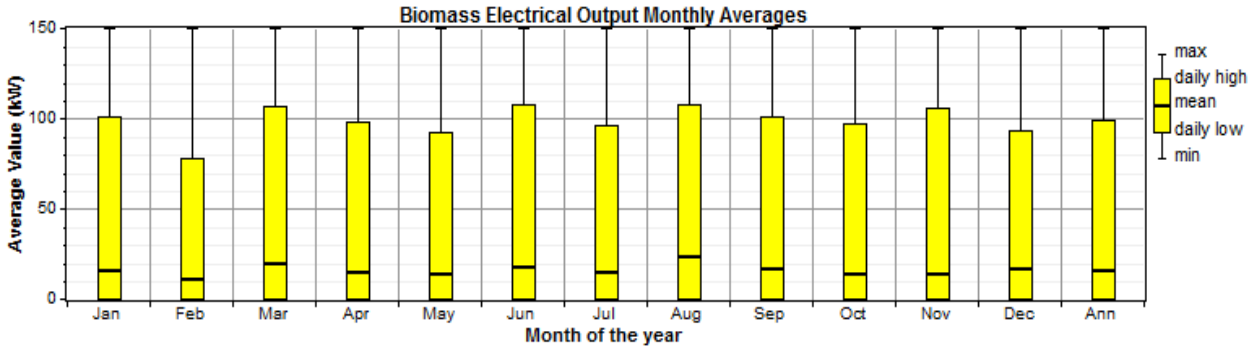

Fig. 5.18 Biomass generator electric output for optimised power System 1.

Table 5.8 and Fig 5.19 show the ORC turbine electrical configuration and electricity output respectively. As evident in Table 5.8, the rated capacity of the ORC turbine is 220 kW and its mean output is 198 kW. The ORC turbine operates for 8,613 hours annually. The efficiency of the ORC is 88.6 %.

Table 5.8 ORC turbine electrical configuration for optimised power System 1.

Quantity	Value	Units
Rated capacity	220	kW
Mean output	198	kW
Capacity factor	88.6	%
Total production	1,708,035	kWh/yr
Minimum output	85.6	kW
Maximum output	220	kW
Hours of operation	8,613	h/yr

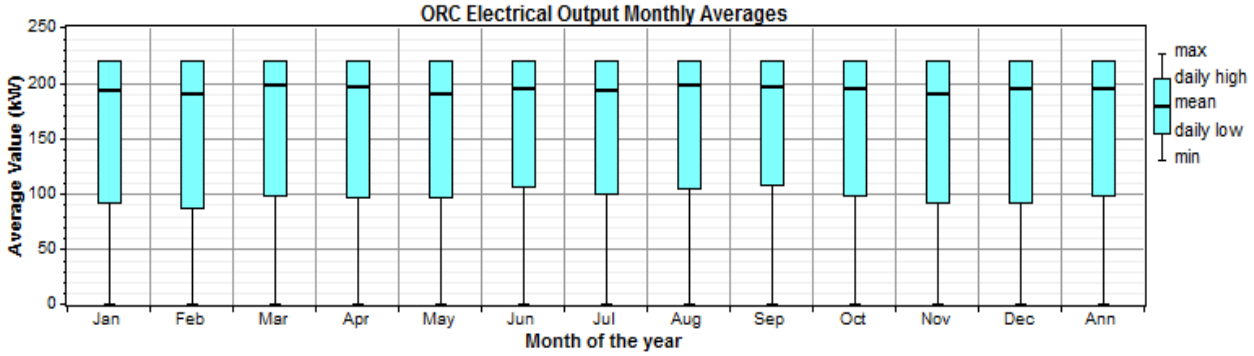

Fig. 5.19 ORC turbine electric output for optimised power System 1.

Table 5.9 Battery system architecture for optimised power System 1.

Quantity	Value
String size	1
Strings in parallel	100
Batteries	100
Bus voltage (V)	6

Tables 5.9 and 5.10 provide the battery architecture and electrical configuration respectively. Table 5.10 shows that for the optimised power System 1 it requires 100 batteries. The current produced by each battery is 6 Volts. The nominal capacity and usable capacity of the battery are 694 kWh and 416 kWh respectively (see Table 5.10). The average battery wear cost is 0.046 $/kWh and average life of 9.05 year. There is throughput of 106,524 kWh annually through the battery bank.

Table 5.10 Battery system electrical configuration for optimised power System 1.

Quantity	Value	Units
Nominal capacity	694	kWh
Usable nominal capacity	416	kWh
Autonomy	2.03	h
Lifetime throughput	964,520	kWh
Battery wear cost	0.046	$/kWh
Average energy cost	0.029	$/kWh
Energy in	118,952	kWh/yr
Energy out	95,278	kWh/yr
Storage depletion	119	kWh/yr
Losses	23,554	kWh/yr
Annual throughput	106,524	kWh/yr
Expected life	9.05	yr

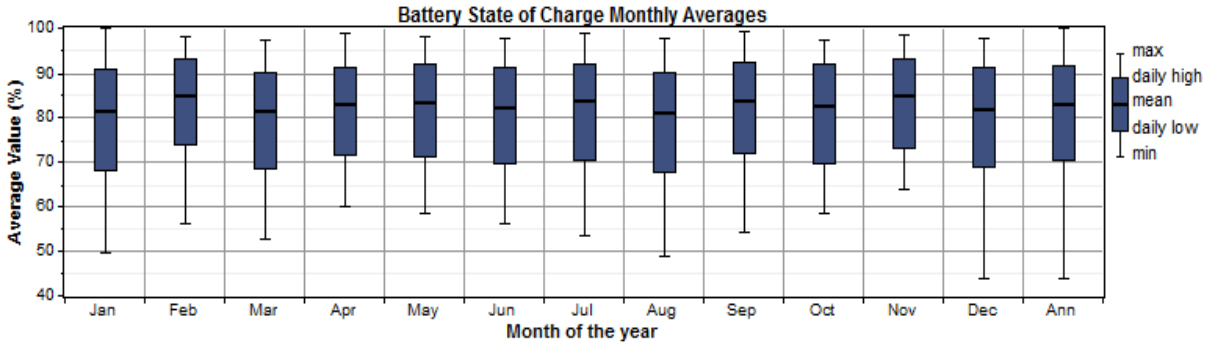

Fig. 5.20 Battery system charging state (%) for optimised power System 1.

The monthly battery state of charge throughout the year is shown in Fig. 5.20. It is evident from Fig. 5.20 that a minimum state of charge for the battery is around 40%, which means that one cannot go beyond this for the battery due to breakdown. Most of the times in the year the battery is almost 80% charged.

Table 5.11 shows the converter electrical configuration. The capacity of the inverter is found to be 90 kW with a mean output of 9.8 kW. The efficiency of the inverter is 10.9% while it operates for 2,292 hours annually. There is a loss of 9,528 kWh of energy annually. Fig. 5.21 shows the electrical output of the inverter. The inverter produces almost constant power in all the months.

The different renewable energy systems are presented in Table. 5.12. If the system operates only on biomass the cost is more as compared to case in which the system operates on a combination of biomass and ORC. For the case of biomass driven system the cost is maximum i.e $5,495,906.

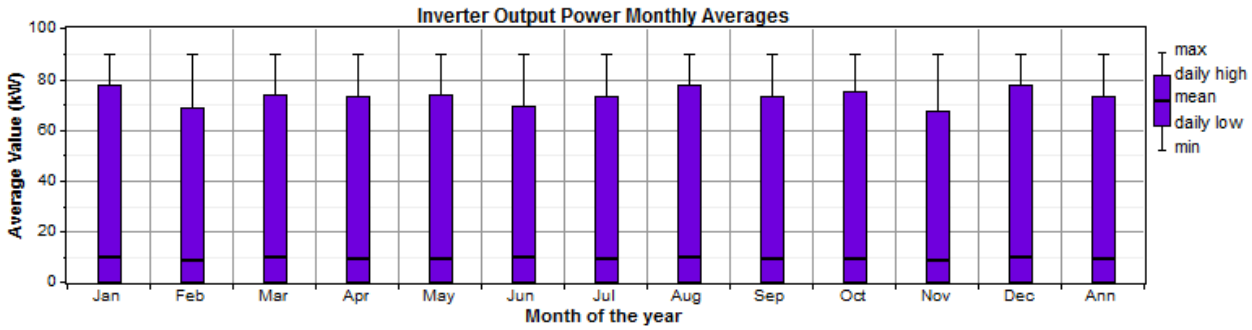

Fig. 5.21 Inverter electrical output for optimised power System 1.

Table 5.11 Converter electrical configuration for optimised power System 1.

Quantity	Inverter	Rectifier	Units
Capacity	90.0	90.0	kW
Mean output	9.8	13.6	kW
Minimum output	0.0	0.00	kW
Maximum output	90	27.5	kW
Capacity factor	10.9	15.1	%
Hours of operation	2,292	6,466	h/yr
Energy in	95,278	139,951	kWh/yr
Energy out	85,751	118,952	kWh/yr
Losses	9,528	20,999	kWh/yr

Table 5.12 Total net present cost for different optimised power System 1.

Power Structure	Biomass generator (kW)	ORC (kW)	Battery quantity and type (Surrette 6CS25P)	Converter capacity (kW)	Total net present cost ($)
1	150	220	100	90	2,700,496
2	250	220	-	-	3,485,647
3	300	-	200	200	5,495,906

5.1.3 Optimisation of Overall Exergy Efficiency of System 1.

Fig. 5.22 shows the optimisation results of the overall exergy efficiency of System 1. As the function call increases, the exergy efficiency increases from 33.4 % to 50.2%. After 1047 function call the exergy efficiency converges to 50.2%. In this regard, further increase in function call will not have any effect on the overall exergy efficiency of the System 1.

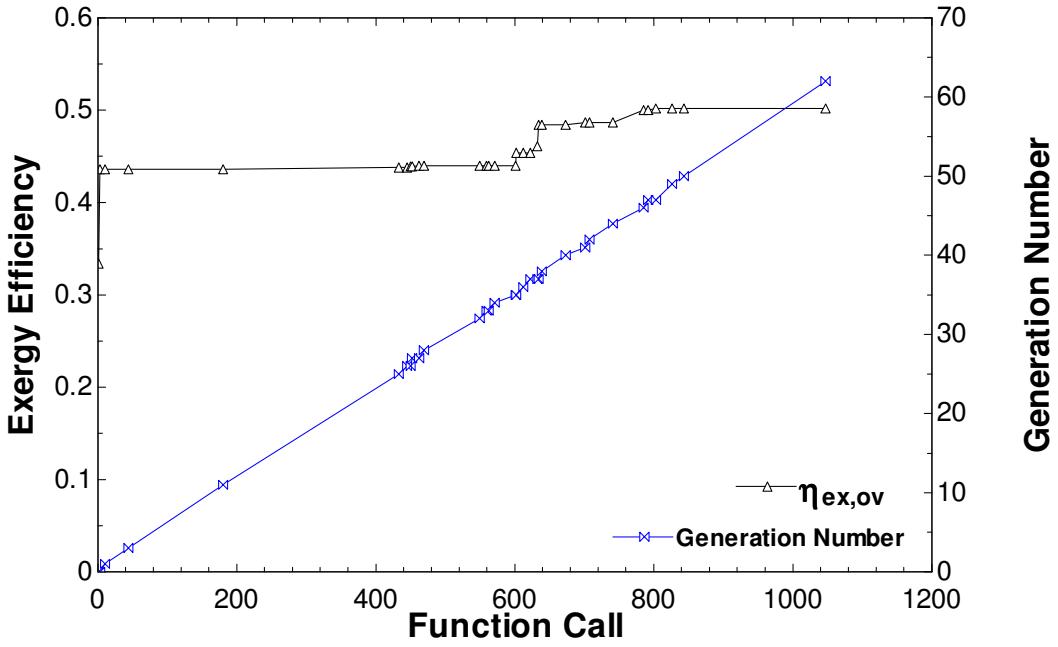

Fig. 5.22 Optimisation of overall exergy efficiency of System 1.

5.2 Results of System 2

5.2.1 Energy and Exergy Analyses of System 2

The exergy destruction rates for the major components of System 2 are determined and shown in Fig. 5.23. The maximum destruction rate occurs in the concentrated solar collector, the next highest takes place in the wind turbine and the third highest destruction rate occurs in the storage tank. To improve the performance of the overall system, the efforts are needed to reduce the exergy destruction in the wind turbine, concentrated solar collector, and storage tank. Table 5.13 provides the energy and exergy efficiencies of the various component of System 2.

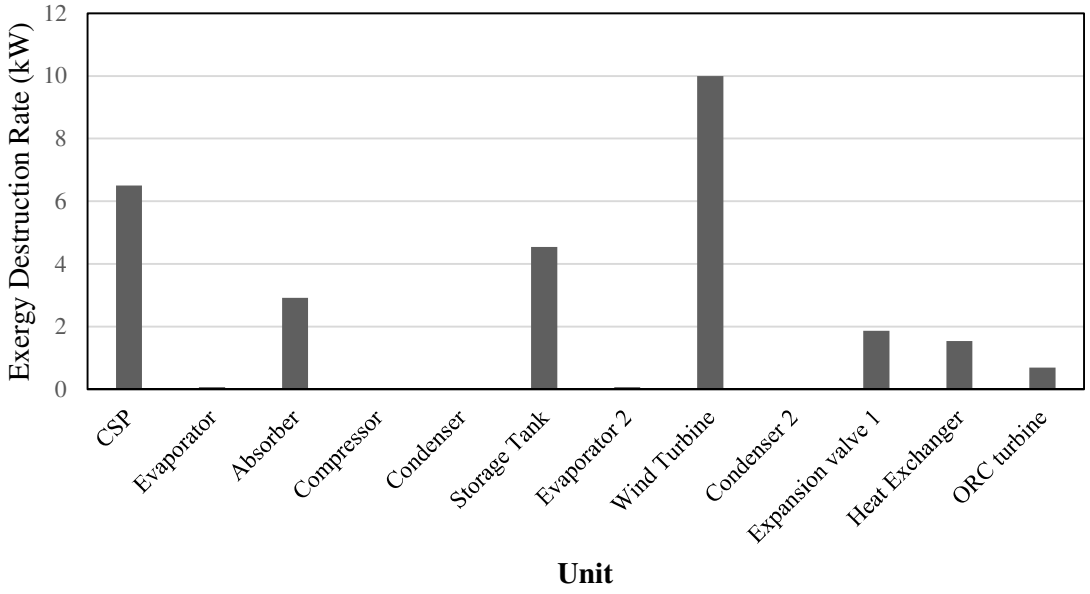

Fig. 5.23 Exergy destruction rates of selected units of System 2.

The effects of ambient temperature on the overall energy and exergy efficiencies of the System 2 are shown in Fig. 5.24. As the ambient temperature changes from 25℃ to 35℃, there is no change in the overall energy efficiency while the overall exergy efficiency of the system changes from 16.2% to 16.9%. The reason for this trend is that with increasing the ambient temperature the exergetic input of the absorption chiller generator decreases and the exergetic output of the absorption increases resulting in the increase in exergy efficiency of the system.

Table 5.13 Parameter values from modeling and energy and exergy analyses of the System 2.

Parameter	Value
Output of ORC turbine (kW)	7.77
Cooling load (kW)	24.1
Energy efficiency of ORC (%)	15.8
Exergy efficiency of ORC (%)	84.5
Overall energy efficiency of the System (%)	34.6
Overall exergy efficiency of the System (%)	16.2
Energetic COP of the ground source heat pump	5.27
Exergetic COP of the ground source heat pump	0.32
Energetic COP of the absorption chiller	0.77
Exergetic COP of the absorption chiller	0.27

The variations of energetic and exergetic COPs of the absorption cooling cycle with ambient temperature are shown in Fig. 5.25. As the ambient temperature increases from 25℃ to 35℃, there is no change in the energetic COP while the exergetic COP increases from 0.27 to 0.43. This is due to the fact that as the ambient temperature increases the exergetic COP of the evaporator increases resulting in the increase in exergetic COP.

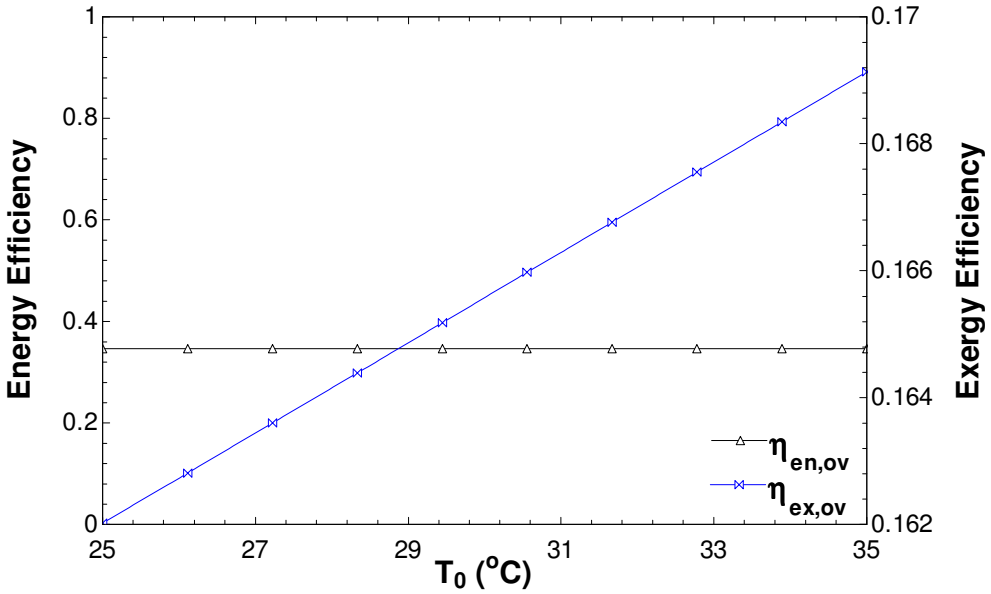

Fig. 5.24 Effect of ambient temperature (T_0) on the overall energy and exergy efficiencies of System 2.

Fig. 5.26 shows the variations of ambient temperature with energetic and exergetic COP of the ground source heat pump. As the ambient temperature increases, the exergetic COP

decreases while the energetic COP remains same. The exergetic COP changes from 0.32 to 0.16 as the ambient temperature changes from 25℃ o 35℃. The reason for the above change is that as the ambient temperature increases the exergetic output of the condenser of the ground source heat pump decreases.

The effects of ambient temperature on the energy and exergy efficiencies of the Organic Rankine Cycle are shown in Fig. 5.27. As the ambient temperature changes from 25℃ to 35℃ the exergy efficiency of the ORC increases from 84.5% to 98.1% while the energy efficiency remains the same. This is due to the fact that as the ambient temperature increases the exergy destruction due to heat loss from the boiler of the ORC i.e. storage tank decreases resulting in the increase in exergy efficiency of the ORC.

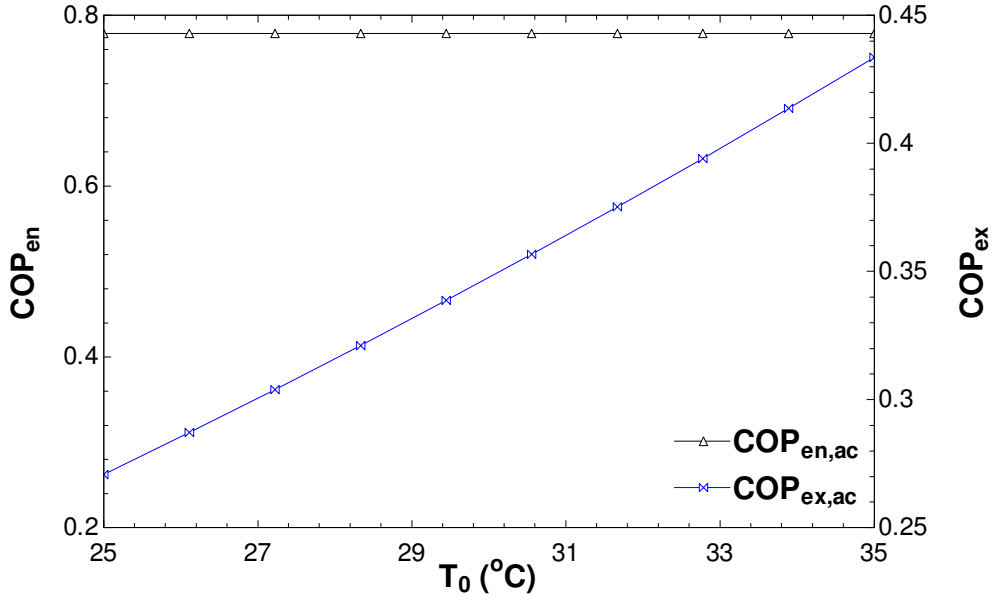

Fig. 5.25 Effect of ambient temperature (T_0) on the energetic and exergetic COPs of the absorption chiller.

The effects of outlet temperature of the concentrated solar collector on the overall energy and exergy efficiencies of the system are shown in Fig. 5.28. As the temperature increases from 140℃ to 180℃ , both the energy and exergy efficiencies decrease. This is due to the fact that as the outlet temperature of oil increases the heat loss and thermal exergy loss in the storage tank increases while the output of the storage tank is fixed.

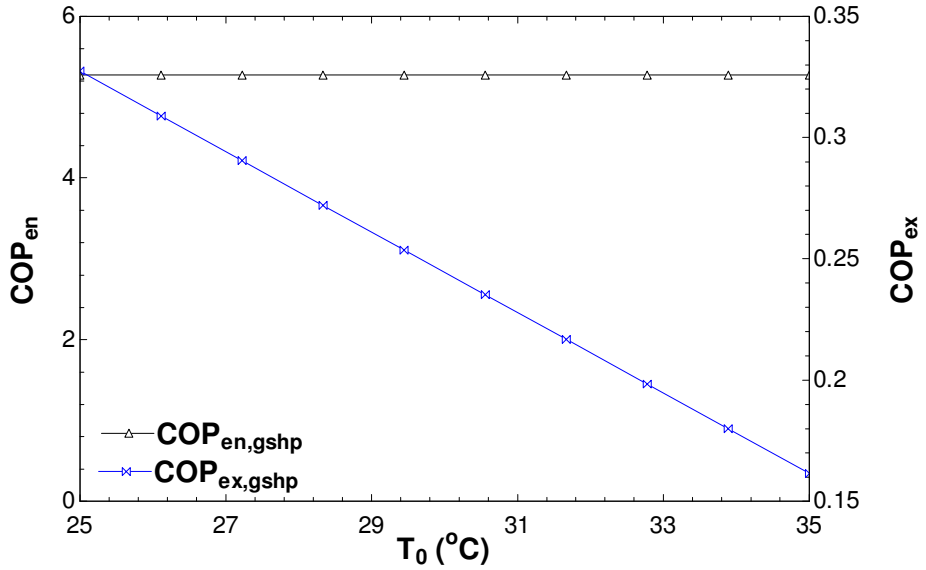

Fig. 5.26 Effect of ambient temperature (T_0) on the energetic and exergetic COPs of the ground source heat pump.

Fig. 5.29 shows the effects of aperture area on the overall energy and exergy efficiencies of the system. As the aperture area changes from 120 m^2 to 200 m^2 the energy efficiency of the system decreases from 37.0% to 32.0% and the exergy efficiency decreases from 19.0% to 13.1%. This is due to the fact that as the aperture area increases the solar input to the system increases and the output of the system also increases but the rate at which solar input increases is higher than the work output rate.

Fig. 5.30 shows the effect of solar irradiation on the overall energy and exergy efficiencies of the system. As the solar irradiation changes from 0.4 kW/m^2 to 1.0 kW/m^2 the overall energy efficiency of the system changes from 41.3% to 31.5% while the overall exergy efficiency decreases from 24.0% to 12.4%. The reason for this kind of the trend is that as on increasing the solar irradiation the energy input to the system increases as well as the energy output of the system increases but the rate at which energy input increase is more the rate at which output increase resulting in the decrease in the energy and exergy efficiencies of the overall system.

Fig. 5.31 shows the effect of ORC turbine inlet pressure (P_{16}) on the overall energy and exergy efficiencies of System 2. As the inlet pressure of the turbine increases from 600 kPa to 1200 kPa, the overall exergy efficiency of the system increases from 13.2 % to 17.2 % while the overall energy efficiency of the system increases from 31.7% to 35.7%.

The increase in the turbine inlet pressure results in increase in the work output of the ORC turbine which eventually leads to the increase in overall energy and exergy efficiencies of the system.

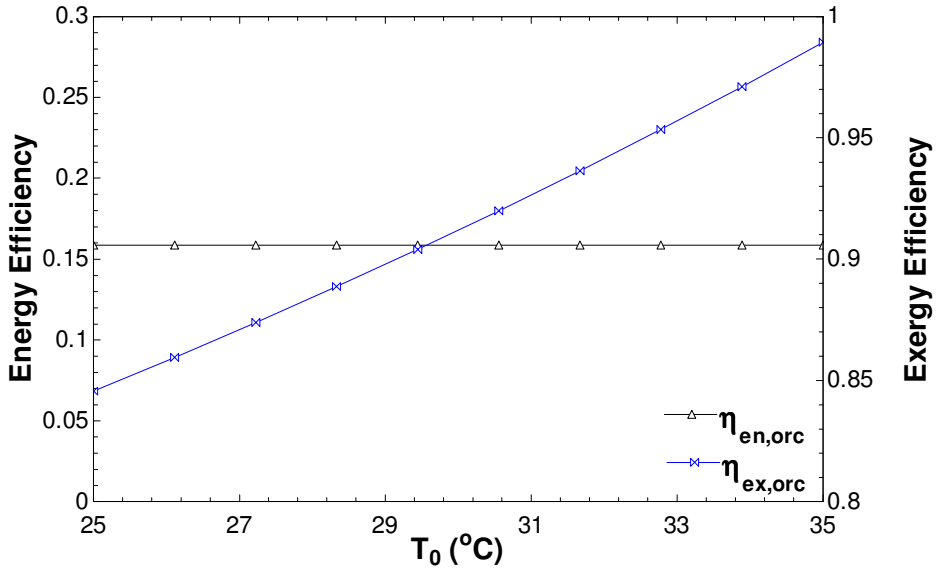

Fig. 5.27 Effect of ambient temperature (T_0) on the overall energy and exergy efficiencies of the ORC.

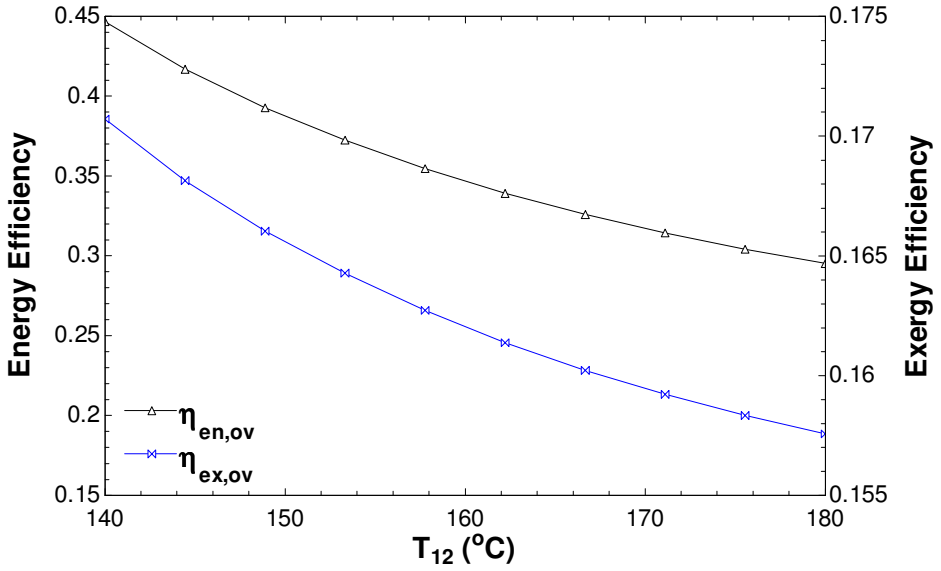

Fig. 5.28 Effect of overall energy and exergy efficiencies of System 2 with the oil outlet temperature (T_{12}) of the concentrated solar collector

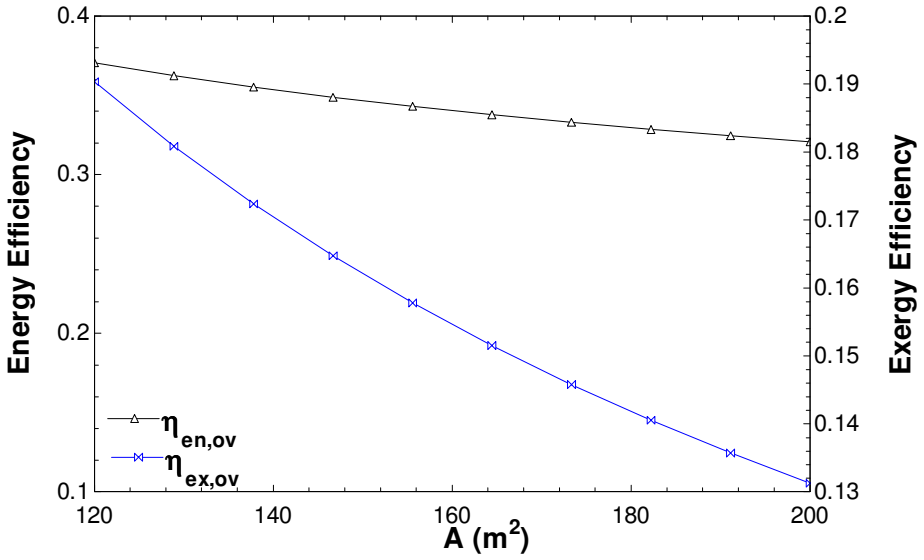

Fig. 5.29 Effect of aperture area of the concentrated solar panel on the overall energy and exergy efficiencies of System 2.

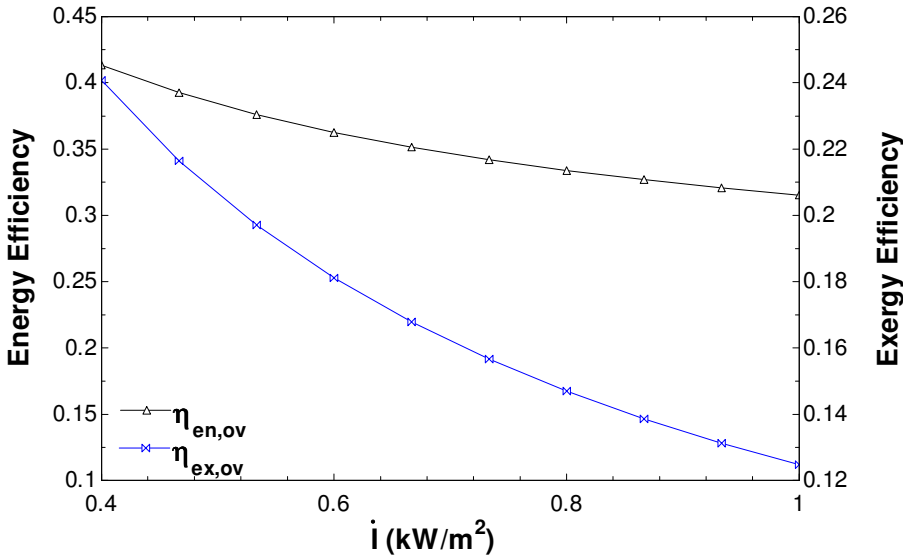

Fig. 5.30 Effect of solar irradiation on the overall energy and exergy efficiencies of System 2.

Fig. 5.32 shows the variations of energy and exergy efficiencies of the ORC with the turbine inlet pressure. As the turbine inlet pressure changes from 600 kPa to 1200 kPa, the exergy efficiency of the ORC increases from 58.2% to 91.5% while the energy efficiency of the ORC increases from 9.0% to 18.1%.

The effects of outlet temperature of the turbine on the energy and exergy efficiencies of the ORC are shown in Fig. 5.33. As the outlet temperature of the turbine changes from 55℃ to 65℃ , the energy efficiency of the ORC decreases from 17.7 % to 13.9% while the exergy efficiency of the ORC changes from 94.8% to 74.1%. The reason for this kind of the trend is that as the outlet temperature of the turbine increases the work output of the turbine decreases resulting in the decrease in energy and exergy efficiencies of the ORC.

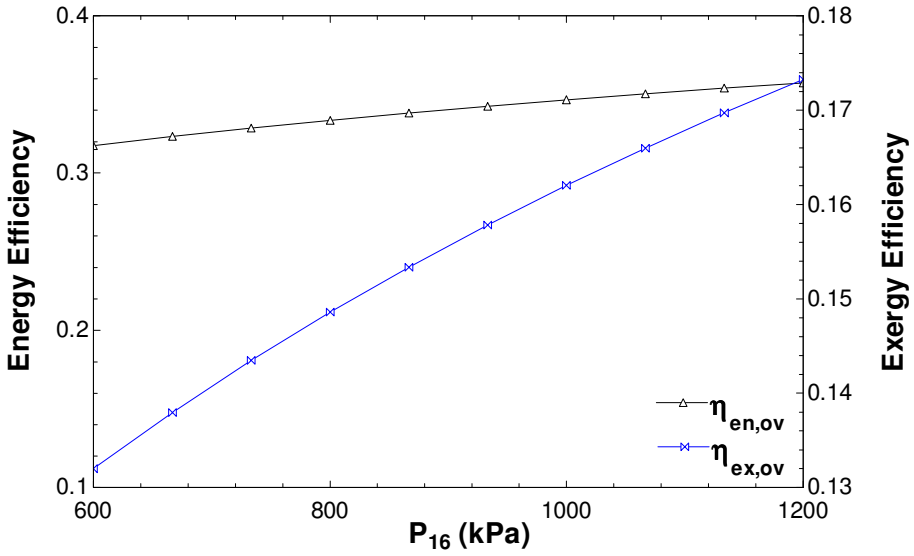

Fig. 5.31 Effect of ORC turbine inlet pressure (P_{16}) on the overall energy and exergy efficiencies of System 2.

Fig. 5.34 shows the effects of outlet temperature of the turbine on the overall energy and exergy efficiencies of the System 2. As the outlet temperature of the turbine changes from 55℃ to 65℃, the overall energy efficiency of the system decreases from 35.4 % to 33.9% while the overall exergy efficiency of the system changes from 16.9% to 15.4%. The reason for this kind of the trend is that as the outlet temperature of the turbine increases, the work output of the turbine decreases resulting in the decrease in overall energy and exergy efficiencies of the system.

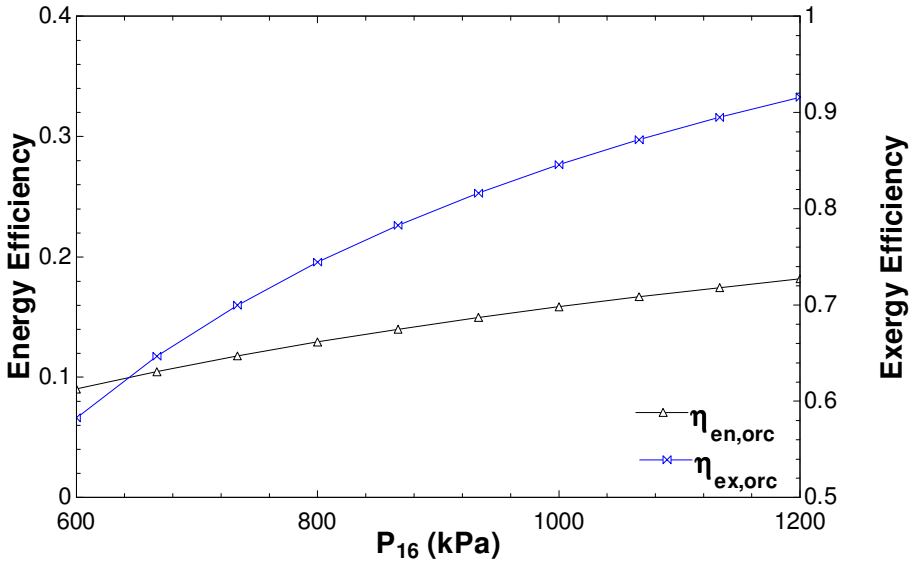

Fig. 5.32 Effect of ORC turbine inlet pressure (P_{16}) on the energy and exergy efficiencies of the ORC.

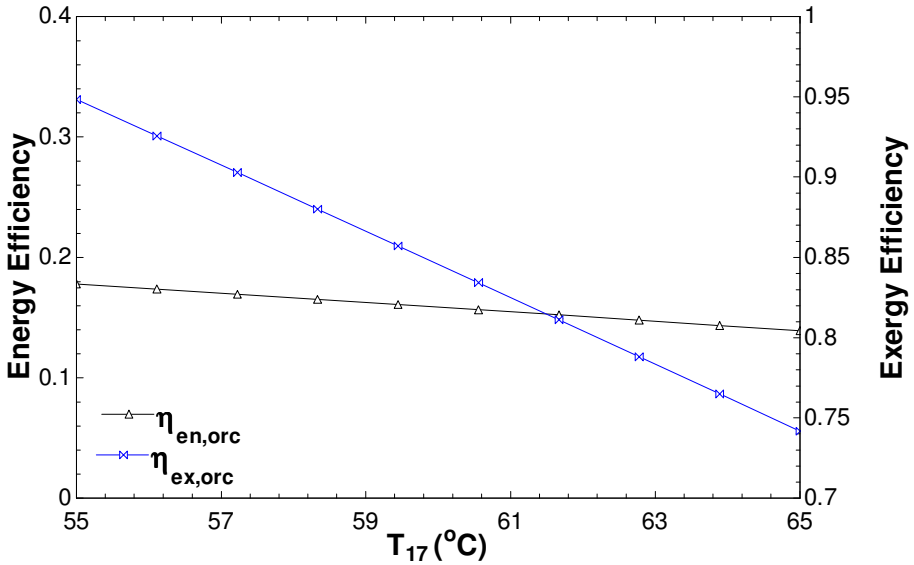

Fig. 5.33 Effect of outlet temperature of the turbine on the energy and exergy efficiencies of the ORC.

Fig. 5.35 shows the effects of the inlet temperature of the ORC pump on the energy and exergy efficiencies of the ORC. As the temperature increases from 17℃ to 27℃, the energy efficiency of the ORC changes from 15.1% to 15.8% while the exergy efficiency of the ORC decreases from 84.7% to 84.5%. The reason for this kind of increase in

energy efficiency is that as the inlet temperature of the ORC pump increases, the work input of the ORC decreases resulting in increase in the energy efficiency of the ORC. The exergy efficiency of the ORC decreases because of the fact that as inlet temperature of the ORC pump increases exergy destruction of the pump increases.

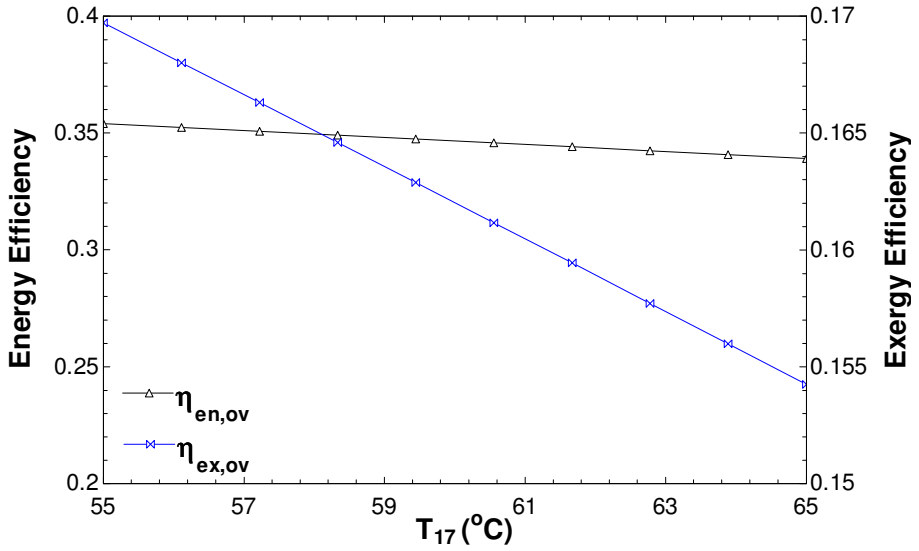

Fig. 5.34 Effect of outlet temperature of the turbine on the overall energy and exergy efficiencies of System 2.

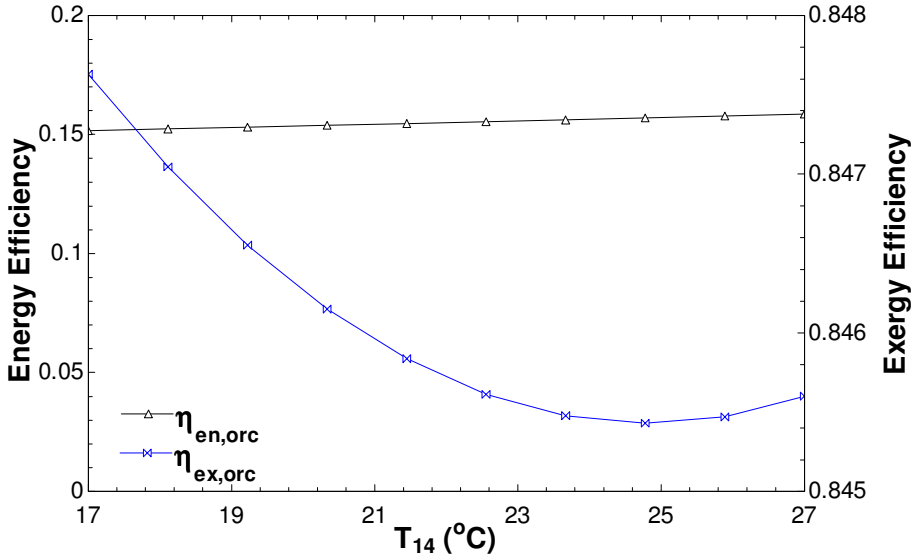

Fig. 5.35 Effect of inlet temperature of the ORC pump on the energy and exergy efficiencies of the ORC.

Fig. 5.36 shows the effects of the inlet temperature of the ORC pump on the overall energy and exergy efficiencies of System 2. As the temperature increases from 17 ^{O}C to 27 ^{O}C, the overall exergy efficiency of the system changes from 34.0% to 34.6% while there is no change in the overall energy efficiency of the system.

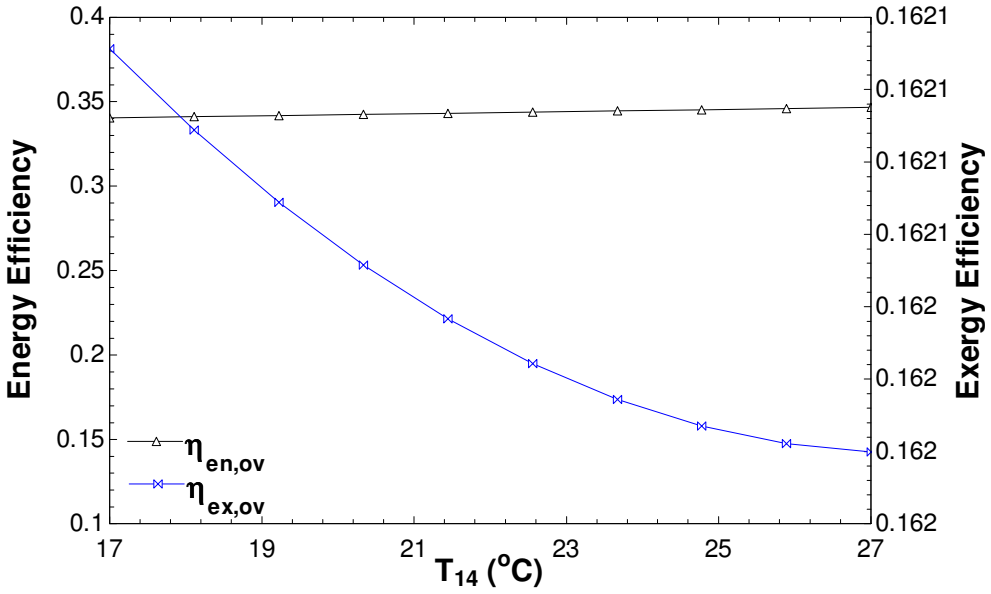

Fig. 5.36 Effect of inlet temperature of the ORC pump on overall energy and exergy efficiencies of System 2.

Fig. 5.37 shows the effects of outlet pressure of the compressor on the energetic and exergetic COPs of the ground source heat pump. As the pressure changes from 1250 kPa to 1500 kPa, the energetic COP of ground source heat pump changes from 5.27 to 5.81 while the exergetic COP of the ground source heat pump changes from 0.32 to 0.36. The reason for this kind of this trend is that as the outlet pressure of the compressor increases the output of the ground source heat pump increases resulting in the increase in the energetic and exergetic COP of the ground source heat pump.

Fig. 5.38 shows the effects of the inlet temperature of the concentrated solar panel on the overall energy and exergy efficiencies of the System 2. As the temperature increases from 80^{O}C to 100^{O}C, the overall energy efficiency of the system changes from 44.1% to 34.6% while the overall exergy efficiency of the system changes from 17.0% to 16.2%. The more inlet temperature of the concentrated solar panel means the energy from the oil is

not fully utilised resulting in the decrease in overall energy and exergy efficiencies of the system.

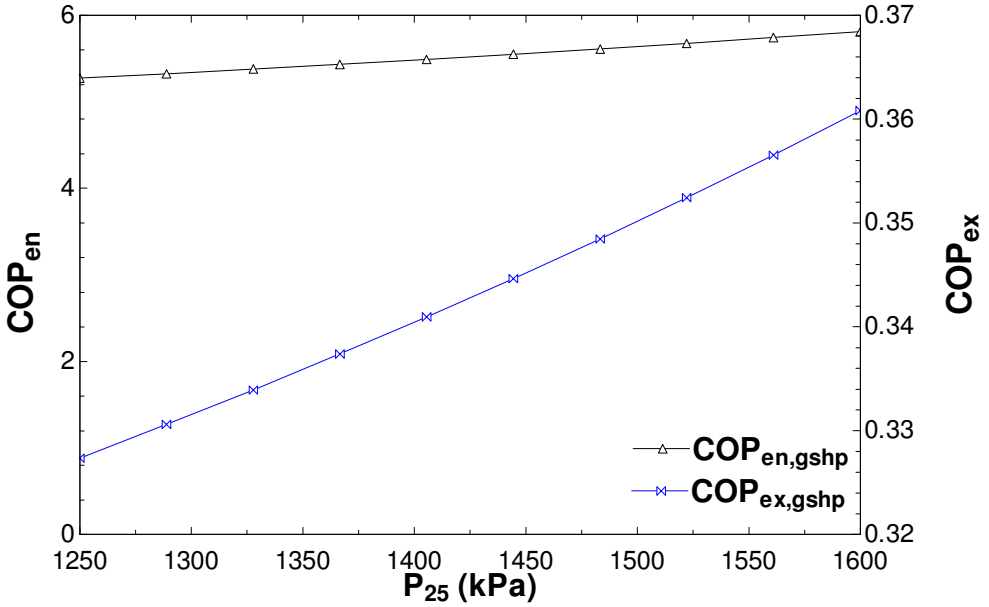

Fig. 5.37 Effects of outlet pressure of the compressor (P_{25}) on the energetic and exergetic COPs of the ground source heat pump.

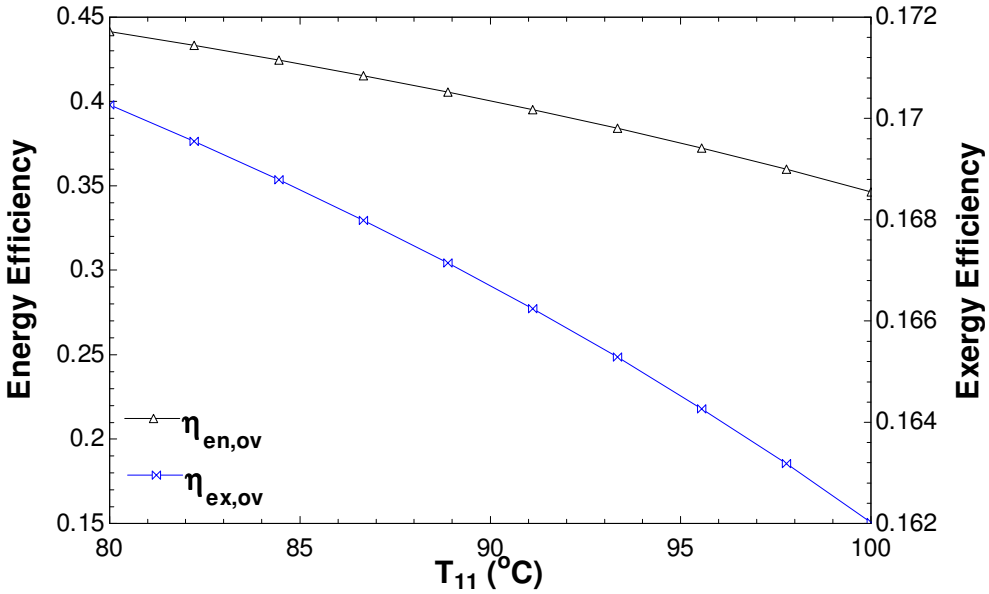

Fig. 5.38 Effect of inlet temperature of the concentrated solar panel on the overall energy and exergy efficiencies of the System 2.

Fig. 5.39 shows the effect of inlet temperature of the vapor absorption generator on the energetic and exergetic COP of the vapor absorption cycle. As the generator temperature increases from 110 ^{O}C to 130 ^{O}C, the energetic COP does not change while the exergetic COP changes from 0.29 to 0.25. This is due to the fact as the generator temperature increases the exergetic input to the vapor absorption cycle increases while the output remains the same resulting in the decrease in exergetic COP of the vapor absorption cycle.

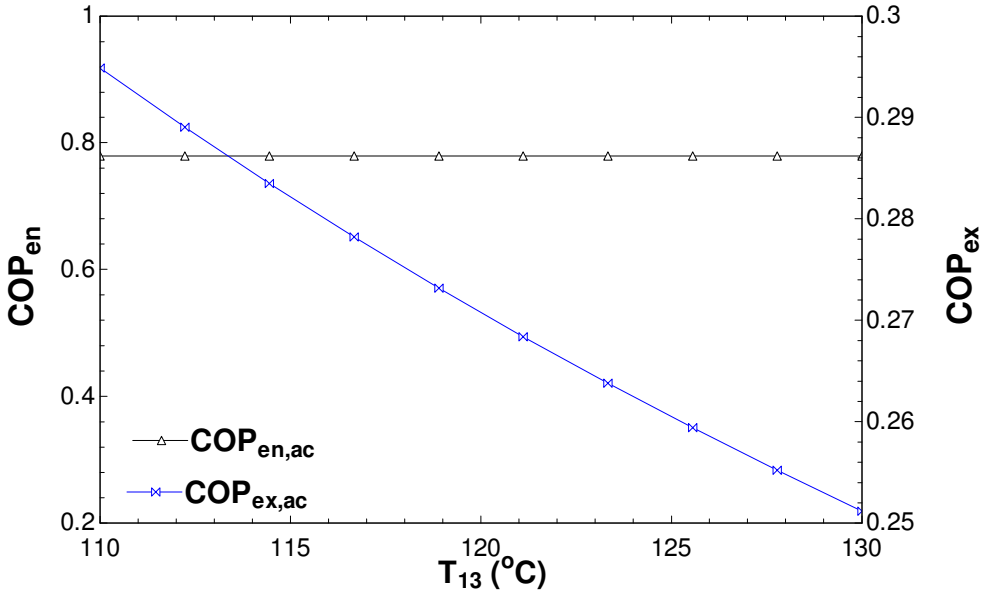

Fig. 5.39 Effect of inlet temperature of the vapor absorption generator on the energetic and exergetic COP of the vapor absorption cycle.

The effect of inlet temperature of the vapor absorption generator on the overall energy and exergy efficiency of System 2 is shown in Fig. 5.40. As the generator temperature increases from 110^{O}C to 130^{O}C the overall energy efficiency of the system increases from 24.7% to 44.5% while the overall exergy efficiency of the system changes from 15.3% to 17.0%. The reason for this kind of the trend is that as the inlet temperature of the vapor absorption generator increases the heat loss from the storage tank decreases resulting in the increase in overall energy and exergy efficiencies of the system.

The effect of wind velocity on the overall energy and exergy efficiencies of System 2 is shown in Fig. 5.41. As the wind velocity changes from 3 m/s to 6 m/s the overall energy

efficiency of the system increases from 32.5% to 36.8% while the overall exergy efficiency of the system also increases from 11.3% to 21.1%. The reason for this kind of trend is that as the velocity of wind increases, the work output of the wind turbine increases resulting in the increase in overall exergy and energy efficiencies of the system.

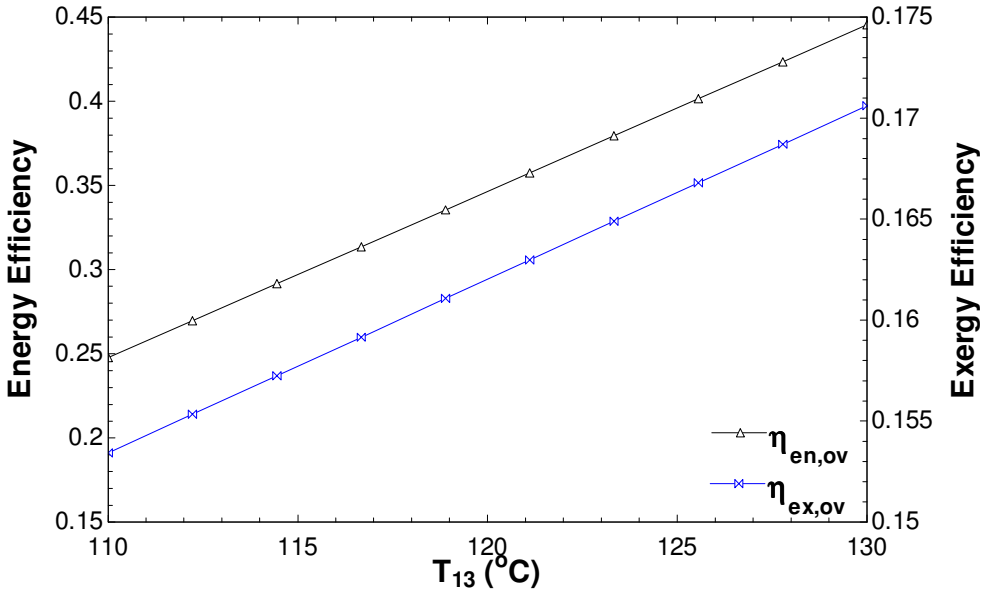

Fig.5.40 Effects of inlet temperature of the vapor absorption generator on the overall energy and exergy efficiencies of System 2.

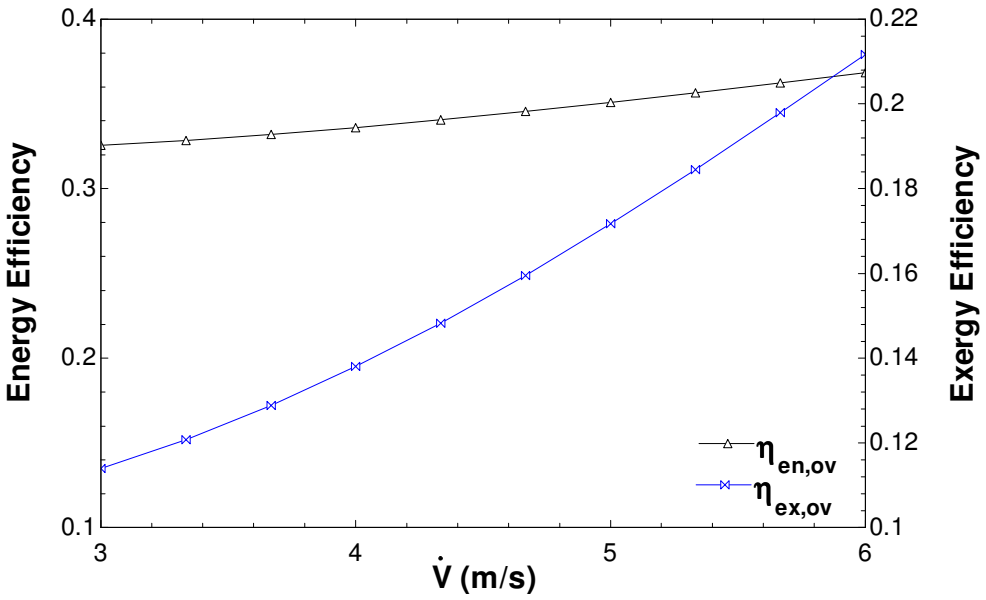

Fig. 5.41 Effect of wind velocity on the overall energy and exergy efficiencies of System 2.

5.2.2 Optimised power System 2

Fig. 5.42 shows the schematic diagram for the System 2 design studied in HOMER. The total connected load is 41 kWh daily. ORC has been model as a generator with the fuel to be considered as isopentane. Table 5.14 shows that it requires ORC of 3 kW, 6 batteries of 6 Volt capacity each, 2 kW rectifier and 2 kW inverter to meet the energy demand of the building for System 2. Table 5.16 shows the cost summary of the optimised system having the cost of electricity as $0.186/kWh and the total cost of the system as $35,502.

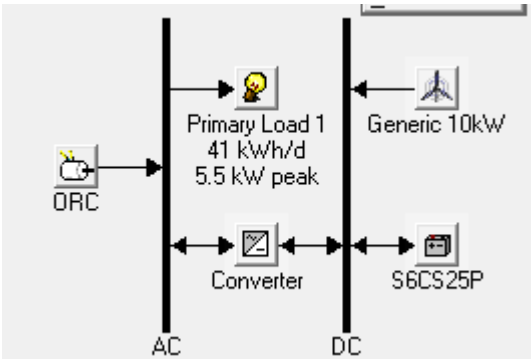

Fig. 5.42 Optimised power System 2.

Table 5.14 Architecture of the optimised power System 2.

ORC	3 kW
Battery	6 Surrette 6CS25P
Inverter	2 kW
Rectifier	2 kW

Table 5.15 Cost summary of the optimised power System 2.

Total net present cost	$ 35,502
Levelised cost of energy	$ 0.186/kWh
Operating cost	$ 1,964/yr

Table 5.16 shows the total net present cost of the optimised renewable energy system for System 2 based on all components which is further divided as capital, replacement, salvage and other costs. Fig. 5.43 shows the cash flow summary of the optimised renewable energy system.

Table 5.16 Total net present cost for optimised power System 2.

Component	Capital Cost ($)	Replacement Cost ($)	Operation and maintenance Cost ($)	Fuel Cost ($)	Salvage Cost ($)	Total Cost ($)
ORC	3,000	13,760	2,242	0	-178	18,825
Surrette 6CS25P	6,000	3,571	3,835	0	-1,025	12,381
Converter	1,400	417	2,557	0	-78	4,296
System	10,400	17,749	8,634	0	-1,281	35,502

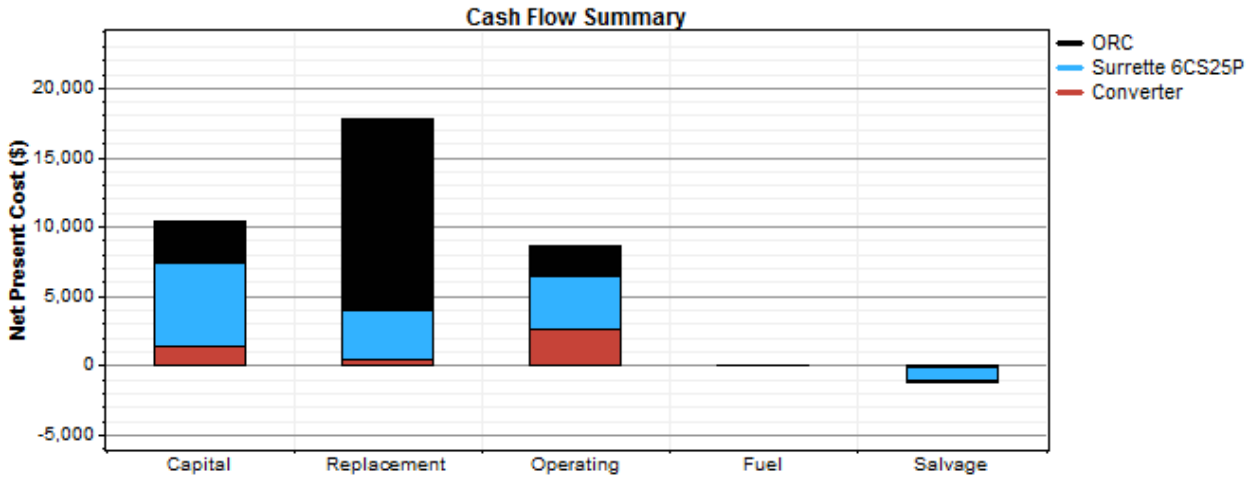

Fig. 5.43 Cash flow summary of the optimised power System 2 based on the selected component.

Table 5.17 shows the annualised cost of the optimised system for System 2 with a detailed cost type. The annualised cost helps in determining the levelised cost of electricity. Fig. 5.44 shows the annualised cash flow summary of the optimised system for System 2.The salvage value is taken as negative (-ve) since it is added value or it the money actually we save at the end of the project. As salvage cost of any component depends upon its replacement cost instead of the initial capital cost.

Table 5.17 Annualised cost of the optimised power System 2.

Component	Capital Cost ($)	Replacement Cost ($)	Operation and maintenance Cost ($)	Fuel Cost ($)	Salvage Cost ($)	Total Cost ($)
ORC	235	1,076	208	8,525	-25	10,370
Surrette 6CS25P	469	279	100	0	-27	323
Converter	110	33	200	0	-6	336
System	814	1,388	558	8,525	-149	12,886

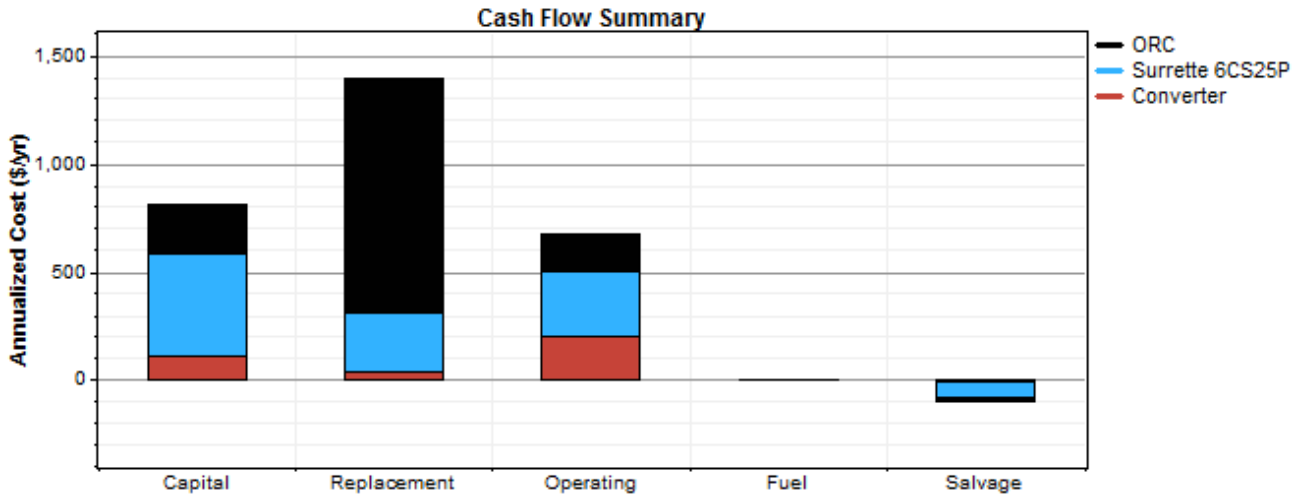

Fig. 5.44 Annualised cash flow summary of the optimised power System 2 based on the selected component.

Fig. 5.45 shows the nominal cash flow summary of the optimised renewable energy system with the detailed component. Discounted cash summary of the optimised renewable energy system is presented in Fig. 5.46.

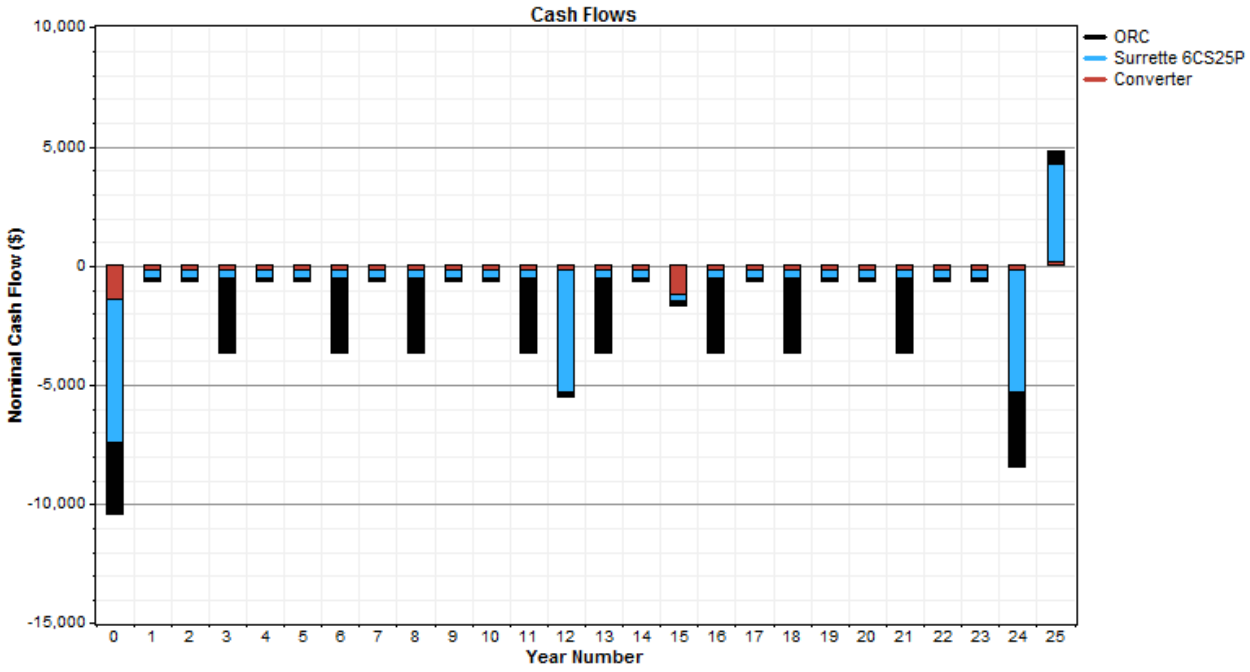

Fig. 5.45 Nominal cash flow summary of the optimised power System 2.

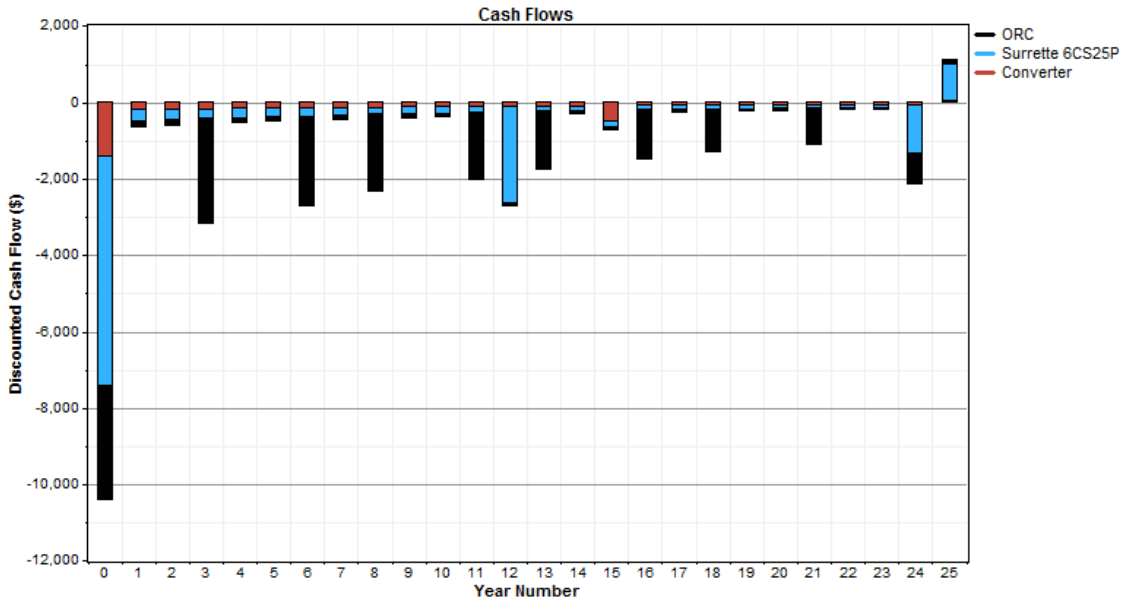

Fig. 5.46 Discount cash flow summary of the optimised power System 2.

Table 5.18 Optimised power System 2 electrical configuration.

Component	Production (kWh/yr)	Fraction (%)
ORC	17,274	100
Excess electricity	0.000136	0

As seen from Table 5.18, the electricity produced by ORC is the 100 % of the total electricity produced as 17,274 kWh. The excess electricity produced by System 2 is almost zero. Fig. 5.47 shows the monthly production of electricity produced by ORC.

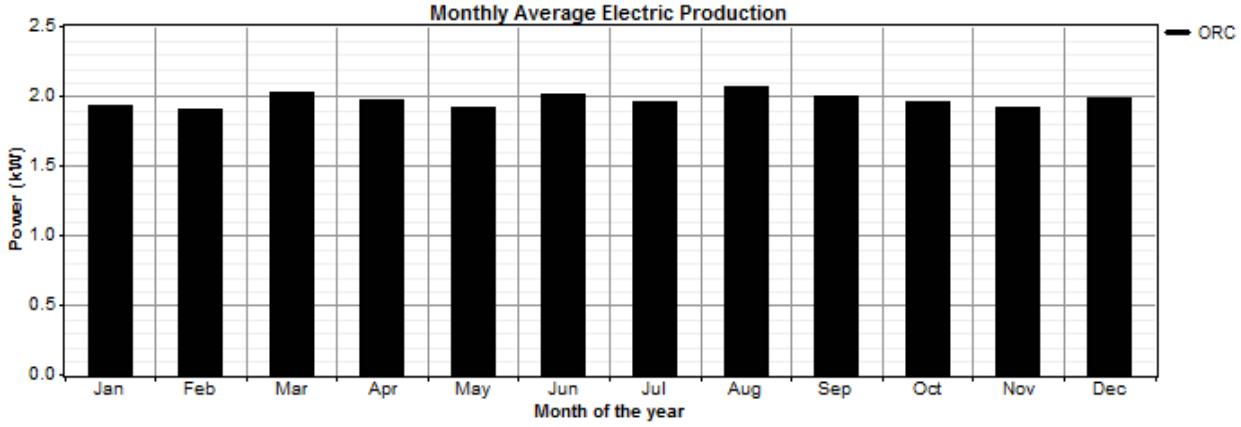

Fig. 5.47 Monthly production of electricity for the optimised power System 2.

Table 5.19 summarised the electrical configuraion of the ORC turbine used in System 2. The rated capacity of the turbine for optimum performance of the system is 3.0 kW with a mean output of 2.95 kW. The efficiency of the ORC turbine is found to be 65.7%. Fig. 5.48 shows the electircal output of the ORC turbine monthwise.

Table 5.19 ORC electrical configuration for System 2.

Quantity	Value	Units
Rated capacity	3.0	kW
Mean output	2.95	kW
Capacity factor	65.7	%
Total production	17,277	kWh/yr

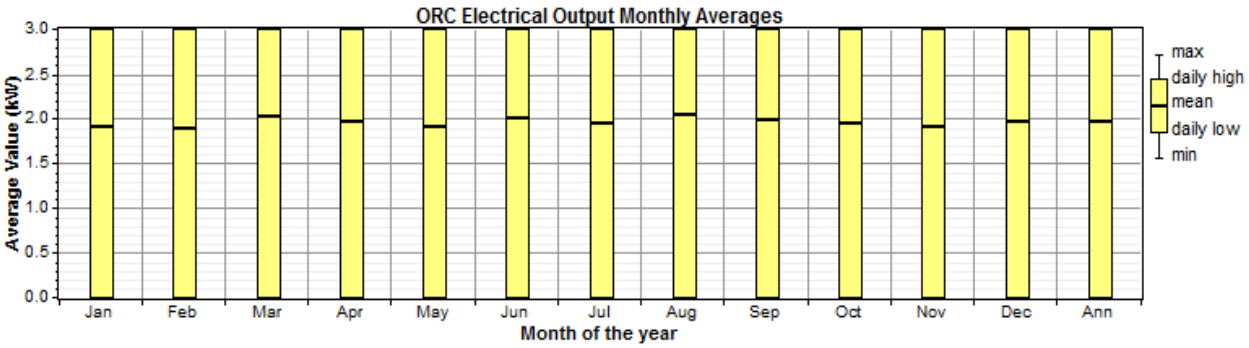

Fig. 5.48 ORC turbine electric output for optimised power System 2.

Tables 5.20 and 5.21 show the battery architecture and the electrical configuration respectively. Table 5.20 shows that for the optimised power system it requires 6 batteries. The voltage produced by each battery is 6 Volts. The nominal capacity and usable capacity of the battery are 41.6 kWh and 25.0 kWh respectively (see Table 5.21). The average battery cost is 0.093 $/kWh and its average life is 12.0 year. There is throughput of 4,557 kWh annually through the battery bank.

Table 5.20 Battery structure for System 2.

Quantity	Value
String size	1
Strings in parallel	6
Batteries	6
Bus voltage (V)	6

Table 5.21 Battery electrical configuration for System 2.

Quantity	Value	Units
Nominal capacity	41.6	kWh
Usable nominal capacity	25.0	kWh
Autonomy	14.6	h
Lifetime throughput	57,871	kWh
Battery wear cost	0.093	$/kWh
Average energy cost	0.000	$/kWh
Energy in	5,022	kWh/yr
Energy out	4,076	kWh/yr
Storage depletion	0	kWh/yr
Losses	995	kWh/yr
Annual throughput	4,557	kWh/yr
Expected life	12.0	yr

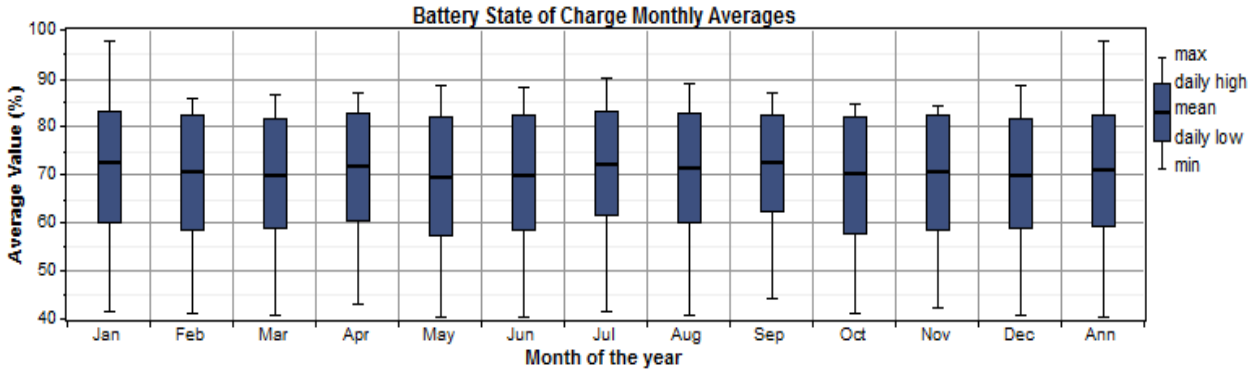

Fig. 5.49 Battery system charge state (%) for optimised power System 2.

The monthly battery state of charge throughout the year is shown in Fig. 5.49. It is evident from the Fig. 5.49 that minimum state of charge for the battery is 40% i.e. one cannot go below this for the battery due to breakdown. From the Fig.5.49 it is found that average battery charge is around 70%.

Table 5.22 shows the inverter electrical configuration. The capacity of the inverter is found to be 2.00 kW with the mean output of 0.42 kW. The efficiency of the inverter is 20.9 % while it operates for 3,556 hours annually. There is a loss of 408 kWh of energy annually. Fig. 5.50 shows the electrical output of the inverter. Fig. 5.51 shows the rectifier output monthly wise.

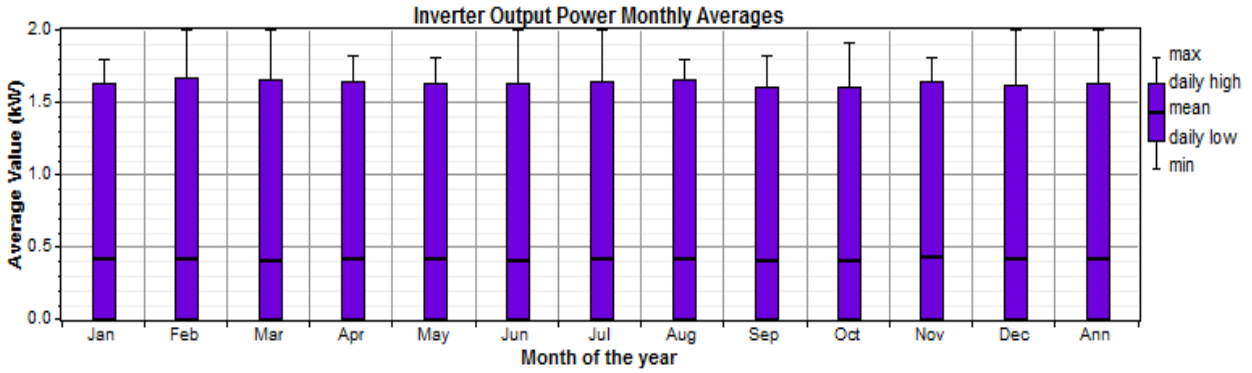

Fig. 5.50 Inverter electric output for optimised power System 2.

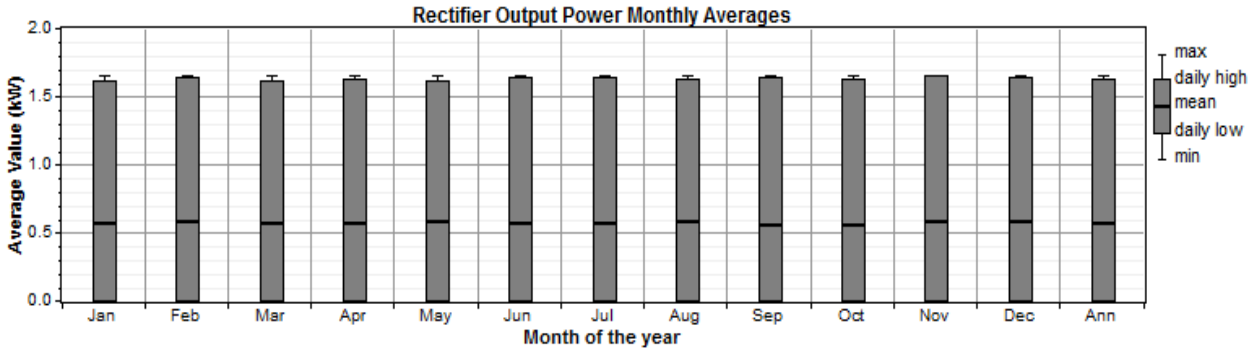

Fig. 5.51 Rectifier electric output for optimised power System 2.

Table 5.22 Converter electrical configuration.

Quantity	Inverter	Rectifier	Units
Capacity	2.00	2.00	kW
Mean output	0.42	0.58	kW
Minimum output	0.00	0.00	kW
Maximum output	2.00	1.65	kW
Capacity factor	20.9	29.0	%
Hours of operation	3,556	5,203	h/yr
Energy in	4,076	5,979	kWh/yr
Energy out	3,688	5,082	kWh/yr
Losses	408	897	kWh/yr

5.2.3 Optimisation of Overall Exergy Efficiency of System 2

Fig. 5.52 shows the optimisation results of overall exergy efficiency of System 2. As the number of function call increases the value of overall exergy efficiency increases until it converges. The exergy efficiency converges after 10000 function call. The value of overall exergy efficiency converges at 18.8%, respectively.

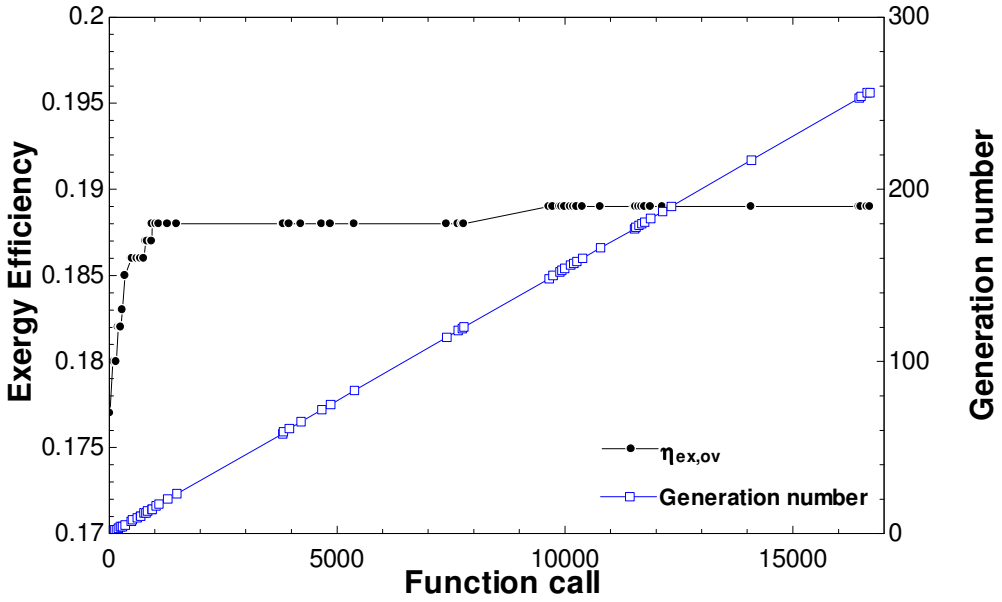

Fig. 5.52 Optimisation of overall exergy efficiency of System 2.

5.3 Results of System 3

5.3.1 Energy and Exergy Analyses of System 3

The exergy destruction rates for the major components of System 3 are determined and shown in Fig. 5.53. The maximum destruction rate occurs in the CSP and the next highest take place in the HEX 2 and the third highest destruction rate occurs in the condenser 3.

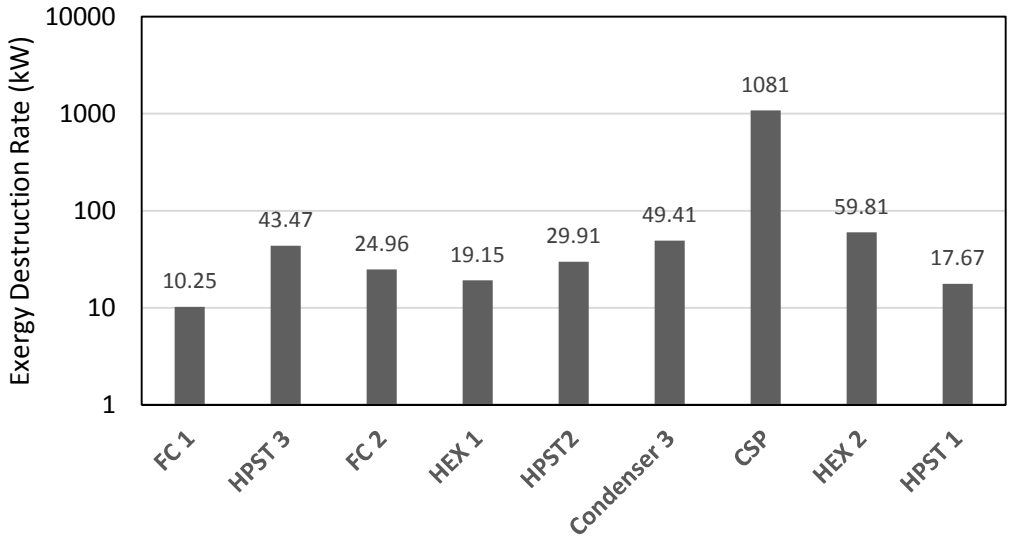

Fig. 5.53 Exergy destruction rates of selected units of System 3.

Table 5.23 Parameter values from modeling and energy and exergy analyses of System 3.

Parameter	Value
Output of LPST 1 (kW)	64.04
Output of HPST 1 (kW)	131.4
Cooling load (kW)	140
Energy efficiency of RC 1(%)	20.2
Exergy efficiency of RC 1(%)	49.8
Overall system energy efficiency (%)	20.2
Overall system exergy efficiency (%)	19.2

The variation of energetic and exergetic COPs of the vapor absorption cycle with ambient temperature are shown in Fig. 5.54. As the ambient temperature increases from 15℃ to 35℃, there is no change in the energetic COP while the exergetic COP increases from 0.11 to 0.33. This is due to the fact that as the ambient temperature increases, the exergetic output of the evaporator increases resulting in the increase in exergetic COP.

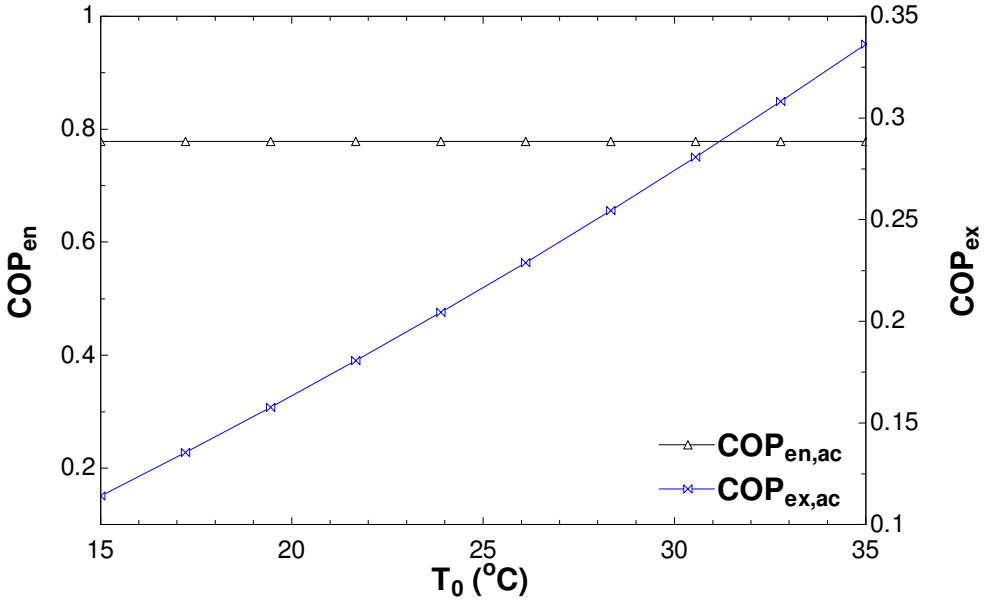

Fig. 5.54 Effect of ambient temperature (T_0) on the energetic and exergetic COPs of the vapor absorption chiller.

The effects of the ambient temperature on the energy and exergy efficiencies of the Rankine Cycle 1 are shown in Fig. 5.55. As the ambient temperature changes, the energy efficiency remains the same while the exergy efficiency increases from 47.54% to

52.45%. This trend is due to the fact that as the ambient temperature increases, the exergetic input of the Rankine Cycle 1 decreases.

The effects of ambient temperature on the overall energy and exergy efficiencies of System 3 are shown in Fig. 5.56. As the ambient temperature changes from 15℃ to 35℃, there is no change in the overall energy efficiency while the exergy efficiency of the overall system changes from 18.8% to 19.7%. The reason for this trend is that on increasing the ambient temperature, the exergetic input of the sun decreases and the exergetic output of the absorption increases resulting in the increase in exergy efficiency of the system.

The effects of oil outlet temperature on the energy and exergy efficiencies of Rankine Cycle 1 are shown in Fig. 5.57. As the ambient temperature changes from 240℃ to 300℃, there is no change in the energy efficiency while the exergy efficiency changes from 50.6% to 47.1%. The reason for this kind of trend is that an increase in oil inlet temperature increases the exergetic input of the Rankine Cycle 1.

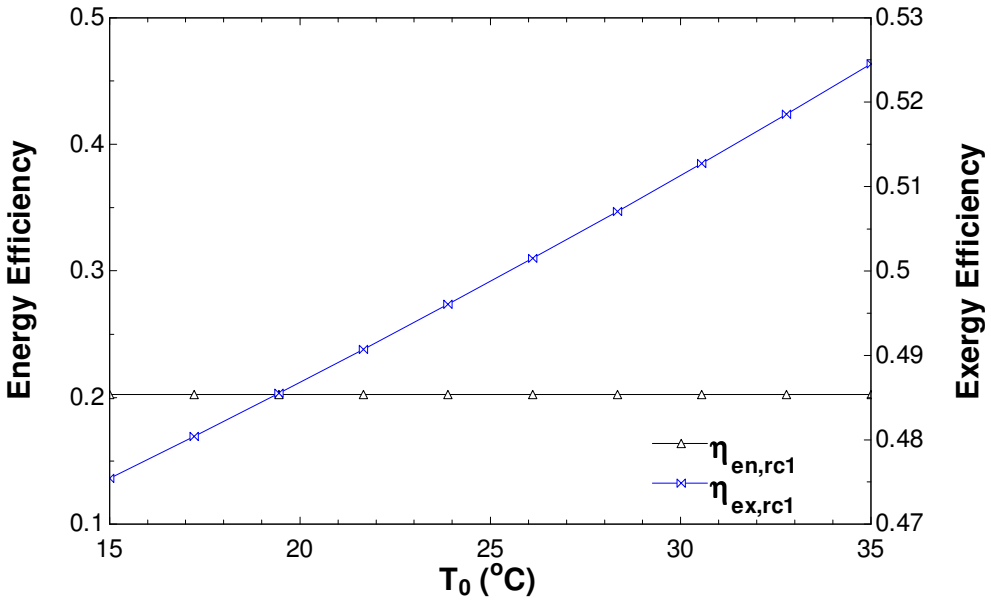

Fig. 5.55 Effect of ambient temperature (T_0) on the energy and exergy efficiencies of RC 1.

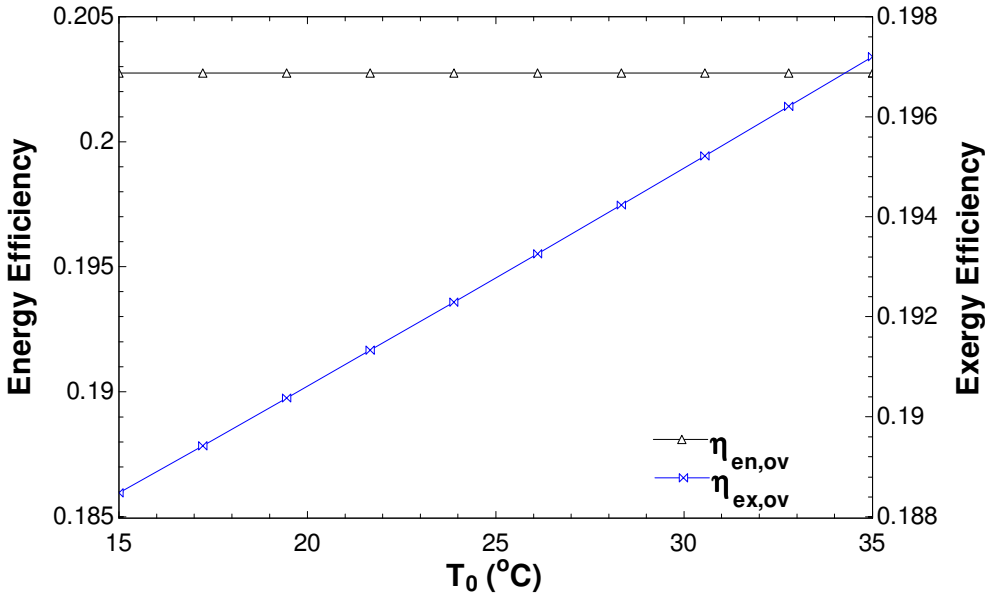

Fig. 5.56 Effect of ambient temperature (T_0) on the overall energy and exergy efficiencies of System 3.

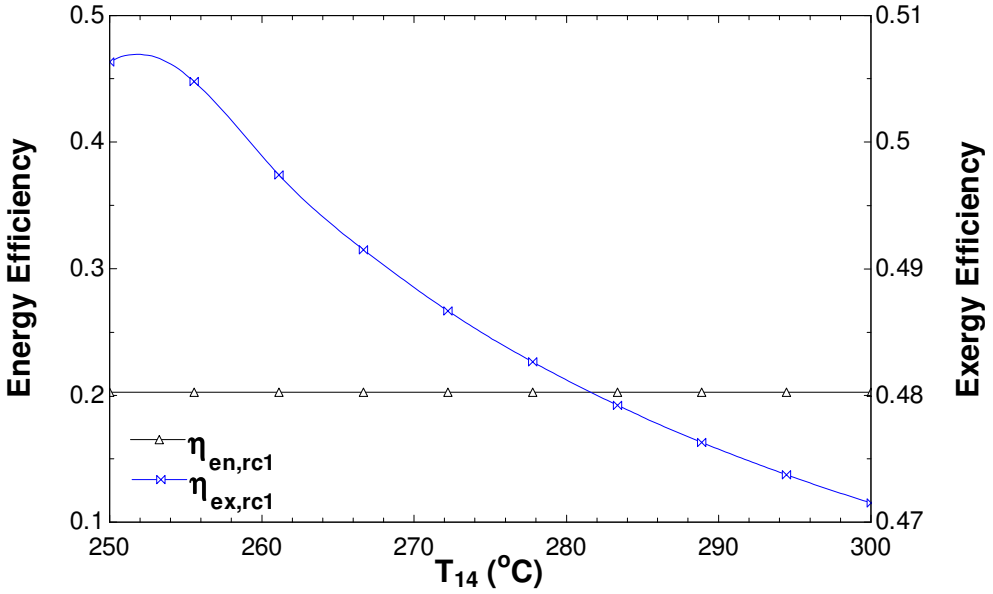

Fig. 5.57 Effect of oil outlet temperature (T_{14}) on the energy and exergy efficiencies of RC 1.

Fig. 5.58 shows the effects of oil outlet temperature on the overall energy and exergy efficiencies of System 3. By increasing the oil outlet temperature both energy and exergy efficiencies of the System 3 increases.

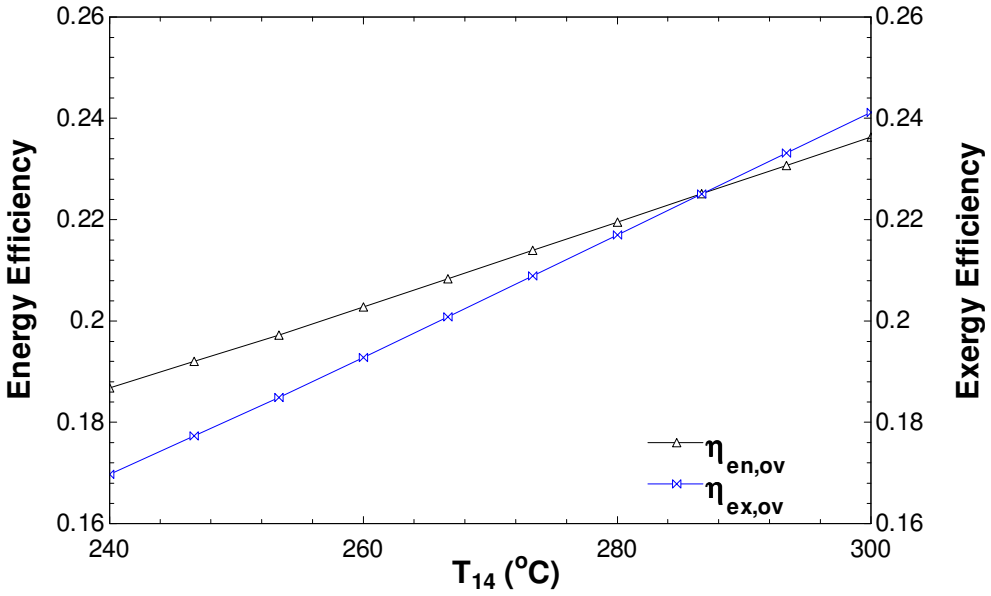

Fig. 5.58 Effect of oil outlet temperature (T_{14}) on the overall energy and exergy efficiencies of System 3.

5.3.2 Optimisation of System 3

Fig. 5.59 shows the schematic diagram for the System 3 design in HOMER. The total connected load is 1,151 kWh daily. Table 5.24 shows that it requires 120 kW high pressure turbine, 50 kW low pressure turbine, 20 batteries of 6 Volt capacity each, 20 kW rectifier and 20 kW inverter for System 3. Table 5.25 shows the cost summary of the optimised system having the cost of electricity as \$0.111/kWh and the total cost of the system as \$598,474.

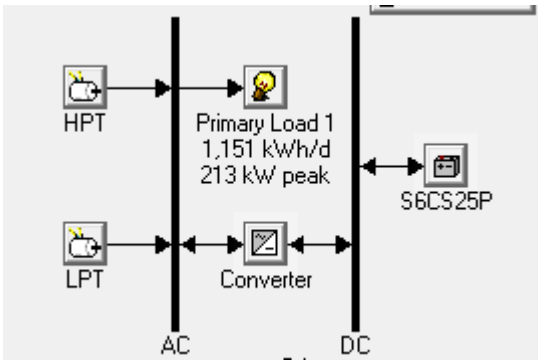

Fig. 5.59 Optimisation power System 3.

Table 5.24 Optimised power System 3 architecture.

HPT	120 kW
LPT	50 kW
Surrette 6CS25P	20
Inverter	20 kW
Rectifier	20 kW

Table 5.25 Cost summary of the optimised power System 3.

Total net present cost	$ 598,474
Levelised cost of energy	$ 0.111/kWh
Operating cost	$ 31,641/yr

Fig. 5.60 shows the cash flow summary of the optimised power System 3. The capital cost of the HPT is around 55% of the total capital cost of the system while on the other hand the LPT is more cheaper in terms of initial capital cost but costly in terms of operation cost.

Table 5.26 shows the total net present cost of the optimised power System 3 according to the component wise as well as the description like as capital, replacement, salvage and other costs. The cost of the LPT is around 43% of the total cost of the system.

Table 5.26 Optimised renewable energy power system net present costs for System 3.

Component	Capital Cost ($)	Replacement Cost ($)	Operation and Maintenance Cost ($)	Fuel Cost ($)	Salvage Cost ($)	Total Cost ($)
HPT	110,000	161,556	1,274	0	-17,755	255,076
LPT	50,000	200,546	10,698	0	-7,357	253,887
Surrette 6CS25P	20,000	14,827	12,783	0	-1,062	46,548
Converter	14,000	4,173	25,567	0	-777	42,963
System	194,000	381,102	50,322	0	-26,951	598,474

Table 5.27 shows the annualised cost of the optimised system with detailed cost type. The annual cost for the HPT is found to be more compared to LPT. The annualised cost helps in determining the levelised cost of electricity. Fig. 5.61 shows the annualised cash flow

summary of the optimised system. The salvage value is taken as negative (-ve) since it is added value or it the money actually we save at the end of the project. As salvage cost of any component depends upon its replacement cost instead of the initial capital cost.

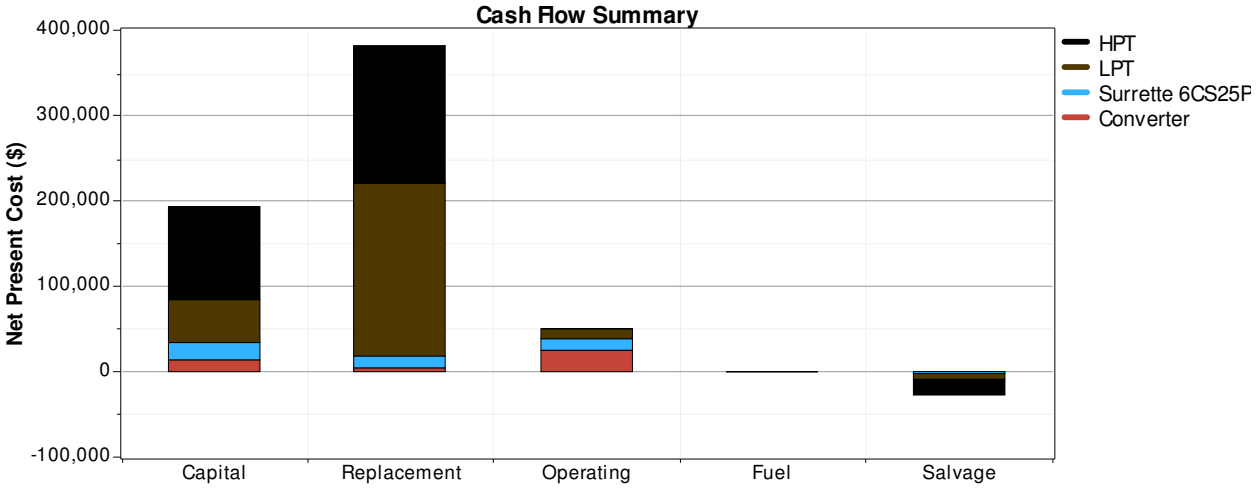

Fig. 5.60 Cash flow summary of the optimised power System 3 based on the selected component..

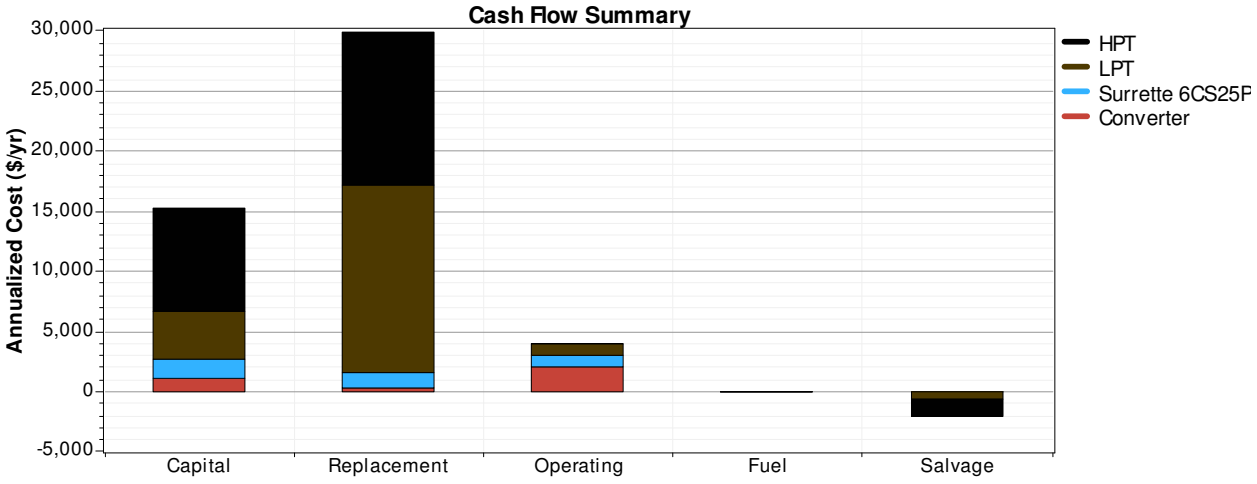

Fig. 5.61 Annual cash flow summary of the optimised power System 3 based on the selected component.

The nominal cash summary of the optimised renewable energy system for System 3 is presented in Fig. 5.62. The nominal cash is the amount that one gets after subtracting the annual income from the actual cost.

Fig. 5.63 shows the discounted cash flow summary of the optimised renewable energy system with the detailed component cost. The monthly production of the electricity is shown in Fig. 5.64. It is clear from the Fig. 5.64 that the electricity produced by HPT is more compare to LPT. Table 5.28 give the optimised power system electrical configuration. It is found that the power produced by the HPT is around 54% of the total power produced. The excess electricity produced by System 3 is 33.7 (kWh/yr) i.e. 0.0078% of the total power produced.

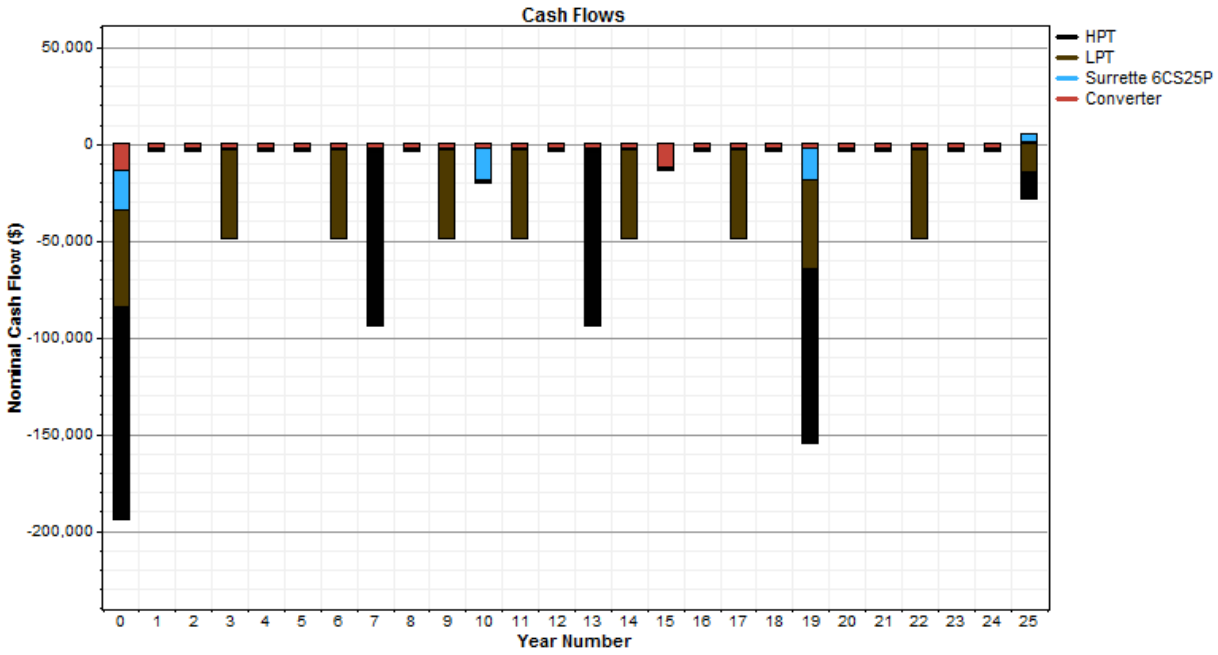

Fig. 5.62 Nominal cash flow summary of the optimised power System 3.

Table 5.27 Optimised renewable energy system annualised costs for System 3.

Component	Capital Cost ($)	Replacement Cost ($)	Operation and Maintenance Cost ($)	Fuel Cost ($)	Salvage Cost ($)	Total Cost ($)
HPT	8,605	12,638	100	0	-1389	19,954
LPT	3,911	15,688	837	0	-576	19,861
Surrette 6CS25P	1,565	1,160	1,000	0	-83	3,641
Converter	1,095	326	2,000	0	-61	3,361
System	15,176	29,812	3,937	0	-2108	46,817

Table 5.28 Optimised renewable energy power system electrical configuration for System 3.

Component	Production (kWh/yr)	Fraction (%)
HPT	230,763	54
LPT	200,002	46
Excess electricity	33.7	0.0078

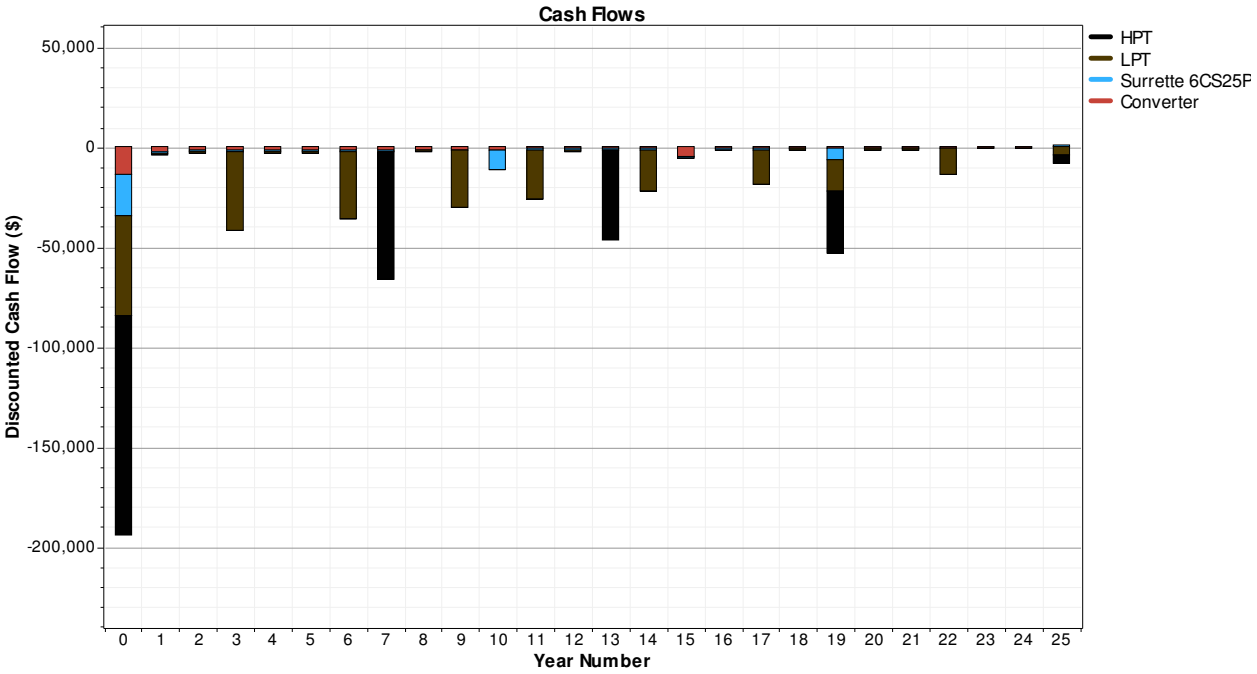

Fig. 5.63 Discounted cash flow summary of the optimised power system 3.

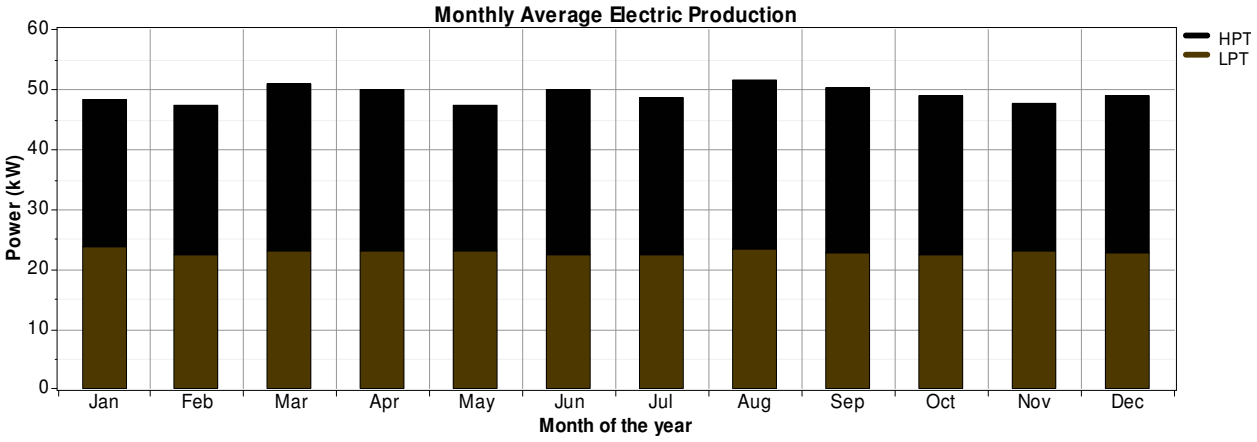

Fig. 5.64 Monthly production of electricity for optimised power System 3.

Table 5.29 HPT electrical configuration for System 3.

Quantity	Value	Units
Rated capacity	120	kW
Mean output	92.6	kW
Minimum output	56.6	kW
Capacity factor	22.0	%
Total production	49,396	kWh/yr
Maximum output	120	kW
Hours of operation	2,492	h/yr

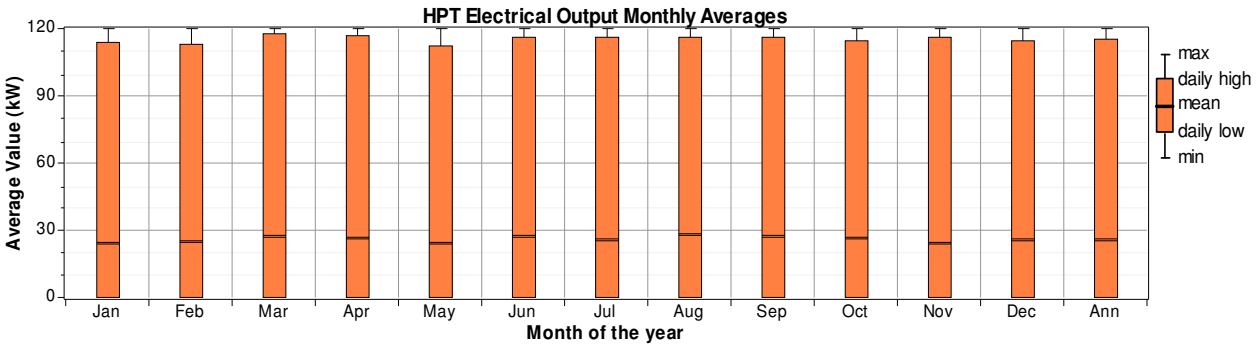

Fig. 5.65 HPT electric output for optimised power System 3.

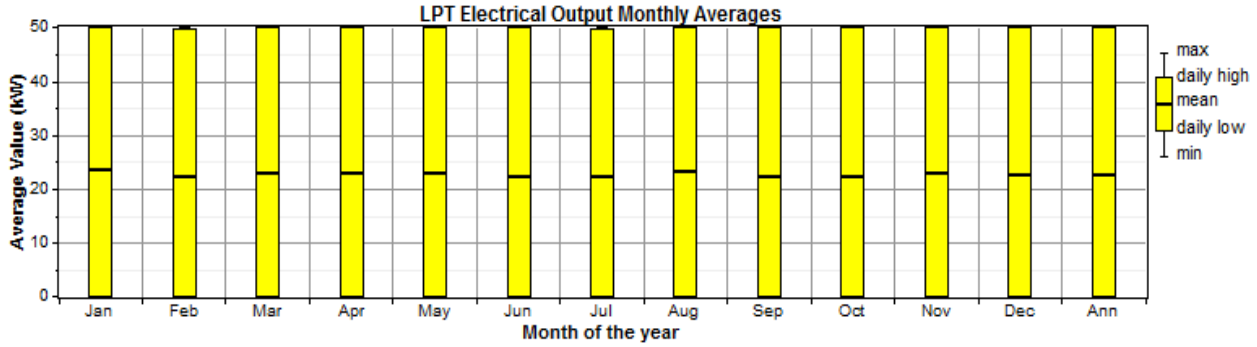

Fig. 5.66 LPT electric output for optimised power System 3.

Table 5.29 shows the electrical configuration of the HPT. The mean output from the HPT is 92.6 kW with the efficiency of 22.0%. The total hours of operation are 2,492 in a year. Table 5.30 provides the electrical configuration of the LPT considered in the study for System 3. It shows that the rated capacity of the LPT is 50 kW while the mean output is 35.8 kW. The efficiency of LPT is found to be as 45.7%. The LPT produces 200,002 kWh of power annually.

Table 5.30 LPT electrical configuration for System 3.

Quantity	Value	Units
Rated capacity	50	kW
Mean output	35.8	kW
Capacity factor	45.7	%
Total production	200,002	kWh/yr
Minimum output	15	kW
Maximum output	50	kW
Hours of operation	5,579	h/yr

Table 5.31 shows the converter electrical configuration. The capacity of the inverter is found to be 20 kW with the mean output of 1.9 kW. The efficiency of the inverter is 9.6% while it operates for 1,726 hours annually. There is a loss of 1,874 kWh of energy annually. The capacity of the rectifier is found be as 13.4% with a mean of 2.7 kW and 7,033 hours of operation annually.

Table 5.31 Converter electrical configuration for optimised power System 1

Quantity	Inverter	Rectifier	Units
Capacity	20	20	kW
Mean output	1.9	2.7	kW
Minimum output	0.0	0.0	kW
Maximum output	20	5.5	kW
Capacity factor	9.6	13.4	%
Hours of operation	1,726	7,033	h/yr
Energy in	18,738	27,544	kWh/yr
Energy out	16,864	23,413	kWh/yr
Losses	1,874	4,132	kWh/yr

Fig. 5.65 shows the electric output of the HPT. The output from the HPT is around 30 kW in most months of the year. Fig. 5.66 shows the output of the LPT. The power generated by LPT is almost same in all months with an average of around 25 kW.

Fig. 5.67 shows the electrical output of the inverter. The power produced by the inverter is almost same in all months with an average of around 3 kW. Fig. 5.69 shows the rectifier output power. The power produced by the rectifier is almost same in all months except in the month of March.

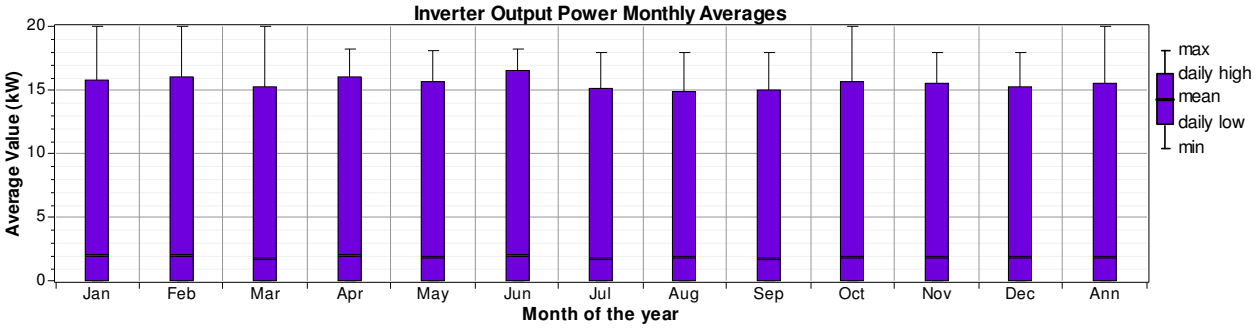

Fig. 5.67 Inverter electric output for optimised power System 3.

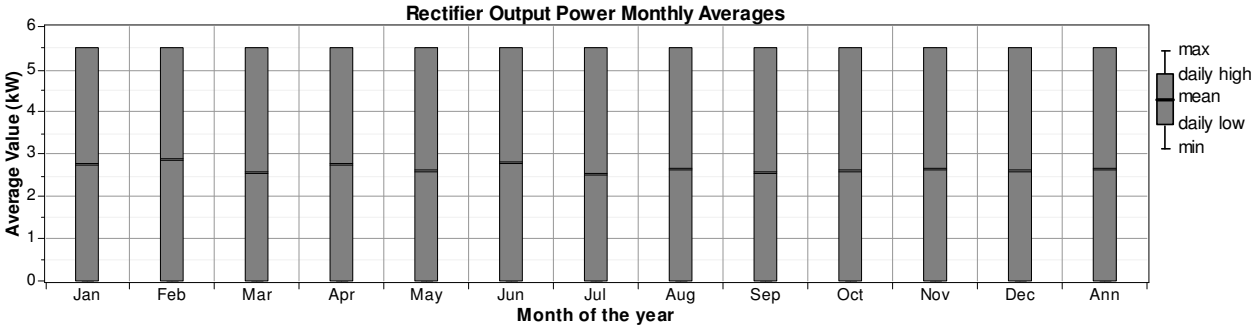

Fig. 5.68 Rectifier electric output for optimised power System 3.

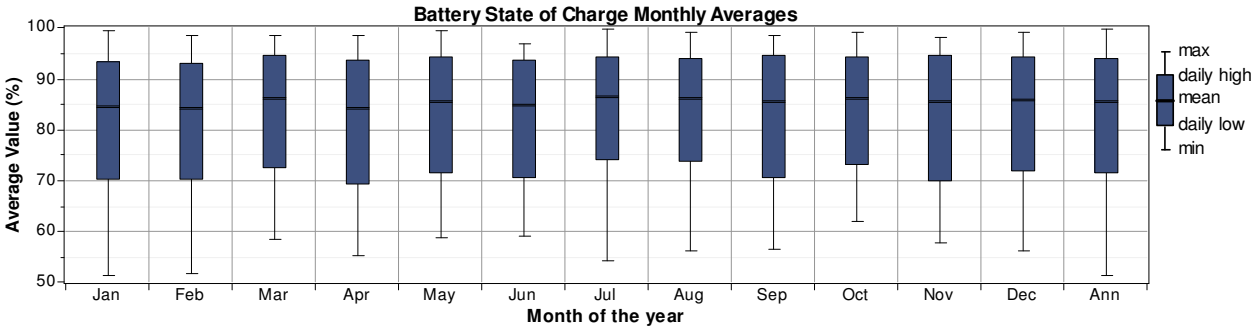

Fig. 5.69 Battery state of charge for optimised power System 3.

The monthly battery state of charge throughout the year is shown in Fig. 5.70. It is evident from the Fig. 5.70 that minimum state of charge for the battery is around 50%, and hence one cannot go beyond this due to breakdown. Most of the time in the year battery is 85% charge.

5.3.3 Optimisation of Overall Exergy Efficiency of System 3

The optimisation study results of overall exergy efficiency of System 3 are shown in Fig. 5.70. As the function call increases, the overall exergy efficiency of System 3 increases until it converges to a maximum value. The overall exergy efficiency converges at a value of 43.0% when the function call reaches 625.

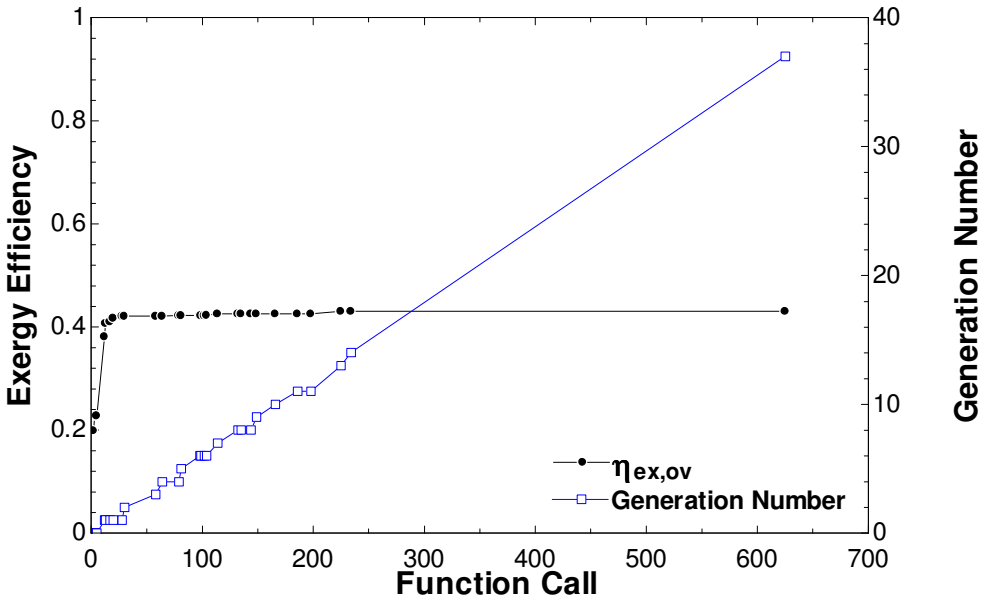

Fig. 5.70 Optimisation of overall exergy efficiency of System 3.

Chapter 6: Conclusions and Recommendations

This study presents three renewable energy based multigeneration systems for residential building applications. The assessment considers building size, occupancy, energy load, and geographic location in the energy and exergy analyses of the systems, supported by real-time simulation of each case using HOMER software. The optimisation studies of each system address the key factors for sustainable development; renewability, total energy consumption, and emissions.

6.1 Conclusions

The following conclusions are extracted from this thesis study:

- The total net present cost for the optimised power System 1 is found to be $2,700,496, with a renewable fraction of 100% with no carbon dioxide or other emissions.
- The levelised cost of energy for System 1 is $ 0.117/kWh.
- The exergy analysis results of System 1 reveal that the combustion chamber followed by the concentrated solar panel, have the largest exergy destructions of the components within the system.
- The exergy efficiency value for System 1 is found to be 34.9%, while the energy efficiency is found to be 91.0%.
- The total net present cost for the optimised power System 2 is found to be $ 35,502, with 100% renewable fraction and no emissions of carbon dioxide or other pollutants.
- The levelised cost of energy for System 2 is found to be $ 0.186/kWh.
- The exergy efficiency for System 2 is found to be 16.2%, and energy efficiency is 34.6%.
- The exergy analysis for System 2 indicates maximum exergy destructions occur in the concentrated solar panel, followed by the wind turbine.
- The total net present cost for the optimised power System 3 is found to be $ 598,474, with no emissions, referring to 100% renewable fraction.
- The levelised cost of energy for System 3 is found to be $ 0.111/kWh.

- The exergy and energy efficiencies of System 3 are to be found 19.2%, and 20.2% respectively.
- The maximum exergy destructions for System 3 occur in the concentrated solar panel, followed by the heat exchanger 2.
- For the comparison case considering each system for the same building and conditions, System 1 is found to have the minimum net present cost and levelised cost of electricity, with values of $ 26,001 and $ 0.136/kWh, respectively.
- On the basis of exergy efficiency, System 1 is found to be the most efficient and effective one and obviously superior to other two systems, namely System 2 and System 3.

6.2 Recommendations

Sustainable energy systems for building applications are investigated in this thesis study and the analysis results presented here provide engineers and designers across the globe with potential solutions to reduce environmental impact of residential buildings for various locations and climates by utilizing regionally available renewable resources. The following recommendations are made based on the results of this thesis study:

- Energy storage systems should be integrated into Systems 1 and 3 to improve year-round sustainability.
- Reduced-scale experimental units of the investigated systems should be built and monitored in different locations to provide practical results for varying climates and renewable resource availability, as well as to identify areas for system improvement based on real-world conditions.
- Structurally integrated photovoltaic systems—i.e. rooftop arrays, windows installations—should be studied to increase the efficiencies of the developed systems.
- Future research should extend the renewable energy system-based assessment presented in this work to include building-specific emissions—i.e. materials used, lifecycle impact of residential structures—to provide further insight into building sustainability.

- Policy-makers should consider energy resources within green building standards—i.e. LEED, BREEAM, etc.—in rating schemes for future building projects to encourage integration of renewable energy systems.

References

Ahmadi, P., I. Dincer and M. A. Rosen (2013a). "Development and assessment of an integrated biomass-based multi-generation energy System." Energy 56(0): 155-166.

Ahmadi, P., I. Dincer and M. A. Rosen (2013b). "Performance assessment and optimization of a novel integrated multigeneration System for residential buildings." Energy and Buildings 67: 568-578.

Ameri, M., P. Ahmadi and A. Hamidi (2009). "Energy, exergy and exergoeconomic analysis of a steam power plant: A case study." International Journal of Energy Research 33(5): 499-512.

Balta, M. T., I. Dincer and A. Hepbasli (2010). "Performance and sustainability assessment of energy options for building HVAC applications." Energy and Buildings 42(8): 1320-1328.

Beccali, M., S. Brunone, M. Cellura and V. Franzitta (2008). "Energy, economic and environmental analysis on RET-hydrogen Systems in residential buildings." Renewable Energy 33(3): 366-382.

Bejan, A. (2002). "Fundamentals of exergy analysis, entropy generation minimization, and the generation of flow architecture." International Journal of Energy Research 26(7): 0-43.

Bejan, A., G. Tsatsaronis and M. Moran (1995). Thermal design and optimization, Wiley-Interscience.

Bingöl, E., B. Kılkış and C. Eralp (2011). "Exergy based performance analysis of high efficiency poly-generation Systems for sustainable building applications." Energy and Buildings 43(11): 3074-3081.

Blieske, M., J. E. D. Gauthier and X. Huang (2009). "Design and Performance Evaluation of a Trigeneration System Incorporating Hydraulic Storage and an Inverted Brayton Cycle." Journal of Engineering for Gas Turbines and Power 131(1): 012302.

Calise, F., M. D. d'Accadia and L. Vanoli (2012). "Design and dynamic simulation of a novel solar trigeneration System based on hybrid photovoltaic/thermal collectors (PVT)." Energy Conversion and Management 60(0): 214-225.

Caliskan, H., I. Dincer and A. Hepbasli (2011). "Exergetic and sustainability performance comparison of novel and conventional air cooling Systems for building applications." Energy and Buildings 43(6): 1461-1472.

Caliskan, H., I. Dincer and A. Hepbasli (2013). "Thermoeconomic analysis of a building energy System integrated with energy storage options." Energy Conversion and Management 76: 274-281.

Chen, Q., W. Han, J.-j. Zheng, J. Sui and H.-g. Jin (2014). "The exergy and energy level analysis of a combined cooling, heating and power System driven by a small scale gas turbine at off design condition." Applied Thermal Engineering 66(1-2): 590-602.

Cohce, M. K., I. Dincer and M. A. Rosen (2011). "Energy and exergy analyses of a biomass-based hydrogen production System." Bioresour Technol 102(18): 8466-8474.

Coskun, C., Z. Oktay and I. Dincer (2009). "New energy and exergy parameters for geothermal district heating Systems." Applied Thermal Engineering 29(11-12): 2235-2242.

Dagdougui, H., R. Minciardi, A. Ouammi, M. Robba and R. Sacile (2012). "Modeling and optimization of a hybrid System for the energy supply of a “Green” building." Energy Conversion and Management 64: 351-363.

Deshmukh, M. K. and S. S. Deshmukh (2008). "Modeling of hybrid renewable energy Systems." Renewable and Sustainable Energy Reviews 12(1): 235-249.

Dincer, I. and M. A. Rosen (2012). Exergy: energy, environment and sustainable development, Newnes.

Dincer, I. and C. Zamfirescu (2012). "Potential options to greenize energy Systems." Energy 46(1): 5-15.

Ebrahimi, M., A. Keshavarz and A. Jamali (2012). "Energy and exergy analyses of a micro-steam CCHP cycle for a residential building." Energy and Buildings 45: 202-210.

Herrando, M., C. N. Markides and K. Hellgardt (2014). "A UK-based assessment of hybrid PV and solar-thermal Systems for domestic heating and power: System performance." Applied Energy 122: 288-309.

Hosseini, M., I. Dincer and M. A. Rosen (2013). "Hybrid solar–fuel cell combined heat and power Systems for residential applications: Energy and exergy analyses." Journal of Power Sources 221: 372-380.

Joshi, A. S., A. Tiwari, G. N. Tiwari, I. Dincer and B. V. Reddy (2009). "Performance evaluation of a hybrid photovoltaic thermal (PV/T) (glass-to-glass) System." International Journal of Thermal Sciences 48(1): 154-164.

Li, Y., X. Wang, D. Li and Y. Ding (2012). "A trigeneration System based on compressed air and thermal energy storage." Applied Energy 99: 316-323.

Lubis, L. I., M. Kanoglu, I. Dincer and M. A. Rosen (2011). "Thermodynamic analysis of a hybrid geothermal heat pump System." Geothermics 40(3): 233-238.

Ma, Q., R. Z. Wang, Y. J. Dai and X. Q. Zhai (2006). "Performance analysis on a hybrid air-conditioning System of a green building." Energy and Buildings 38(5): 447-453.

Mammoli, A., P. Vorobieff, H. Barsun, R. Burnett and D. Fisher (2010). "Energetic, economic and environmental performance of a solar-thermal-assisted HVAC System." Energy and Buildings 42(9): 1524-1535.

Mwasha, A., R. G. Williams and J. Iwaro (2011). "Modeling the performance of residential building envelope: The role of sustainable energy performance indicators." Energy and Buildings 43(9): 2108-2117.

Ozgener, O. (2010). "Use of solar assisted geothermal heat pump and small wind turbine Systems for heating agricultural and residential buildings." Energy 35(1): 262-268.

Rosiek, S and F.J. Batlles(2013) "Renewable energy solutions for building cooling, heating and power system installed in an institutional building, Case study in southern Spain." Renewable and Sustainable Energy Reviews 26 147–168.

Sakulpipatsin, P., L. C. M. Itard, H. J. van der Kooi, E. C. Boelman and P. G. Luscuere (2010). "An exergy application for analysis of buildings and HVAC systems." Energy and Buildings 42(1): 90-99.

Schmidt, D. (2009). "Low exergy systems for high-performance buildings and communities." Energy and Buildings 41(3): 331-336.

Smith, A. D., P. J. Mago and N. Fumo (2013). "Benefits of thermal energy storage option combined with CHP system for different commercial building types." Sustainable Energy Technologies and Assessments 1: 3-12.

Srinivas, T., A. V. S. S. K. S. Gupta and B. V. Reddy (2007). "Parametric simulation of steam injected gas turbine combined cycle." Proceedings of the Institution of Mechanical Engineers, Part A: Journal of Power and Energy 221(7): 873-883.

Stender, J. (1993). Parallel Genetic Algorithms: Theory and Applications, IOS Press.

Toja-Silva, F. and A. Rovira (2013). "A First and Second Thermodynamics Law Analysis of a Hydrogen-Fueled Microgas Turbine for Combined Heat and Power Generation." Journal of Engineering for Gas Turbines and Power 136(2): 021501.

Twidell, J. and A. D. Weir (2006). Renewable Energy Resources, Taylor & Francis.

Vučićević, B., M. Jovanović, N. Afgan and V. Turanjanin (2014). "Assessing the sustainability of the energy use of residential buildings in Belgrade through multi-criteria analysis." Energy and Buildings 69: 51-61.

Yang, L., E. Entchev, M. Ghorab, E. J. Lee and E. C. Kang (2014). "Energy and cost analyses of a hybrid renewable microgeneration system serving multiple residential and small office buildings." Applied Thermal Engineering 65(1-2): 477-486.